A Novel in vitro PDE7 Inhibitor Inhibits IL-2 Gene Expression in Activated T Cells and Induces Apoptosis in a B-cell Line and Monocytic Cell Line

Author: Chenjia Xu

Boston College

The Graduate School of Arts and Sciences

Department of Biology

A NOVEL IN VITRO PDE7 INHIBITOR INHIBITS IL-2 GENE EXPRESSION IN ACTIVATED T CELLS AND INDUCES APOPTOSIS IN A B-CELL LINE AND MONOCYTIC CELL LINE

a dissertation

by

CHENJIA XU

submitted in partial fulfillment of the requirements

for the degree of

Doctor of Philosophy

August 2013

ABSTRACT

A NOVEL IN VITRO PDE7 INHIBITOR INHIBITS IL-2 GENE EXPRESSION IN ACTIVATED T CELLS AND INDUCES APOPTOSIS IN A B-CELL LINE AND MONOCYTIC CELL LINE

Author: Chenjia Xu

Advisor: Thomas C. Chiles, Ph.D.

Elevating intracellular cAMP levels can result in a wide range of anti-inflammatory effects and growth arrest and apoptosis in cancer cells, marking phosphodiesterases (PDEs) as potential targets for inflammatory diseases and cancer treatment. PDE7A is proposed to be a new therapeutic target for its ubiquitous expression in proinflammatory and immune cells. A Barbituric acid based compound, BC12 was identified as an *in vitro* PDE7 inhibitor in fission-yeast-based high-throughput screen. Analysis of this compound on the activation of Jurkat T lymphocytes, mouse and human primary T cells reveals inhibition of IL-2 production, though cell viability is not significantly impacted. Real-time RT-PCR and mRNA stability assays indicate that the inhibition of IL-2 production by BC12 is attributable to transcriptional repression without accelerating *IL-2* mRNA decay. By contrast, compounds of similar structure with that of BC12 exhibit varying effects on IL-2 production that does not correlate with their *in vitro* PDE7 inhibitory activity, suggesting that the *in vivo* target of BC12 responsible for these effects may not be PDE7. Our study further reveals that BC12 inhibits *IL-2* transcription through targeting NFAT and NFκB-mediated pathways. Preliminary investigation on

other T helper cell cytokine secretion indicates that BC12 has a potential to selectively inhibit Th2 cytokines. Our data suggest that BC12 may present a novel anti-inflammatory drug for its immunosuppressive and potential immunomodulatory effects. Analysis of BC12 on a human B-cell line and a monocytic cell line demonstrate its pro-apoptotic effects in a dose-dependent manner. Titration of BC12 on human diffuse large B-cell lymphoma (DLBCL), LY18 cells, and human primary B cells reveals that BC12 induces cell death more effectively in DLBCL LY18 cells than normal B cells, suggesting the anti-cancer potential of this compound.

This dissertation is dedicated to my mom, Yanyan Chen,

for her endless love

and the courage she seeded in my heart.

ACKNOWLEDGEMENTS

First, I would like to express my deepest appreciation to my advisor, Dr. Thomas Chiles. Without his patient guidance and persistent support, this dissertation would not have been possible. I would also like to thank my second advisor, Dr. Charles Hoffman, for his knowledge, encouragement and support.

I want to express many thanks to Dr. Fay Dufort for her assistance, support and friendship over the past six years. I also want to thank my other colleagues in Chiles lab and in the Biology department, past and present. I have had the great pleasure to work in this excellent environment, where people share knowledge, passion and love with each other.

I must thank my family and friends for their continuous support and encouragement over the years. I especially want to thank my father, who has always been there for me. I want to thank my husband, Chong, for the confidence in me when I doubted myself, for the comfort and encouragement when I felt frustrated and for the support whenever I needed it.

Finally, I would like to thank my newborn baby, Aidan. He has been with me during the frustration and has given me strength to become a better person.

TABLE OF CONTENTS

Dedication i

Acknowledgements ii

Table of Contents iii

List of Figures v

List of Abbreviations viii

Introduction 1

I. Cyclic Nucleotide Phosphodiesterases and Their Role in Immune System 1

II. The Immune System 9

III. T Lymphocytes 10

IV. The Cytokine Interleukin-2 17

V. B lymphocytes 31

VI. Monocytes 33

Material and Methods 36

Antibodies and Reagents 36

T Lymphocyte Isolation, Cell Culture and Stimulation 37

Enzyme-Linked Immunosorbent Assay (ELISA) 38

Nuclear Extraction for Western Blotting 39

Whole Cell Extraction for Western Blotting 39

Western Blotting 40

Reverse Transcription and Real-Time PCR 40

Viability Assay and Cell Cycle Analysis 41

BrdU Incorporation 42

Terminal Deoxynucleotidyltransferase dUTP Nick End Labeling (TUNEL) Assay 42

Caspase 3 Staining by Flow Cytometry 42

Nuclear Extraction and Electrophoretic Mobility-Shift Assay (EMSA) 43

Chapter One: An *in vitro* PDE7 inhibitor inhibits *IL-2* gene expression in activated T cells by repressing NFκB and NFAT -mediated transcription 45

Results 46

Figures and Legends 62

Chapter Two: BC12 induces apoptosis in LY18, U937 cells and primary B cells 120

Results 121

Figures and Legends 128

Discussion 158

I. Chapter One 158

II. Chapter Two 167

References 171

LIST OF FIGURES

1.	BC12 inhibits IL-2 secretion in Jurkat cells in a dose-dependent manner.	62
2.	BC12 does not significantly reduce cell viability.	64
3.	Time course of IL-2 inhibition by BC12.	66
4.	BC12 inhibits IL-2 intracellular protein production.	68
5.	BC12 decreases IL-2 mRNA level in activated Jurkat cells.	70
6.	BC12 does not affect IL-2 mRNA stability.	72
7.	BC12 and its derivatives have different PDE7A and 7B inhibitory activity.	74
8.	BC12 and its derivatives have various effects on IL-2 secretion.	77
9.	BC12 inhibits IL-2 expression not through PDE.	79
10.	BC12 augments activation signal towards AP-1 pathway.	81
11.	Microarray analysis of *IL-2* gene regulators suggests NFκB the most likely transcription factor responsible for down-regulation of *IL-2* gene.	83
12.	BC12 inhibits IκBα turnover at early time points.	85
13.	BC12 inhibits nuclear translocation of some NFκB family proteins.	87
14.	BC12 does not affect nuclear translocation of NFAT and AP-1 family.	89
15.	BC12 inhibits the binding of NFκB to the consensus NFκB-binding probe.	91
16.	BC12 inhibits the binding of NFAT to the NFAT-binding probes.	93
17.	BC12 and its analogs have different effects on Transcription factor binding activity.	96
18.	BC12 and BC12-4 inhibit IL-2 secretion in activated mouse primary T cells.	98

19.	BC12, BC12-4 and BC12-6 do not significantly reduce mouse primary T cell viability.	100
20.	BC12 inhibits mouse primary T cell proliferation.	102
21.	BC12 induces a moderate level of increase in hypodiploid DNA resulting in apoptosis in mouse primary T cells.	104
22.	BC12 augments activation signals in activated mouse primary T cells.	106
23.	BC12 inhibits IL-2 secretion in activated human primary T cells.	108
24.	BC12 induces cell death in human primary T cells.	110
25.	BC12 and BC12-4, but not BC12-6, inhibit IL-2 secretion in activated human primary T cells.	112
26.	BC12 decreases the IL-2 mRNA level in activated human primary T cells.	114
27.	BC12 selectively inhibits Th2 cytokines over Th1.	116
28.	*In vitro* PDE7 inhibitors have various effects on LY18 cell viability.	128
29.	BC12 induces dose-dependent decrease of cell viability in LY18 cells.	130
30.	BC12 induces apoptosis in LY18 cells.	132
31.	BC12 activates caspase pathway in LY18 cells.	134
32.	BC12 induces PARP cleavage and activation in LY18 cells.	136
33.	BC12 analogs have various effects on LY18 cell viability.	138
34.	BC12 does not inhibit cell cycle progression in LY18 cells.	140
35.	BC12 induces cell death in human primary B cells.	142
36.	*In vitro* PDE7 inhibitors have various effects on U937 cell viability.	144
37.	BC12 induces dose-dependent decrease of cell viability in U937 cells.	146
38.	BC12 induces apoptosis in U937 cells.	148

39. BC12 activates caspase pathway in U937 cells. 150

40. BC12 induces PARP cleavage and activation in U937 cells. 152

41. BC12 does not inhibit cell cycle progression in U937 cells. 154

42. BC12 does not inhibit DNA synthesis in U937 cells. 156

LIST OF ABBREVIATIONS

5-FOA	5-fluoroorotic acid
AC	Adenylyl cyclase
AICD	Activation-induced cell death
ALL	Acute lymphoblastic leukemia
AP-1	Activator protein 1
APC	Antigen presenting cells
ARE	AU-rich element
at-RA	*all-trans* retinoic acid
BCR	B cell receptor
cAMP	Adenosine 3', 5'-cyclic monophosphate
CBP	CREB binding protein
CCR2	CC-chemokine Receptor 2
CD28RE	CD28 responsive element
C/EBP	CCAAT/enhancer-binding protein
CLL	Chronic lymphocytic leukemia
CLP	Common lymphoid progenitor
CMP	Common myeloid progenitor
COPD	Chronic obstructive pulmonary disease
CRE	cAMP-response element
CREB	cAMP response element-binding protein
CREM	cAMP response element modulator
CsA	Cyclosporin A
cSMAC	Central supramolecular activation cluster
CtBP	C-terminal-binding protein
CTL	Cytotoxic T lymphocyte
DAG	Diacylglycerol
DLBCL	Diffuse large B-cell lymphoma
DN	Double negative
DP	Double positive

ECL	Enhanced chemiluminescence
Egr-1	Early growth response protein-1
ELISA	Enzyme-Linked Immunosorbent Assay
EMSA	Nuclear Extraction and Electrophoretic Mobility-Shift Assay
EPAC	Exchange protein directly activated by cAMP
ERK	Extracellular-signal-regulated kinase
FBS	Fetal bovine serum
FLNA	Filamin A
GABP	GA binding protein
GCs	Glucocorticoids
GMP	Granulocyte-monocyte progenitor
Grb2	Growth factor receptor-bound protein 2
HDAC	Histone deacetylase
HRP	Horseradish peroxidase
HSC	Hematopoietic stem cell
HTS	High-throughput fission-yeast-based screen
IFN	Interferon
Ig	Immunoglobulin
IKK	IκB kinase
IL-2	Interleukin-2
IL-2R	Interleukin-2 receptor
IP_3	Inositol triphosphate
IS	Immunological synapse
ITAM	Immunoreceptor tyrosine-based activation motif
iTreg	Induced T regulatory cell
JNK	c-Jun N-terminal kinase
JRE	c-Jun N-terminal kinase response element
Lck	Lymphocyte protein-tyrosine kinase
MEP	Megakaryocyte–erythroid progenitor
MHC	Major histocompatibility complex

mTOR	Mammalian target of rapamycin
NAB2	NGFI-A-binding protein 2
NFAT	Nuclear factor of activated T-cells
NFκB	Nuclear factor kappa B
NHL	Non-Hodgkin's lymphoma
NLS	Nuclear localization signal
nTregs	Natural T regulatory cell
NURD	Nucleosome remodeling and DNA methylation complex
OCI-LY18	Ontario Cancer Institute-LY18
Oct	Octamer-binding protein
PARP	Poly ADP Ribose Polymerase
PBMC	Peripheral blood mononuclear cell
PDE	Phosphodiesterase
PDK	Phosphoinositide-dependent protein kinase
PHA	Phytohaemagglutanin
PI3K	Phosphatidylinositol 3-kinase
PIP_2	Phosphatidylinositol 3,4-phosphate
PIP_3	Phosphatidylinositol 3,4,5-phosphate
PKA	Protein kinase A
PKB	Protein kinase B
PKC	Protein kinase C
PLC	Phospholipase C
PMA	Phorbol myristate acetate
PTK	Protein tyrosine kinase
RA	Rheumatoid arthritis
RAR	Retinoic acid receptor
ROR	Retinoic acid-related orphan receptor
SLE	Systemic lupus erythematosus
Sos	Son of sevenless
Stat	Signal transducer and activator of transcription

Syk	Spleen tyrosine kinase
TCR	T-cell receptor
TGF	Tumor growth factor
TNF	Tumor necrosis factor
TUNEL	Terminal Deoxynucleotidyltransferase dUTP Nick End Labeling
UTR	Untranslated region
ZAP-70	Z-chain associated protein kinase-70
ZEB	Zinc finger E-box-binding protein

INTRODUCTION

I. Cyclic Nucleotide Phosphodiesterases and Their Roles in Immune System

A. cAMP Signaling in Immune System

Adenosine 3', 5'-cyclic monophosphate (cAMP) is a ubiquitous second messenger that plays a central role in signal transduction and regulation of cellular responses. It is generated by adenylyl cyclase (AC) and hydrolyzed by phosphodiesterase (PDE) [1, 2]. The intracellular level of cAMP is precisely controlled and organized spatially and temporally. Adenylyl cyclases are activated through occupation of respective upstream G protein receptors by their ligands. There are at least ten isoforms of adenylyl cyclase and eleven families of phosphodiesterases in mammalian cells that allow tissue and differentiation specific regulation and compartmentalization of cAMP signaling [2]. Protein kinase A (PKA) and exchange protein directly activated by cAMP (EPAC) are the major effector enzymes of cAMP signaling [1]. Binding of cAMP to PKA releases catalytic domains of the kinase from regulatory domains. These catalytic domains are free to translocate and phosphorylate enzymes, transcription factors and ion channels, and therefore regulate a large scale of cellular response and gene expression [2]. Targeting cAMP pathway can be achieved through respective G-protein coupled receptors, adenylyl cyclases, phosphodiesterases, and downstream PKA activity. However, increasing of adenylyl cyclase activity only results in transient change of cAMP level due to compensation of increased downstream PDE activity [3].

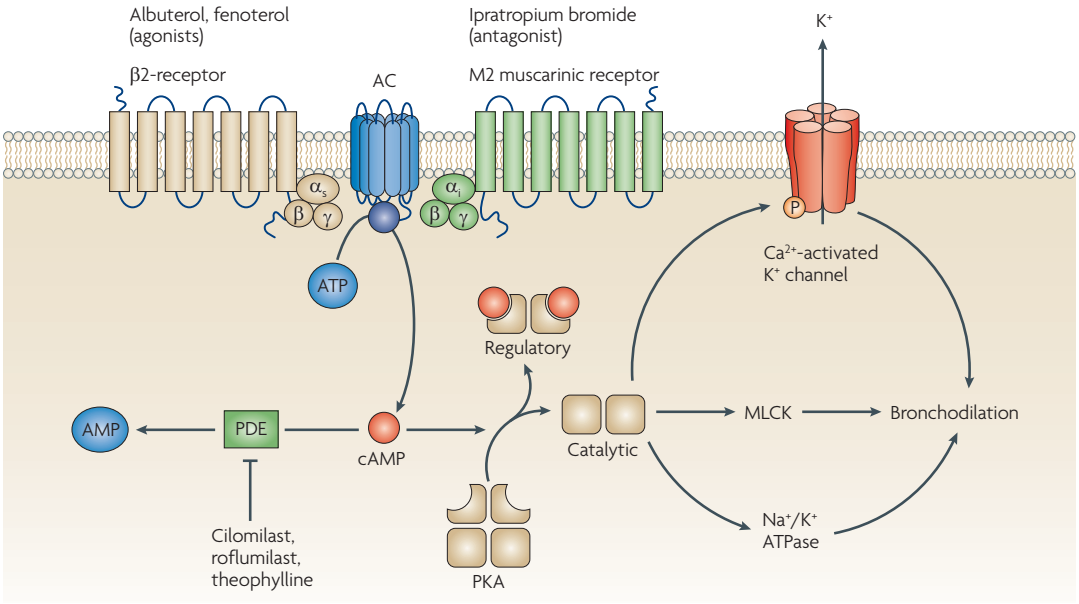

Figure 1. cAMP signaling pathways in asthma therapy [2]. The figure is lifted from *Pierre, S., Eschenhagen, T., Geisslinger, G., and Scholich, K. 2009. Nat Rev Drug Discov. 8(4):321-35.*

In the early 1970s, cAMP was reported as a general immunomodulator through an inhibitory action on immunologic and inflammatory functions [4]. Elevation of intracellular cAMP levels results in a wide range of anti-inflammatory effects, such as decreased pro-inflammatory cytokine generation, decreased proliferative response, and decreased surface marker expression in leukocytes [5]. Manipulating cAMP levels in immune cells has many clinical applications [6]. Several drugs for inflammatory diseases, such as asthma and chronic obstructive pulmonary disease (COPD), act through increasing cAMP levels (Figure 1) [2, 6].

Additionally, the cAMP signaling pathway has also drawn increasing attention as a regulator of hematopoietic cell proliferation and apoptosis. It has been frequently reported that elevation of cAMP level arrests proliferation or induces apoptosis in malignant lymphoid cells [6–10]. However, the mechanism of cAMP-mediated apoptosis

remains largely undiscovered. Although PKA is believed to be required in mediating apoptosis in most cases, the cAMP-mediated apoptosis in diffuse large B-cell lymphoma was reported to be associated with inhibition of the phosphatidylinositol 3-kinase (PI3K)/Akt pathway [10]. The expression level of the pro-apoptotic protein, Bim, from Bcl-2 family, is up-regulated in response to cAMP/PKA activation in lymphoid cells, which may be the link between PKA and caspase activation [8].

B. PDE and Immune Cells

The multigenic family of cyclic nucleotide phosphodiesterase (PDE) hydrolyze the 3' ribose phosphate bond of cAMP or cGMP to their respective 5' -monophosphate and is the only way to degrade these cyclic nucleotides [1]. PDEs that hydrolyze cyclic pyrimidine monophosphates have also been discovered but have received little attention [11]. PDEs with homology greater than 65% in their catalytic cores are considered as the same family [1, 11]. There are at least 21 PDE genes expressed in mammalian cells that are divided into 11 families [1, 12]. Each gene produces one or more protein products due to splicing variation, yielding at least 80 different PDE proteins [1, 12]. Different PDE families share some structural similarity, including a conserved catalytic domain, and also own specificity in the respects of biochemical properties, substrate specificity, cellular localization, tissue-specific expression, and their sensitivity to pharmacological agents. PDE4, PDE7 and PDE8 are cAMP specific [1, 6]. Among the large PDE superfamily, PDE 3B, 4A, 4B, 4D and 7A1 are predominant in immune cells [5, 13].

Besides tissue-specific expression, PDE isoenzymes display remarkable specific cellular and subcellular localization. Subsequent compartmentalization of PDE activity in

cells makes it a potential target for specific pathways and disease processes [1]. Therefore, PDE inhibition is one of the major mechanisms applied to target cAMP signaling pathway for therapeutic purpose. The first PDE inhibitor, theophylline, was identified in 1962 [14]. Since then, more selective and potent inhibitors for each PDE family have been synthesized and characterized. As a nonselective PDE inhibitor, theophylline has proven effective in controlling asthma through increasing cAMP levels (Figure 1) [1, 2].

Over the last two decades, there have been extensive efforts in developing PDE4 inhibitors as therapeutic agents due to their anti-inflammatory properties. PDE4 is the major isoenzyme found in most T cell populations and PDE4 inhibitors have been shown to inhibit tumor necrosis factor (TNF) α production [15]. PDE4 specific inhibitors cilomilast and roflumilast reached stage III of clinical trials for treating asthma and COPD, but their usage is limited due to severe side effects of vomiting and nausea [1, 2, 16, 17].

Recently, increasing attention has been drawn to the ability of PDE4 inhibitors to induce apoptosis in malignant lymphoid cells, which opens a new therapeutic area of cancer treatment [6–10]. Theophylline and PDE4 inhibitors were reported to augment glucocorticoid-mediated apoptotic effects in B cell chronic lymphocytic leukemia (B-CLL) [9].

For the present, most of the PDE inhibitors are still used in biomedical and pharmaceutical research to study the functions of PDE isoenzymes [1]. The potential of PDE inhibitors as therapeutic agents is promising whereas their usage is still limited, calling for more specific PDE inhibitors for a better benefit-risk ratio [1].

C. PDE7 Family: Expression and Function in Immune Cells

PDE7 is a cAMP-specific PDE family characterized as high affinity for cAMP (K_m=0.2 μM) and low V_{max}, but no sensitivity to PDE4 inhibitors such as rolipram [1]. It was first isolated at the gene level from a human glioblastoma cDNA library in 1993 [18]. Since then, two genes have been identified in the PDE7 family, PDE7A and PDE7B, in mouse, rat and human [11, 18–21]. Although these two genes share structural similarity, they exhibit distinct distribution patterns [21, 22].

PDE7A mRNA is highly expressed in human proinflammatory and immune cells, as well as in endothelial cells [22]. Three splice variants derived from the same gene have been identified. PDE7A1, the most well understood splice variant, is abundant in T lymphocytes, bronchial epithelial cells, airway and vascular smooth muscle cells, lung fibroblasts, and eosinophils. PDE7A2 has only been detected in cardiac myocytes at the protein level. PDE7A3 was found expressed in human $CD4^+$ T cells after stimulation with anti-CD3/CD28 antibodies but not naive T cells [11, 22, 23]. PDE7A was also reported to be expressed in human B-lymphocytes and its expression is up-regulated by elevation of intracellular cAMP as a compensatory feedback mechanism [24]. The overall expression of PDE7A mirrors the distribution of PDE4, which leads to a reasonable speculation of its potential to be another anti-inflammatory target [22].

PDE7B was cloned and characterized using a bioinformatics approach in 2000. The deduced amino acid sequence of human PDE7B is 64% identical to that of PDE7A, with 67.1% identity in the catalytic domain and almost identical cAMP binding sites [19, 20]. PDE7B mRNA is most abundantly expressed in the brain, heart, skeletal muscle and

pancreas, with little overlapping in distribution compared to PDE7A, indicating tissue-specific functions of these two isoenzymes [19, 21, 24]. Three PDE7B splice variants were identified in rats, with PDE7B1 most widely distributed and PDE7B2 restricted to testis. PDE7B1 was proposed to play a role in neural activity and memory function [19–21, 24]. It is notable that PDE7B mRNA is also detected in a low transcriptional level in T-lymphocytes [24].

In addition to the ubiquitous expression of PDE7A in immune cells, accumulating evidence support that PDE7A plays a role in regulating inflammatory responses. Both PDE7A1 and 7A3 are up-regulated in T cells after stimulation [23, 25]. Li et al. reported that PDE7A antisense oligonucleotides inhibited cell proliferation and IL-2 production in both Hut78 T cell line and primary $CD4^+$ T lymphocytes. The inhibition was associated with an increase in the cAMP level and could be reversed by a PKA antagonist [25]. However, PDE7A deficient mice were reported to have functional T cells, but unexpectedly exhibit a significantly enhanced antibody response, opposing the role of PDE7A in T cell activation but suggesting its potential role in B cell function [26].

Although PDE7B was considered not present at an appreciable level in immune cells, it was recently reported that B-CLL cells overexpressed PDE7B [7]. Both selective inhibition of PDE7 and dual inhibition of PDE4/7 kill CLL cells at concentrations that have little effects on normal B cells, suggesting PDE7B as a potential therapeutic target for CLL [7]. However, inhibitors that selectively and potently inhibit PDE7B are in need to confirm its role in CLL malignancy.

D. Fission-yeast-based High Throughput Screen for PDE Inhibitors

The discovery of selective inhibitors to PDE7 family has allowed more efficient assessment of its specific role in immune function and clinical potential. BRL50481, a pure competitive inhibitor discovered in 2004, is the only commercially available PDE7 inhibitor to date [27]. It effectively inhibits PDE7A with IC_{50} of 200 nM, while moderately inhibits PDE7B [28]. BRL50481was found to act additively with PDE4 inhibitors to suppress TNFα release from stimulated human monocytes [27]. Although PDE7 has shown a remarkable potential to serve as therapeutic targets, there are only a few selective PDE7 inhibitors that have been identified so far, and specific inhibitors to either isoenzyme or each splice variant are not available [28]. The identification and characterization of a selective PDE7A or 7B inhibitor or activator would facilitate the studies of PDE7A versus PDE7B functions, as well as generate more specific therapeutic agents.

Since most of the inhibitor development is based on structural characterization of active sites and novel synthesis, those newly developed inhibitors are not readily available to the research community. Our collaborator, Dr. Hoffman at Boston College, developed a novel fission yeast-based high throughput screen to identify new PDE inhibitors. The fission yeast *Schizosaccharomyces pombe* responses to extracellular glucose levels through a cAMP-signaling pathway. High glucose levels activate adenylyl cyclase through a G protein coupled receptor, generate a cAMP signal and lead to subsequent PKA activation. A fusion gene *fbp1-ura4* is under a promoter repressed by PKA activity in response to cellular cAMP level. Yeast grown in a high glucose

environment require uracil to survive unless cAMP signaling is inhibited. Defects in glucose signaling pathway result in constitutive expression of *fbp1-ura4* fusion gene, allowing yeast strains grow in high glucose environment lacking uracil, while conferring sensitivity to 5-fluoroorotic acid (5-FOA) [28].

Fission yeast strains with defects in glucose signaling were constructed with mammalian PDE genes as the only PDE activity. PDE inhibitors augment intracellular cAMP level and confer 5-FOA-resistant growth. Therefore, this platform can be used to screen for compounds with PDE inhibitory activity in a high-throughput fashion [28].

E. Identification, Structure and In-vitro Characterization of BC12 and Related Compounds

A series of novel compounds were identified as PDE7A or 7B inhibitors by the Hoffman lab based on their ability to stimulate 5-FOA-resistant growth in PDE7A or PDE7B recombinant fission yeast stains. *In vitro* PDE assays confirmed the PDE7 inhibitory activity of these compounds. Among them, BC12 is one of the best PDE7A inhibitors in both high-throughput screening and *in vitro* assay. The IC_{50} on purified PDE7A catalytic domain is 1 μM, compared to 0.2 μM of BRL50481. Interestingly, BC12 acts as an activator on PDE7B catalytic domain with AC_{200}= 0.1 μM. To further confirm, PDE7B from rat cell extracts was used as a substrate. BC12 acts as an inhibitor of full-length rat PDE7B with IC_{50} of 200 nM (Thomas Rich, personal communication). Based on the high throughput screening and *in vitro* PDE assay, BC12 is a potent *in vitro* PDE7A and 7B inhibitor.

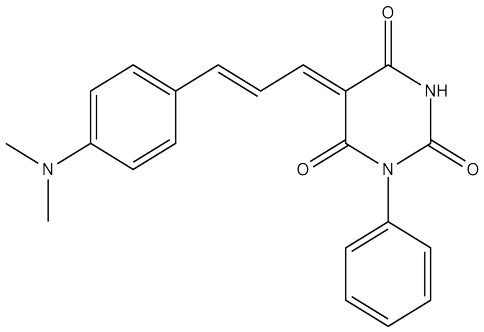

Figure 2. The Molecular Structure of BC12

Structurally, BC12 is a barbituric based compound (Figure 2). Barbiturates are used for the treatment of intracranial hypertension, but the effect of neuroprotection is also associated with a loss of protective immunity. It has been reported that barbiturates exhibit immunosuppressive and immunomodulatory actions on lymphocyte and leukocyte function, including inhibition on T cell proliferation, differentiation, and cytokine production [29, 30].

A series of analogs of BC12 were tested for their PDE inhibitory activity. Among 7 derivative compounds, BC12-6 is the best PDE7 inhibitor and BC12-4 has no PDE7 inhibitory effect when tested in the 5-FOA growth assay.

As a potent novel PDE7 inhibitor characterized in both fission-yeast growth assay and *in vitro* PDE assay, BC12 is a promising candidate for its potential immunomodulatory effects. My study will focus on the effects of BC12 and its derivative compounds on mammalian immune cells.

II. The Immune System

The immune system is the protective barrier of an organism and the defensive mechanism against invading pathogens.

The immune system has two branches: innate immune system and adaptive immune system. The cells and molecules of both branches work as an integrated host defense system. Innate immunity serves as the first line of defense, which acts within minutes of infection and is followed later by early-induced responses. These responses can keep the infection under control in the early stages as well as influence the development of the adaptive immune response that will take several days. The innate immune system recognizes the common features of pathogens, and does not provide lasting protective immunity [31].

When the innate immune system fails to eliminate infectious organisms, an adaptive immune response is triggered, which is a stronger response with highly specific recognition of diverse foreign pathogens. The adaptive immune system comprises T lymphocytes, including $CD8^+$ cytotoxic T lymphocytes and $CD4^+$ T helper cells, and B lymphocytes, which mediate humoral responses. Both T and B lymphocytes develop through clonal expansion and differentiation into antigen-specific effector lymphocytes, and also generates memory lymphocytes that allow more rapid and efficient response upon re-infection [31].

III. T Lymphocytes

A. The Development of T Lymphocytes

Like all other blood cells, T lymphocytes derive from self-renewing hematopoietic stem cells (HSC) in bone marrow. The fate determination of a pluripotent progenitor cell requires specific inductive signals and specified microenvironment. T cell progenitors migrate at a very early stage to thymus to develop into mature T cells [31].

The developmental process in thymus can be distinguished by distinctive expression of cell-surface markers, and are divided into: double negative (DN) $CD4^-CD8^-$ stage, double positive (DP) $CD4^+CD8^+$ stage and single positive (SP) $CD4^+$ or $CD8^+$ stage (Figure 3) [32]. DN stage can be further broken down into four sub-stages based on the differential expression of surface protein CD44 and CD25 [33]. Immature DN thymocytes undergo receptor gene rearrangement that produces a diverse repertoire of T-cell receptors (TCRs) of individually unique antigen specificity. Rearrangement of two sets of receptor genes gives rise to two distinct T-cell lineages: more than 95% α:β T cells and the rest γ:δ T cells [31]. After successful rearrangement of β-chain gene in α:β lineage cells, subsequently formed pre-T-cell receptor (preTCR) signals cells to proliferate, upregulate CD4 and CD8 expression, and initiate the rearrangement of the α-chain gene [31]. These developing cells go through positive selection by engagement of their TCR by self-major histocompatibility complex (MHC) molecules and negative selection by eliminating self-reactive cells [31]. T cells expressing receptors that recognize self MHC II are positively selected to the $CD4^+$ lineage and those expressing receptors that recognize self MHC I are selected to the $CD8^+$ lineage [32]. In the specific environment of the thymus, T cells are selected to generate a repertoire of self-MHC restricted and self-tolerant mature T cells.

Mature T cells leave the thymus and recirculate between the bloodstream and peripheral lymphoid tissues where they may encounter foreign antigens. They remain naive T cells until they encounter antigens in lymphoid tissues [31].

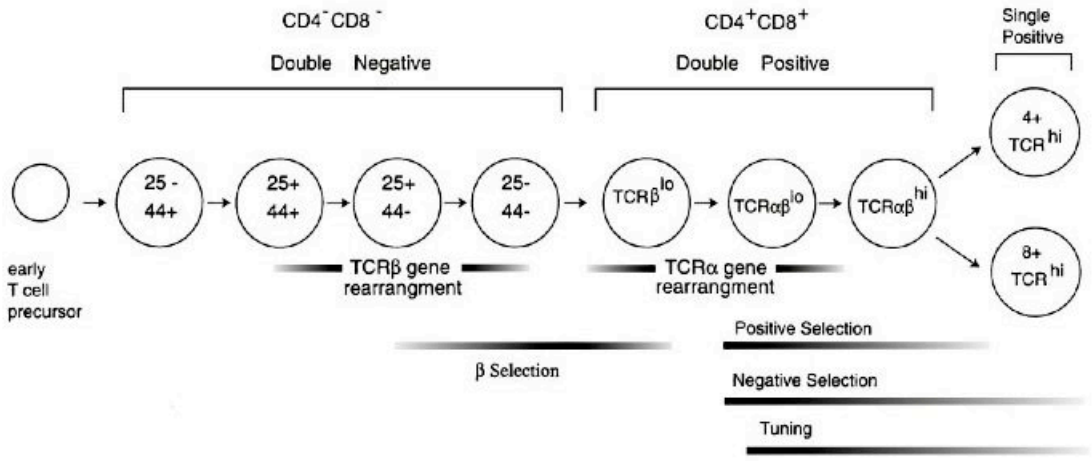

Figure 3. The stages of T cell development [32]. The figure is lifted from E. Sebzda, S. Mariathasan, T. Ohteki, R. Jones, M. F. Bachmann, and P. S. Ohashi, *Annual review of immunology*, vol. 17, no. 3, pp. 829–874, 1999.

B. Activation and Differentiation

Naive T cells are activated to proliferate and differentiate into effector T cells when they encounter their specific antigen presented in the form of peptide: MHC by antigen presenting cells (APC) in peripheral lymphoid tissues. Both ligation of TCR and costimulatory signals are required to trigger activation of naive T cells. Upon activation, T cells re-enter G_1 phase of cell cycle and express an essential cytokine interleukin-2 (IL-2) along with the α chain of IL-2 receptor (IL-2R). The α chain assembles with IL-2Rβ chain and common receptor γ chain to form a high-affinity IL-2 receptor, which binds to IL-2 to trigger the progression of cell cycle and following activation events [31].

Naive $CD8^+$ T cells are determined to become cytotoxic T lymphocytes (CTL), while naive $CD4^+$ T cells can be induced by distinct cytokine cues from innate immune cells to different effector T-cell subsets, including Th1, Th2 and Th17 cells. Th1 cells,

which predominately produce IL-2, interferon (IFN) γ, and tumor-necrosis factor (TNF) β, are primarily responsible for initiating cell-mediated immunity [34]. Th2 cells produce IL-4, IL-5, IL-6 and IL-13, promote humoral immunity mediated by B lymphocytes, and stimulate the differentiation and activation of eosinophils [34]. Th17 cells are characterized by the production of pro-inflammatory cytokines IL-17A, IL-17F and IL-22. They reside mainly at barrier surfaces and play an important role in autoimmunity [35]. The function of these effector cells is limited by another subset of T cells, regulatory T cells, including natural Treg cells (nTregs) and induced Treg cells (iTregs) [36]. nTreg cells develop in thymus during positive selection and suppress function of autoreactive T lymphocytes that have escaped negative selection. iTregs are generated in periphery after antigen-specific stimulation from naive $CD4^+$ T cells [36]. Treg cells produce high level of inhibitory cytokines IL-10 and tumor growth factor (TGF) β and suppress effector T cell and dendritic cell function [37].

The decision to differentiate into which effectors or regulatory cells is determined mainly by cytokines naive $CD4^+$ T cells are exposed to during activation, and controlled by specific transcription factors. IL-12, produced by dendritic cells and macrophages, and IFNγ produced by activated T cells are the principal cytokines to induce Th1 development [36]. Activation of signal transducer and activator of transcription 4 (Stat4) by IL-12 and Stat1 by IFNγ leads to expression of the central transcription factor for Th1 programming, T-bet [36]. IL-4 is the main cytokine that directs Th2 differentiation. Stat6, activated by IL-4, drives production of GATA-3, the central transcription factor for Th2 programming [36]. The differentiation of Th1 and Th2 effector cells are self-reinforcing and counter-inhibiting [36]. Development of Th17 and extrathymic iTreg cells share the

requirement of TGF β, while differentiation into either Th17 or iTregs depends on the dominance of signaling by IL-6 or *all-trans* retinoic acid (*at*-RA) [38, 39]. Binding of *at*-RA to the retinoic acid receptor (RAR) can potently inhibit Th17 development and promote Treg development [40–43], whereas signaling via IL-6 activates Stat3 and the lineage-determining transcription factor for Th17, an isoform of retinoic acid-related orphan receptor γ (RORγ), which is expressed in T cells (RORγt) [44].

C. Signaling Events to T cell Activation: the TCR and CD28 Costimulatory Signals

T lymphocyte activation requires two signals, engagement of the TCR/CD3 complex with antigen peptide/MHC molecule, and an additional signal from costimulatory molecules present on antigen-presenting cells (APC). The major costimulatory signal is provided by ligation of the T cell surface molecule CD28 with its ligands CD80/CD86 (B7-1/B7-2) [45]. Signaling from the TCR in the absence of costimulation renders a long lasting hyporesponsive state known as T cell anergy, which is important for peripheral tolerance.

The TCR/CD3 complex is comprised of the polymorphic α and β subunits (γ and δ subunits in γ:δ lineage T cells) in association with the invariant TCR ζ chain, and γ, δ, and ε chains of CD3 molecule [46]. Signals from the TCR are transduced by ζ chain and all three CD3 chains, which contain the immunoreceptor tyrosine-based activation motif (ITAM) [46]. Phosphorylation of ITAM by membrane-bound Src family kinases Fyn and lymphocyte protein-tyrosine kinase (Lck) recruits additional protein tyrosine kinases (PTKs) to the TCR, such as z-chain associated protein kinase-70 (ZAP-70) [47].

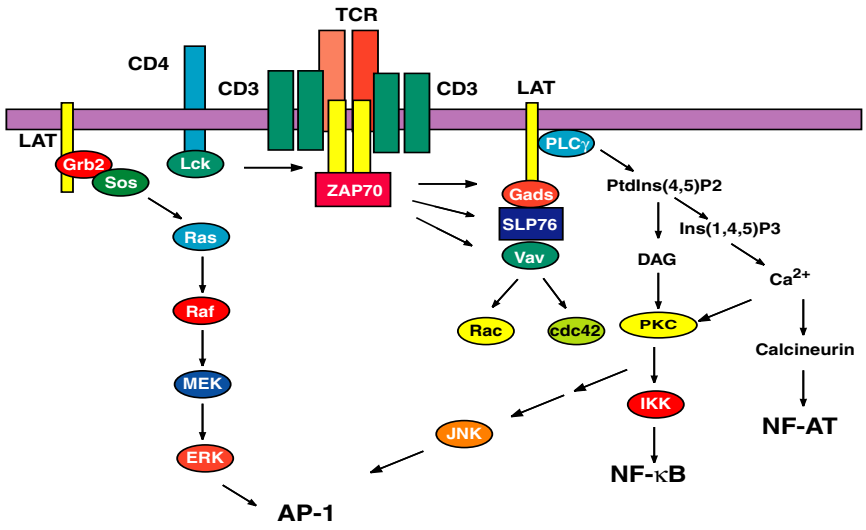

Figure 4. Signaling pathways activated by the TCR and CD28 molecules that lead to IL-2 production in T helper cells [48]**. The figure is lifted from S. L. Gaffen and K. D. Liu, *Cytokine*, vol. 28, no. 3, pp. 109–23, Nov. 2004.**

ZAP-70 phosphorylates a series of downstream adaptor proteins such as LAT, and also phospholipase Cγ 1 (PLCγ 1), which catalyzes the hydrolysis of phophatidylinositol lipids, generating inositol triphosphate (IP_3) and diacylglycerol (DAG) [46]. IP_3 induces intracellular calcium release, which in turn activates calcineurin, and together with DAG, activates protein kinase C (PKC). LAT recruits growth factor receptor-bound protein 2 (Grb2) and guanine nucleotide exchange protein son of sevenless (Sos), which activates Ras/ extracellular-signal-regulated kinase (ERK) pathway (Figure 4) [47]. Calcineurin is upstream of nuclear factor of activated T-cells (NFAT), PKC can activate c-Jun N-terminal kinase (JNK) and nuclear factor kappa B (NFκB) pathways, and ERK activates the transcription factor c-Fos. All these components regulate the expression of the *IL-2* gene [48].

CD28 signal is required in most cases for optimal IL-2 production and T cell activation, and for preventing the induction of anergy [49]. The function of CD28 can be partially attributed to augmentation of the TCR mediated signaling and therefore lower the TCR activation threshold, by facilitating the clustering of lipid rafts and formation of the immunological synapse (IS) [50]. However, the molecular basis of CD28 signaling is still largely controversy [50].

CD28 is a 44-kDa homo-dimeric protein expressed on the cell surface of resting and activated T cells [51]. The cytoplasmic domain of CD28 molecule lacks catalytic activity, and instead, it signals through binding to other signaling proteins via consensus motifs [51]. The phosphorylated YMNM motif in the cytoplasmic tail of CD28 can bind to adaptor protein Grb2 and the Src homology 2 (SH2) domain of PI3K [51]. In addition to Sos/Ras pathway, Grb2 can also recruit guanine nucleotide exchange factor Vav1, which activates Rho family protein such as Rac1, and subsequently JNK pathway [51]. PI3K catalyzes the production of phosphatidylinositol 3,4-phosphate (PIP_2) and phosphatidylinositol 3,4,5-phosphate (PIP_3), which associate with phosphoinositide-dependent protein kinase 1 (PDK1) that in turn activates protein kinase B (PKB, or known as Akt). CD28 mediated PI3K/PKB pathway can provide survival signal to T cells by directly inhibiting apoptotic machinery [51], and control protein synthesis, cell metabolism and proliferation.

Downstream of YMNM motif, CD28 possesses two proline-rich motifs that can bind to additional signaling proteins, including PKCθ and an actin-binding scaffold protein Filamin A (FLNA) [51]. FLNA is reported to be important for the movement of PKCθ to the central supramolecular activation cluster (cSMAC) [51]. PKCθ provides the

bridge between CD28 signaling to NFκB pathway, which is considered to be the most relevant CD28 biochemical target [52].

D. Acute lymphoblastic leukemia and Jurkat cells

Acute lymphoblastic leukemia (ALL) is a malignant disorder of lymphoid progenitor cells that are committed to differentiate into T- or B-cell lineage [53]. It is the most common childhood malignancies [53]. Although the cure rate in children is higher than 80%, relapsed ALL remains a leading cause of childhood mortality [53]. T precursor ALL comprises about 25% of ALL [54].

Jurkat cells were established from the peripheral blood of a 14-year-old boy with ALL during the first relapse in 1977 [54]. It was originally designated JM cell line after the patient's name [54]. It is a $CD4^+$ T cell line and carries leukemia properties identical to fresh leukemic cells [54]. It is used in research as a producer of cytokine IL-2 [55]. IL-2 is only produced by Jurkat cells treated with stimuli, such as phorbol esters with either lectins or monoclonal antibodies directly ligating TCR. My study will focus on Jurkat cells as a model system for IL-2 production and T cell activation.

IV. The Cytokine Interleukin-2

A. Biological Function of IL-2

IL-2 was discovered in 1976 as a growth-promoting activity for T lymphocytes, and was the first Type I cytokine identified at the molecular level [56]. IL-2 is a four α–helical, secreted glycoprotein with a molecular weight of 15.5 kDa [48]. *De novo* synthesis of IL-2, followed by the ligand specific IL-2 receptor α chain (IL-2Rα), is the

immediate consequence of T cell activation [57]. IL-2Rα itself binds IL-2 with low affinity. IL-2Rβ combined with the common cytokine receptor γ chain (γ_c), binds with IL-2 with intermediate affinity. IL-2Rα/β/γ_c complex form a high affinity IL-2 receptor, and transduce IL-2 signals through the cytoplasmic domains of IL-2Rβ and γ_c [57]. IL-2 signals activate at least three main signaling pathways, including PI3K/Akt, Ras-MAP kinase, and Janus kinase (Jak)/Stat5 pathways [57].

The *in vitro* function of IL-2 as a potent T cell growth factor has been well recognized. IL-2 is the most potent growth factor to stimulate T cell proliferation, survival and activation, and using monoclonal antibodies specific for IL-2 or IL-2R can efficiently inhibit T cell proliferation *in vitro* [58]. IL-2 also sensitizes activated T cells for activation-induced cell death (AICD) by Fas and Fas ligand induced apoptosis [59].

Later studies have revealed IL-2 as a pleiotropic cytokine that influences lymphocyte differentiation, immune responses and homeostasis [66, 67]. IL-2 or IL-2R knock-out mice develop severe autoimmunity instead of immune deficiency diseases [68, 69] , indicating a crucial role of IL-2 in peripheral T cell tolerance. It has been proven that a failure of production of $CD4^+CD25^+$(also known as IL-2Rα) regulatory T cells is the underlying cause of the lethal autoimmunity in IL-2 deficient mice [70, 71]. Treg cells do not produce IL-2, but consistently express a high affinity IL-2 receptor [65] and depend highly on IL-2 signaling for their generation and homeostasis [66–68].

Recent reports reevaluated the complex roles of IL-2 as a broad regulator of $CD4^+$ T helper cell differentiation [67, 75, 76]. Although IL-2 does not specifically induce one type of helper T cells to differentiate, it modulates expression of cytokine receptors and transcription factors to either promote or inhibit helper T cell differentiation [69]. IL-2

induces the expression of IL-12 receptor β2 subunit (IL-12Rβ2) and of T-bet via Stat5 pathway, thereby promoting Th1 cell differentiation [69]. For Th2 cells, IL-2 augments accessibility of *IL4* gene chromatin [70] and increases the expression level of IL-4 receptor α chain (IL-4Rα) [71]. However, the generation of Th17 cells is inhibited by IL-2 signals [67, 70]. Since Treg and Th17 cells share a common requirement of cytokine TGF β for differentiation, IL-2 signals play a crucial role in the reciprocal balance between Th17 and Treg cells [73].

B. Regulation of IL-2 Expression

IL-2 is produced primarily by $CD4^+$ T lymphocytes upon activation by antigen, although activated $CD8^+$ cells and dendritic cells can also secrete small amounts of it [74]. The production of IL-2 is regulated at multiple levels, with most research emphasis on transcriptional regulation. Chromatin structure and epigenetic modification also play an important role in *IL-2* gene regulation. In addition, posttranscriptional regulation, especially *IL-2* mRNA stability, is also tightly controlled [46, 72, 73].

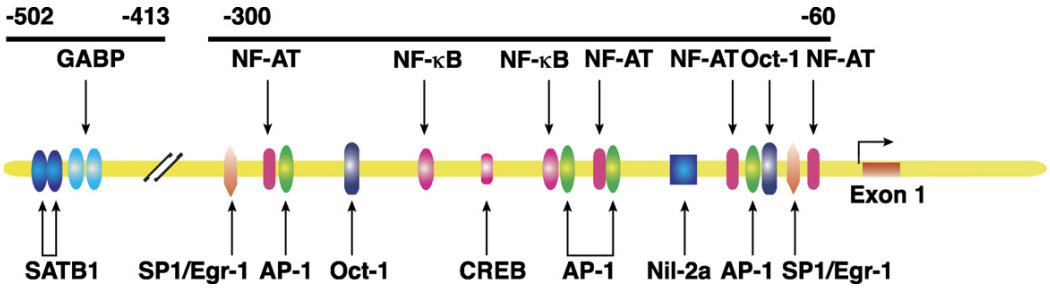

Figure 5. The known regulatory elements and corresponding transcription factors identified in the *IL-2* gene [74]. The figure is lifted from H. P. Kim, J. Imbert, and W. J. Leonard, *Cytokine & growth factor reviews*, vol. 17, no. 5, pp. 349–66, Oct. 2006.

An approximately 300bp minimal enhancer region upstream of the *IL-2* gene transcription start site possesses consensus binding sites for several transcription factors, including NFAT, the activator protein 1 (AP-1), NFκB, and Octamer-binding protein (Oct), as well as additional regulatory sites such as the CD28 responsive element (CD28RE) [76]. All these positive regulatory elements need to be occupied by corresponding transcription factors for optimal *IL-2* transcription (Figure 5) [74].

a. NFAT

The *IL-2* promoter contains four binding sites for NFAT family transcription factors. Five NFAT family members have been identified, NFATc1 (also known as NFAT2 or NFATc), NFATc2 (also known as NFAT1 or NFATp), NFATc3, NFATc4 and NFATc5, among which NFATc1, NFATc2 and NFATc3 all contribute to *IL-2* gene regulation, with NFATc1 and NFATc2 the major players. Except NFATc5, the other four members are regulated by intracellular calcium levels. Calcium influx activates calcineurin, which dephosphorylates NFAT, leading to its nuclear translocation [77].

NFATc2 accounts for 80-90% of NFAT in resting T cells, and rapidly translocates to the nucleus following activation, thus playing an essential role in regulating an early stage response [78]. NFATc1 expression is induced following T cell activation, therefore regulating a later stage of *IL-2* gene transcription. *IL-2* gene expression was minimally altered in mice deficient in either NFATc1 [79] or NFATc2 [80], while severely impaired in mice deficient in both [81].

b. AP-1

AP-1 is a dimer of two basic region-leucine zipper proteins (bZIP), typically composed of Fos and Jun family proteins. c-Fos and c-Jun are the major components to

form AP-1 in the context of regulating *IL-2* gene [74]. c-Jun is the most potent transcriptional activator in the Jun family, and like other Jun proteins, can form both homo- and hetero- dimers. The Fos protein cannot homodimerize; they instead form heterodimers with Jun proteins and thereby enhance their DNA binding affinity [82]. Both c-Fos and c-Jun contain transactivation potency after stimulation, and Fos-Jun heterodimers are more effective at DNA binding and transcriptional activation than Jun-Jun homodimers [76].

Signaling from TCR and CD28 activates JNK through both PKC and Rac mediated pathways [74]. JNK translocates to the nucleus and phosphorylates c-Jun at N-terminal transactivation domain and results in a robust induction of c-Jun transactivation activity [83]. In addition to post-translational regulation, c-Jun activity is also regulated at the expression level. The promoter region of both c-Jun and c-Fos contain AP-1 binding sites, and are therefore regulated by AP-1 itself as a feed-forward mechanism [83]. The expression level of c-Fos is very low in naive T cells and T cell activation requires its *de novo* synthesis [84]. Signaling from TCR activates the Ras-Raf-ERK pathway and leads to the nuclear translocation of ERK to phosphorylate transcription factors, such as Elk1, to initiate the transcription of c-Fos [82].

AP-1 tends to cooperate with other transcription factors, such as NFAT, NFκB and Oct-1, to enhance their DNA binding affinity [46, 72]. Overexpression of Fos and Jun family protein augments NFAT-driven transcription [76], and a dominant -negative mutant of c-Jun inhibits NFAT transcriptional activity and prevents *IL-2* gene transcription [85].

c. NFκB

The *IL-2* promoter contains two NFκB binding sites, with one located in the CD28RE, which is responsible for the responsiveness of *IL-2* gene to CD28 costimulation signal [74]. NFκB is the major target of CD28 signaling to activate *IL-2* transcription.

NFκB family is composed of two groups of proteins, NFκB proteins NFκB1 (p50) and NFκB2 (p52), and Rel proteins RelA (p65), RelB and c-Rel. NFκB1 and NFκB2 are synthesized as precursor proteins p105 and p100, respectively, and processed to yield mature proteins. The mature NFκB proteins contain Rel homology region (RHR), which is responsible for dimerization, DNA binding and interaction with inhibitors of κB (IκB), and also contains a nuclear localization signal (NLS) [86]. In addition to RHR, Rel proteins also contain transcriptional activation domains. Members of the two groups of proteins can form homo- or hetero-dimers as functional NFκB transcription factors [87]. p50-p50 and p52-p52 homo-dimers that lack transcriptional activation domains appear to repress transcription [86].

In the resting state, NFκB dimers are sequestered by IκB proteins in the cytoplasm. Nuclear translocation of NFκB requires liberation from IκB, which depends on degradation of IκB by the proteasome [86]. Phosphorylation of IκB by the IκB kinase (IKK) complex marks it for ubiquitination. IKK is a multi-subunit complex with three core components, an adaptor protein IKKγ (NEMO), and a dimer of catalytic subunits IKKα/β [88]. Signaling from both TCR and CD28 merges to activate PKCθ, which directly phosphorylates Carma1, resulting in recruitment of Bcl10 and Malt1 to the

plasma membrane [89–91]. Carma1, Bcl10 and Malt1, often referred to as the CBM complex, mediate the activation of IKK complex through a mechanism that has not been fully understood [92], which at least involves ubiquitination of IKKγ [93] and phosphorylation of the catalytic subunit IKKβ [90, 91].

Besides the canonical IκB inhibitory mechanism, a non-canonical pathway depends on IKKα–mediated phosphorylation and processing of p100 associated with RelB, generating mature p52/RelB complex that is able to translocate to the nucleus [95]. T cell activation mainly depends on the canonical pathway, with p50, RelA and c-Rel demonstrated targets of TCR or CD28 signaling [88]. Independent of IκB activity, phosphorylation of RelA is also important for its transcriptional activity, partially due to increased association with co-activators such as CREB binding protein (CBP)/p300 [96]. Activated NFκB is generally composed of p50-p65 and p50-c-Rel. p65 probably mediates early time points of *IL-2* gene transcription, and c-Rel contributes to later. c-Rel may be the major NFκB component mediating activation of the CD28RE [97].

d. Oct

The *IL-2* promoter contains two binding sites for Oct family proteins, and both sites contribute to *IL-2* promoter activity [98]. The proximal Oct binding site is a composite element, to which Oct and AP-1 bind cooperatively [99]. Oct-1 is constitutively expressed, while Oct-2 is lymphocyte specific and its expression is induced by stimulation. The Jurkat T cell line was reported to lack Oct-2 protein but completely capable of *IL-2* gene transcription [98].

e. CREB/CREM

The cAMP response element-binding protein (CREB) family consists of CREB, the cAMP response element modulator (CREM) and the activating transcription factor-1 (ATF-1) [96, 97]. CREB family proteins bind to DNA as a dimer through the cAMP-response element (CRE) [100]. *IL-2* gene contains a CRE site at -180 region and mutation of this site almost completely abolishes *IL-2* transcription [102]. T cells from transgenic mice expressing a dominant-negative form of CREB have a remarkable defect in proliferation and IL-2 production following activation [103].

Although sharing a high level of sequence homology with CREB, CREM either forms a homodimer or heterodimer with CREB and functions as a transcriptional repressor [104]. Increased expression of CREMα protein is proposed as the central cause of decreased IL-2 production in systemic lupus erythematosus (SLE) T cells [105]. Antisense CREM enhanced the accessibility of the *IL-2* promoter to endonucleases and prevents the condensation of chromatin [106]. CREB transcriptional activity depends on phosphorylation of serine 133. Once phosphorylated, pCREB associates with its co-activator, CBP, or its paralogue p300, to initiate transcription of target genes [100]. Later, pCREB is dephosphorylated, and CREM is produced and gradually replaces CREB to bind to the CRE site, resulting in downregulation of *IL-2* gene [107].

f. Sp1/Egr-1

An overlapping binding site for two zinc finger transcription factors, Sp1 and the early growth response protein-1 (Egr-1) is located immediately upstream of the distal NFAT/AP-1 binding site within the minimal *IL-2* promoter [108]. In resting cells, only the constitutively expressed Sp1 protein binds to this region, whereas upon stimulation

the inducible protein Egr-1 replaces Sp1 and regulates *IL-2* transcription via synergistic interaction with NFATc1 [109]. NGFI-A-binding protein 2 (NAB2) is recruited by Egr-1 to *IL-2* promoter and acts as a co-activator of T cell function by promoting Egr-1-mediated *IL-2* production [110].

g. GABP

The Ets family transcription factor GA binding protein (GABP) is a heterodimer of GABP α and β that binds to a distal enhancer of the *IL-2* gene upstream of the 300bp minimal promoter region [111]. GABP contributes to *IL-2* transcriptional activation through the ERK and JNK/SAPK pathways [111].

h. Transcriptional Repressors

Besides CREMα mentioned above, several other transcriptional repressors have been identified that contribute to restriction of IL-2 production and induction of T cell anergy.

The zinc finger E-box-binding protein (ZEB) 1 binds to the negative regulatory element NRE-A located at -100 upstream from the TSS [112]. ZEB1 recruits C-terminal-binding protein (CtBP) 2 and histone deacetylase 1 (HDAC1) to repress *IL-2* gene expression [113]. ZEB1 mediated transcriptional repression has been shown to contribute to the *IL-2* gene silencing in activated Th2 cells [114].

The *IL-2* promoter has two consensus binding sites for Ikaros, a component of the nucleosome remodeling and DNA methylation complex (NURD) [115]. Ikaros has been shown to repress *IL-2* gene expression in $CD4^+$ T cells through recruiting chromatin remodeling complexes [115] and therefore is required for anergy induction in $CD4^+$ T cells [111, 112].

NFκB p50-p50 homodimers lack transactivation domains and act as transcriptional repressors [86]. In tolerant $CD4^+$ T cells that do not produce IL-2, the intracellular level of p50 protein is increased [117] and predominant p50-p50 homodimers bind to the NFκB binding site of the IL-2 promoter instead of p50-p65 [118].

i. Epigenetic Modification and Chromatin Remodeling

Epigenetic modifications of the IL-2 promoter region regulate the accessibility of the DNA to transcription factors and serve as a memory of the regulatory event [119]. Anti-CD3/CD28 stimulation of human $CD4^+$ T cells induces active demethylation of a specific CpG site in the NFAT/Oct-1 binding element, and this modification is required for transcription factors binding to DNA and subsequent histone modification [119]. Upstream of the 300bp minimal enhancer, additional CpG methylation sites are also demethylated [120]. CpG demethylation seems to be stable once initiated, and therefore acts as an epigenetic memory to contribute to a more rapid response upon re-activation [115, 116].

Chromatin structure at the *IL-2* promoter region is also dynamically remodeled to become more accessible upon activation. The human *IL-2* promoter can assemble a positioned nucleosome that occludes the binding of transcription factors to functional elements in resting state. The region becomes remodeled upon activation in Jurkat T cells [121]. Costimulation through both TCR and CD28 leads to histone acetylation and loss of cytosine methylation at the *IL-2* promoter, accompanied by extensive remodeling of the chromatin [122].

j. Post-transcriptional Regulation

IL-2 mRNA level is not only regulated at the level of transcriptional initiation, but also mRNA stability. *IL-2* mRNA contains several AU-rich (AUUUA) elements (AREs) in its 3' untranslated region (UTR), which is known as a common indicator of mRNA instability [123]. After stimulation with anti-CD3/CD28 antibodies, the relatively short half-life of *IL-2* mRNA is significantly prolonged [124]. TCR and CD28 costimulation mediated regulation of mRNA stability requires the 3' [125] and 5' -UTR [126] as well as sequences within the coding region [127].

ARE directed mRNA decay can be positively or negatively regulated in response to extracellular stimuli. NF90 is an RNA binding protein that recognizes and binds AREs in 3'-UTR region and therefore decelerates *IL-2* mRNA degradation [125]. NF90 localizes in the nucleus in resting Jurkat cells, and translocates to the cytoplasm in response to stimulation where it binds to mRNA [125]. Nuclear export of NF90, mediated by Akt-dependent phosphorylation in response to CD28 costimulation, is required for *IL-2* mRNA stabilization [121, 124].

Another signaling pathway that contributes to *IL-2* mRNA stabilization is the JNK pathway [126], which functions through a JNK response element (JRE) in the 5'-UTR that binds to two RNA binding proteins, nucleolin and YB-1 [129]. CD28 signaling also acts through sequences within the coding region of exon 2 and exon 4 to stabilize the *IL-2* mRNA [127]. In contrast, CD28 signaling, at later times, enhances IL-2 mRNA decay through sequences localized between exon 3 and the stop codon [127], ensuring a tightly regulated response.

C. Diseases Related to Abnormal Activation of T Cells

Autoimmunity is a loss of tolerance to multiple self-antigens. SLE is an autoimmune disease characterized as autoantibody production and inflammatory cell infiltration into target organs [130]. T cells play a critical role in the pathogenesis of SLE as they regulate and assist autoreactive B cells. T cells from SLE patients resemble naive or anergic T cells in certain ways, but at same time carry characteristics reminiscent of activated T cells [130]. In SLE T cells, the TCR ζ chain is replaced by the Fc receptor (FcR) γ chain, which recruits spleen tyrosine kinase (Syk) instead of ZAP-70 [131]. Syk is a more efficient signal transducer and results in a hyper-phosphorylation of downstream signaling molecules [132] and increased calcium influx [133]. Increased calcium influx leads to abnormally high NFAT dephosphorylation, which accounts for enhanced transcription of multiple target genes such as CD40L (CD154). The interaction of CD40L on the surface of T cells and CD40 on B cells activates B cells and facilitates autoantibody production in SLE [131]. However, SLE T cells have a reduced ability to produce IL-2, despite the increased NFAT activity [130]. Several key transcription factors that regulate *IL-2* expression have decreased expression levels in SLE T cells, including Rel-A [134], c-Fos [135] and CREB [136], while the transcription repressor, CREMα, has increased activity [106]. Impaired IL-2 production is responsible for decreased activation-induced cell death and extensive survival of autoreactive lymphocytes [137], as well as reduced Treg cell function [138].

Treg cells are essential for the maintenance of self-tolerance and immune homeostasis, and therefore play a protective role in autoimmune diseases. Defects in Treg numbers and function have been shown in human autoimmunity and a restoration in

model systems can prevent and reverse disease [139]. Another subset of T helper cells, Th17 cells, and their effector molecules, actively participate in the pathogenesis of multiple autoimmune diseases, such as SLE and rheumatoid arthritis (RA) [140].

Allergic diseases are characterized as a hypersensitive response toward an innocuous antigen, which comprise two main components of the immune response: an abnormal polarization of naive Th0 cells to differentiate into Th2 phenotype and class switching to IgE in B lymphocytes [31]. T cell activation and cytokine secretion are essential mediators in allergy. A preferential skewing to expansion of the Th2 lymphocytes is the crucial forerunner to the pathogenesis of allergic diseases [141]. Excessive Th2 cytokine expression and a reduced production of Th1 cytokine IFNγ is noted in atopic disease [141]. Therefore, preventing or reversing the process of abnormal Th2 polarization has been a focus for the development of new therapeutic strategies to control allergies and asthma [141]. Recently, IL17-producing Th17 cells have been shown to play a role in driving cytokine production, neutrophil recruitment and airway hyperresponsiveness in steroid-resistant asthma [142]. The cytokine IL-17 family has increased levels in asthma and COPD and promotes airway neutrophilia and allergic responses [142]. In contrast, Tregs have shown reductions in numbers and capacity to suppress effector T cells and Th2 cytokine production in asthma [143], implicating their role in modulation and suppression of allergic airway responses.

D. Inhibitors of T cell Activation and Their Therapeutic Uses

Inhibitors of T cell activation are commonly used as immunosuppressants in transplantation, autoimmune diseases, and allergic asthma. Glucocorticoids (GCs) are the

first immunosuppressants used in transplantation [144]. By binding to GC receptors, GCs inhibit AP-1 and NFκB pathways, thus blocking IL-2 production in T cells [144]. Although very potent, they are the least selective inhibitors that affect lymphocytes as well as non-lymphoid cells, therefore causing severe side effects [145].

The most well characterized inhibitors specific for T cell activation are cyclosporin A (CsA) and tarolimus (FK506). They bind to specific immunophilins in T cells and the drug-immunophilin complexes block activation of the calcium calmodulin-dependent serine/threonine phosphatase calcineurin, thus inhibiting NFAT regulated *IL-2* expression [146]. These two drugs have been very useful working either alone, or in combination with GCs for lowering GC doses and reducing side effects [144]. CsA is also commonly used in research for its ability to inhibit IL-2 production and T cell activation.

Another group of T cell inhibitors target the mammalian target of rapamycin (mTOR), such as rapamycin (or sirolimus) and everolimus [144]. mTOR is a serine/threonine protein kinase that acts downstream of IL-2 receptor engagement to regulate mRNA translation [147]. These inhibitors exert anti-inflammatory effects by blocking IL-2 post-receptor signaling and subsequently inhibiting T cell proliferation [136, 140, 141]. mTOR inhibitors and calcineurin inhibitors are currently used in combination to prevent transplant rejection [150].

Other inhibitors targeting various surface and intracellular signaling molecules in T cells are under investigation for their potential use in transplantation and anti-inflammation. For example, R788, a specific Syk inhibitor, ameliorated both skin and kidney symptoms in lupus prone mice [151]. AEB071, an early-T cell activation inhibitor

selectively targeting PKC, showed promising potential for immunosuppression in organ transplantation [150].

V. B lymphocytes

A. B cell development and function

B cells develop from HSC in bone marrow [31]. The process of B cell development requires the specific environment provided by bone marrow stromal cells [31]. The lineage commitment is largely regulated by a combination of transcription factors and signaling pathways [152]. Specifically, Ikaros controls the development of common lymphoid progenitors (CLP) and Pax5 is crucial in both activating B cell specific genes and repressing lineage inappropriate genes [152]. The early developmental stages can be divided into Pro, Pre, Immature and Mature B cells, with the first three stages occur in bone marrow (Figure 6) [31]. Each stage is marked by the rearrangement and expression of immunoglobulin (Ig) genes to make functional B cell receptors (BCR) or their surrogates. Signal transduction by BCR or their surrogate is critical for progression through multiple developmental checkpoints [153]. Ordered Ig gene rearrangement ensures that each immature B cell bears antigen receptors of a single specificity and generates a diverse repertoire of B-cell receptors for antigen recognition [152]. Immature B cells, characterized by the expression of membrane IgM, migrate to the periphery where they undergo further maturation into naive mature B cells [153].

Once encountering antigen in the periphery, naive B cells proliferate and differentiate into antibody secreting plasma cells. Binding of an antigen causes BCR to crosslink, triggering signal transduction pathways that result in changed gene expression

in the nucleus [154]. As a result, B cells enter the cell cycle, migrate to primary lymphoid follicles and ultimately form a germinal center [31]. Some germinal center B cells differentiate into plasmablasts and then into plasma cells, which are responsible for long-lasting antibody secretion. Others differentiate into memory B cells that provide a rapid response when the host reencounters the same antigen [31].

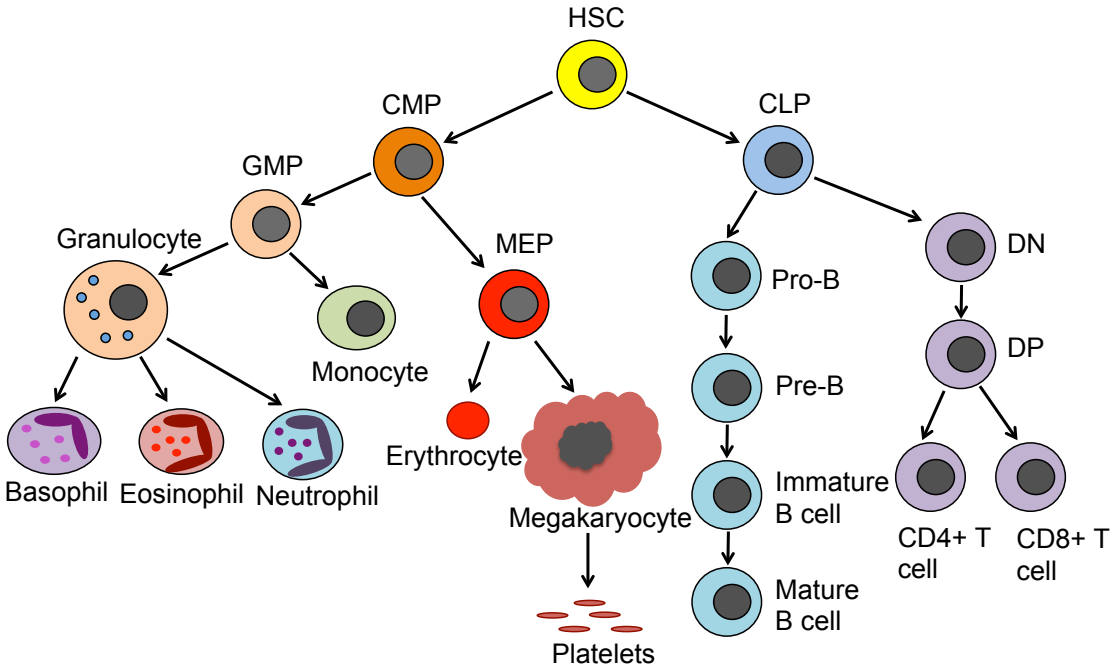

Figure 6. Hematopoiesis. HSC: Hematopoietic stem cell; CLP: common lymphoid progenitor; CMP: common myeloid progenitor; GMP: granulocyte-monocyte progenitor; MEP: megakaryocyte–erythroid progenitor; DN: double negative; DP: double positive.

B. Diffuse large B-cell lymphoma and OCI-LY18

Diffuse large B-cell lymphoma (DLBCL) is the most common type of Non-Hodgkin's lymphoma (NHL) in adults, accounting for approximately 40% of NHL [155]. DLBCL is a heterogeneous mature B-cell malignancy. Gene expression profiling has identified two molecularly distinct forms of DLBCL, one germinal center B-like DLBCL

and the other activated B-like DLBCL [149, 150]. Approximately 30-40% of DLBCL carry *BCL-6* gene rearrangements, resulting in deregulation of the cell cycle and enhanced proliferation; about 20% carry *BCL-2* gene rearrangements, resulting in inhibition of apoptosis [151, 152]

OCI-LY18 (Ontario Cancer Institute-LY18) is a germinal center B-like DLBCL cell line. It was established from the pleural fluid of a 56-year-old male patient, who was diagnosed with a high grade NHL of diffuse large cell immunoblastic type in 1988 [159]. LY18 cells carry chromosome translocations involving bands 8q24, 14q32 and 18q21, which leads to a rearrangement of the *MYC* gene [159] and also carry *p53* and *BCL-2* gene rearrangements [160]. My study uses LY18 cells as a model system for mature B cell malignancy.

VI. Monocytes

A. Monocyte development and function

In addition to common lymphoid progenitors, pluripotent HSC also give rise to common myeloid progenitors (CMP). CMP further develop into granulocyte-monocyte progenitors (GMP) in bone marrow, which in turn give rise to neutrophils, eosinophils, basophils and monocytes (Figure 6) [31]. Differentiation is governed by transcriptional regulation of lineage specific genes. Specifically, PU.1 and CCAAT/enhancer-binding proteins (C/EBPs) regulate the progression of HSC to CMP, then further to the GMP branch, respectively [161]. Increased PU.1 activity further directs GMP to commit to the monocytic lineage [161].

Monocytes are a heterogeneous population of cells with subgroups that differ in size, surface marker expression and function [162]. Human monocytes are divided into two subsets based on the expression of surface markers CD14 and CD16 (FcγR III) [155, 156]. $CD14^{++}CD16^{-}$ monocytes are the most prevalent monocyte subset, constituting approximately 90% of total monocytes in human and are therefore referred to as classical monocytes [155, 157]. Classical monocytes express the CC-chemokine Receptor 2 (CCR2), which plays a key role in mediating monocyte migration from bone marrow into the circulation in response to infection or inflammation [163]. $CD16^{+}$ monocytes are smaller in size and less prevalent. They increase in frequency during infections and are also referred to as proinflammatory monocytes [164].

Monocytes have an essential role in innate immune defense against diverse pathogens, including bacteria, parasites, fungi and viruses, and also contribute to the adaptive immune response [164]. At the site of infection, monocytes mature into macrophages or inflammatory dendritic cells [157, 158]. Macrophages contribute to pathogen elimination mainly by phagocytosis. Macrophages and dendritic cells also function by antigen presentation and therefore help activate T cells [164].

B. U937 cells

The U937 cell line was established from a 37-year-old male patient with histiocytic lymphoma in 1976 [166]. The cell line was identified as having a histiocytic origin by its capacity for lysozyme production and strong esterase activity [166]. The U937 cell line is one of the few established human cell lines exhibiting monocytic characteristics [167]. They can be induced to mature macrophage-like cells in culture

[160, 161]; therefore commonly used the as a model for differentiation of monocytes and macrophages *in vitro*. My study uses U937 cell line as a model system for monocytic malignancy.

MATERIAL AND METHODS

Antibodies and Reagents

Anti-human IL-2 and anti-goat IgG- horseradish peroxidase (HRP) antibodies were obtained from R&D systems (Minneapolis, MN). Anti-β-actin antibody was obtained from Sigma-Aldrich (St. Louis, MO). Anti-mouse Ig-G was obtained from Jackson ImmunoResearch (West Grove, PA). Anti-human CD3 antibody was from eBioscience (San Diego, CA). Anti-human CD28 and anti-human caspase 8 antibodies were purchased from BD Biosciences (San Jose, CA). Anti-mouse IgG-HRP and anti-rabbit Ig-G-HRP were purchased from Santa Cruz Biotechnology (Santa Cruz, CA). Anti-Rel-A antibody was from EMD Millipore (Billerica, MA) and all other antibodies were from Cell Signaling (Danvers, MA). APO-BRDU^{TM} Kit, FITC-BrdU Flow Kit, FITC-conjugated anti-active caspase 3 monoclonal antibody, Fc Block, and BD Cytofix/Cytoperm^{TM} Kit were all obtained from BD Biosciences. Immobilon-P membrane was obtained from EMD Millipore. ECL reagents were obtained from Kirkegaard and Perry Laboratories (Gaitherburg, MD). Lympholyte M was purchased from Accurate Chemical and Scientific (Westbury, NY). Protein Transport Inhibitor (Containing Monensin) was purchased from BD Biosciences. Cyclosporin A *Tolypocladium inflatum* was obtained from Calbiochem, EMD Millipore. Primers, NFAT and AP-1 binding sites of the human IL-2 promoter were synthesized by Integrated DNA Technologies (Coralville, Iowa). NFAT, NFκB and Oct-1 consensus oligonucleotides were purchased from Santa Cruz Biotechnology. RETROscript Kit, TURBO DNase-free Kit, RNaseZap wipe and spray were from Life Technologies (Grand Island, NY).

RealMasterMix SYBR ROX was purchased from 5 Prime (Gaithersburg, MD). RPMI 1640 was purchased from Cellgro, Corning (Manassas, VA). T4 polynucleotide kinase was obtained from New England Biolabs (Ipswich, MA). [γ-^{32}P] ATP was obtained from Perkin Elmer (Waltham, MA). All other chemicals were obtained from Sigma-Aldrich.

T Lymphocyte Isolation, Cell Culture and Stimulation

BALB/cJ mice were obtained from The Jackson Laboratory (Bar Harbor, ME) and housed at Boston College. Mice were cared for and handled at all times in accordance with National Institutes of Health and Boston College guidelines. Mouse T lymphocytes were isolated from mouse spleen by sedimentation on Lympholyte M followed by negative selection using Mouse Pan T cell Isolation Kit II (Miltenyi Biotec, Auburn, CA) according to the manufacturer's protocols. Peripheral venous blood was obtained from healthy volunteers for each study and peripheral blood mononuclear cells (PBMCs) were isolated using Ficoll-Paque according to the Miltenyi online protocol. Total human primary T cells or $CD4^+$ T cells were further separated by negative selection using Human Pan T Cell Isolation Kit II or Human $CD4^+$ T Cell Isolation Kit II (Miltenyi Biotec, Auburn, CA) according to the manufacturer's protocol. The Jurkat cell line (E6-1) was kindly provided by Dr. Charles Hoffman (Boston College, MA). The OCI-LY18 (LY18) cell line was kindly provided by Dr. Raju Chaganti (Memorial Sloan-Kettering Cancer Center, New York, NY). The U937 cell line was obtained from American Type Culture Collection (Manassas, VA). Jurkat cells, LY18 cells, U937 cells and mouse primary T cells were cultured in RPMI 1640 (Atlanta Biologicals, Norcross, GA) supplemented with 10 mM HEPES (pH 7.5), 2 mM L-glutamine, 50 μM 2-

mercaptoethanol, 100 U/ml penicillin, 100 μg/ml streptomycin, and 10% heat-inactivated fetal bovine serum (FBS) (Atlanta Biologicals, Norcross, GA) at a density of 5×10^5-1×10^6 cells/ml. Human T lymphocytes were cultured in RPMI 1640 with 2% heat-inactivated human AB serum and all the supplements listed above except FBS at a density of 1×10^6 cells/ml. Cells were maintained in a 37 ^oC humidified incubator at 5% CO_2 at 95% humidity. T cells were stimulated by the combination of 0.5 μg/ml phytohaemagglutanin (PHA) and 50 ng/ml phorbol myristate acetate (PMA), or 20 ng/ml PMA and 1 μM Ionomycin. For antibody stimulation of human primary T cells, 10 μg/ml anti-mouse antibody diluted in PBS was coated on 96-well flat-button plate by incubating at 37 ^oC for one hour. The plate was washed twice with PBS, followed by incubating 1 μg/ml anti-CD3 antibody for another hour at 37 ^oC and washing with PBS. Human primary T cells (0.2×10^6) were plated in 0.2 ml media as stated above with 1 μg/ml anti-CD28 antibody supplemented in solution.

Enzyme-Linked Immunosorbent Assay (ELISA)

To measure the concentration of IL-2 or other cytokines secreted by cells, Jurkat cells or primary T cell from human or mouse were cultured in 96-well plate at 1×10^6 /ml with each treatment condition in duplicates. At the end of treatment, the plate was centrifuged at 300 ×g for 3 minutes at 4 ^oC. Supernatants were collected and subjected to ELISA according to the manufacturer's instruction provided by Quantikine Human IL-2 kit from R&D Systems (Minneapolis, MN) or by Human Th1/Th2/Th17 Cytokines Multi-Analyte ELISArray kit from SABiosciences (Qiagen, Valencia, CA).

Nuclear Extraction for Western Blotting

Jurkat cells (5×10^6) or mouse primary T cells (1×10^7) were washed with PBS and incubated on ice for 10 minutes in 150 μl hypotonic buffer (20 mM HEPES and 3 mM $MgCl_2$) supplemented with freshly added 2 mM DTT, 1 mM PMSF, and protease inhibitor cocktail. At the end of the incubation, Nonidet P-40 was added to the mixture at a concentration of 0.06%. The mixture was gently vortexed for 5 seconds and subjected to centrifugation for 3 minutes at 300 × g at 4 ^oC. The supernatant was collected and saved as raw cytosolic fraction. The pellet was washed with ice-cold PBS and centrifuged for 3 minutes at 300 × g. After carefully removing all supernatant, the pellet was resuspended in 50 μl of RIPA buffer (20 mM Tris-HCl (pH 7.5), 150 mM NaCl, 1% Nonidet P-40, 1% sodium deoxycholate, and 0.1% SDS) supplemeted with freshly added 2 mM DTT, 10 mM PMSF, and protease inhibitor cocktail, sonicated for 5 seconds and incubated on ice for 20 minutes. After centrifugation at 16,000 × g at 4 ^oC for 10 minutes, the supernatant was saved as nuclear fraction. The raw cytosolic fraction was further centrifuged at 16,000 × g at 4 ^oC for 10 minutes, and the supernatant was saved as cytosolic fraction.

Whole Cell Extraction for Western Blotting

Jurkat cells (4×10^6) or mouse primary T cells (1×10^7) were washed with PBS and centrifuged at 626 × g at 4 ^oC for 8 minutes. The pellet was lysed on ice for 20 minutes in 50 μl cyclin lysis buffer (50 mM Tris-HCl (pH 7.4), 150 mM NaCl, 20 mM EDTA (pH 8), and 0.5% Tween-20) supplemented with freshly added 1 mM DTT, 1 mM PMSF, 1 mM Okadaic acid, 1 mM Na_3VO_4, 10 mM β-glycerophosphate, and 10 mM

NaF. The mixture was subjected to centrifugation at 16,000 × g at 4 °C for 20 minutes, and the supernatant was collected and saved as whole cell extract at -80 °C.

Western Blotting

Nuclear extracts or whole cell extracts were obtained from Jurkat cells or primary T cells. Lysate protein was separated by electrophoresis through a 15% polyacrylamide SDS-gel (SDS-PAGE) for IL-2 detection or 8% or 10% for other proteins and transferred to Immobilon-P membrane. The membrane was blocked in TBS-T (20 mM Tris (pH 7.6), 137 mM NaCl, and 0.05% Tween-20) containing 5% nonfat dry milk for 1 hour and incubated overnight at 4 °C with primary antibody in TBS-T, washed and then incubated with a 1:2500 dilution of secondary IgG-coupled horseradish peroxidase antibody for 1 hour and developed by enhanced chemiluminescence (ECL). Autoradiograms were scanned with Adobe Photoshop 7.0 (Adobe Systems, Inc., San Jose, CA) and the mean density of each band was analyzed by the ImageJ program (NIH, Bethesda, MD).

Reverse Transcription and Real-Time PCR

Jurkat cells (6×10^6) or human primary T cells (1×10^7) were used for each treatment. Cells were centrifuged at 626 × g for 8 minutes at 4 °C and cell pellets were washed with PBS. RNA extraction was done following the protocol provided by Qiagen RNeasy mini kit (Hilden, Germany). The working area was RNase free after RNaseZap treatment. RNA was treated with DNase I at 37 °C for 30 minutes to digest remaining DNA. The concentration of RNA was determined by measuring the absorbance at 260 nm in a spectrophotometer. The purity of RNA was estimated by the ratio of the readings

at 260 nm and 280 nm. At each reverse transcription reaction, 2 μg of RNA was used to generate cDNA using RETROscript Kit according to the manufacturer's instruction. Real-time PCR was performed using the RealMasterMix SYBR ROX on a Mastercycler ep realplex^2 real-time PCR instrument (Eppendorf, Germany). Amplification conditions were as follows: 95 ^{o}C 3 minutes, followed by 40 cycles of 95 ^{o}C 15 seconds, 60 ^{o}C 90 seconds, 72 ^{o}C 15 seconds. For mRNA stability assay, Jurkat cells were stimulated with PHA and PMA for 4 hours before adding 1 μg/ml Cyclosporin A to inhibit *IL-2* transcription. Total RNA was isolated at each time point and reverse transcribed to cDNA. The level of *IL-2* mRNA was determined by real-time PCR following normalization to a house-keeping gene, *β-actin*, with *IL-2* mRNA levels in media cells as the calibrator. Primers were obtained from literature [169].

IL-2 primers: forward: 5'- GAATGGAATTAATAATTACAAGAATCC-3';

reverse: 5'-GACACTGAAGATGTTTCAGTTCTGT-3'.

β-actin primers: forward: 5'-TCACCCACACTGTGCCCATCTACGA-3';

reverse: 5'-CAGCGGAACCGCTCATTGCCAATGG-3'.

Viability Assay and Cell Cycle Analysis

For viability assays, propidium iodide stock solution was diluted at 1 μg/ml in PBS. Approximately 1×10^5 cells were directly added to 500 μl propidium iodide staining solution. Cells were kept on ice protected from light until analysis by flow cytometry. For cell cycle analysis, 0.5 to 1×10^6 cells were washed twice with ice-cold PBS, resuspended in 0.5 ml staining solution (PBS containing 0.1% Triton X-100, 100 μg/ml RNase IIIA and 50 μg/ml propidium iodide) and incubated at 37 ^{o}C for 30 minutes

in dark. DNA content was measured by flow cytometry using a FACSCanto cytometer and BDFACS Diva software (BD Biosciences, San Jose, CA).

BrdU Incorporation

BrdU was added to U937 cell culture at a final concentration of 20 μM for 24 hours before cells were collected. For each condition, 2×10^6 cells were collected and washed with PBS. FITC-BrdU labeling was performed according to the manufacturer's instruction (BD Biosciences) and DNA synthesis was measured by flow cytometry using a FACSCanto cytometer and BDFACS Diva software (BD Biosciences, San Jose, CA).

Terminal Deoxynucleotidyltransferase dUTP Nick End Labeling (TUNEL) Assay

At each time point, LY18 or U937 cells (1×10^6) were collected, washed with PBS, fixed and permeabilized using BD Cytofix/Cytoperm™ Kit following manufacturer's instruction (BD Biosciences). Samples were stored at 4 °C until ready to be labeled. TUNEL assays were performed using APO-BrdU™ kit following manufacturer's instruction (BD Biosciences). Apoptotic cells were labeled with FITC-conjugated anti-BrdU antibody. Samples were analyzed by flow cytometry using a FACSCanto cytometer and BDFACS Diva software.

Caspase 3 Staining by Flow Cytometry

At each time point, LY18 or U937 cells (1×10^6) were collected, washed with PBS, fixed and permeabilized using BD Cytofix/Cytoperm™ Kit following manufacturer's instruction (BD Biosciences). Samples were stored at 4 °C until ready to

be labeled. For caspase 3 labeling, cells were resuspended in 100 µl Perm/Wash solution (BD Cytofix/Cytoperm^{TM} Kit) plus 2 µl Fc block and incubated at 4 ^{o}C for 20 minutes. After washing with 100 µl Perm/Wash, cells were resuspended in 100 µl Perm/Wash plus 20 µl FITC-conjugated anti-active caspase 3 antibody and incubated at 4 ^{o}C for 1 hour. Cells were then washed once with Perm/Wash, resuspended in 500 µl Perm/Wash solution and analyzed by flow cytometry.

Nuclear Extraction and Electrophoretic Mobility-Shift Assay (EMSA)

Jurkat cells (1×10^7) were washed with PBS and incubated on ice for 10 minutes in 5 ml Hypotonic Buffer (20 mM HEPES and 3 mM $MgCl_2$) supplemented with freshly added 2 mM DTT, 1 mM PMSF, and protease inhibitor cocktail. The mixture was subjected to centrifugation at 626 × g for 8 minutes. The supernatant was saved as cytoplasmic fraction. The pellet was resuspended in 50 µl of High Salt Buffer C (30 mM HEPES, 25% glycerol, 450 mM NaCl, 0.3 mM EDTA and 12 mM $MgCl_2$) supplemented with 6 mM DTT, 1 mM PMSF and protease inhibitor cocktail, and incubated on ice for 30 minutes. After centrifugation for 10 minutes at 16,000 × g, the supernatant was collected and diluted with an equal volume of Buffer D (30 mM HEPES, 25% glycerol, 0.3 mM EDTA and 12 mM $MgCl_2$) with the same supplements as buffer C. All nuclear extracts were diluted to 2 mg/ml with the 1:1 mixture of buffer C and D and stored at -80^{o}C. The DNA probes were radiolabeled with [γ-^{32}P] ATP by T4 polynucleotide kinase. 5 µl of nuclear extracts were incubated with 3 µl radiolabeled dsDNA probe (10,000cpm), 1 µg of poly (dI/dC) and 6 µl of dH_2O to a total volume of 15 µl for 20 minutes at room temperature. The reaction mixture was then subjected to separation in

6% nondenaturing gel. The dried gel was autoradiographed over night at -80 ^{o}C. For supershift assays, the nuclear proteins were incubated with 4 μg specific antibodies at 4 ^{o}C for 10 minutes before the probe, poly (dI/dC) and dH_2O were added. The reactions were further conducted for another 20 minutes at room temperature. The sequences of distal NFAT binding site of the human IL-2 promoter [170] and AP-1 binding site of the human IL-2 promoter [171] were obtained from literature. The sequences of the probes used were:

Distal NFAT binding site of the human IL-2 promoter:

5’-GATCGGAGGAAAAACTGTTTCATACAGAAGGCGT-3’;

NFAT consensus oligonucleotide: 5'-CGCCCAAAGAGGAAAATTTGTTTCATA-3'

NFκB consensus oligonucleotide: 5’-AGTTGAGGGGACTTTCCCAGG-3’.

AP-1 binding site of the human IL-2 promoter: 5'- TTCCAAAGAGTCATCAG-3'

Oct-1 consensus oligonucleotide: 5’-TGTCGAATGCAAATCACTAGAA-3’

Chapter One

An *in vitro* PDE7 inhibitor inhibits *IL-2* gene expression in activated T cells by repressing NFκB and NFAT-mediated transcription

RESULTS

BC12 inhibits IL-2 protein production in activated Jurkat cells

The Jurkat T cell line is a common model for studying T cell signaling and IL-2 production [1, 2]. To begin to evaluate the potential immunomodulatory effects of the novel *in vitro* PDE7 inhibitor BC12, we first examined extracellular IL-2 secretion in activated Jurkat cells by ELISA (Figure 1). Jurkat cells were stimulated by a combination of 0.5 μg/ml phytohemagglutinin (PHA) and 50 ng/ml phorbol 12-myristate 13-acetate (PMA). PHA is a plant lectin that binds to cell membrane glycoproteins including TCR-CD3 complex, causing extensive crosslinking of the TCR receptors and triggering signaling [172]. PMA is a structural analog of diacylglycerol, and therefore can stimulate T cells by activating PKC [172]. A combination of PHA and PMA increased IL-2 secretion, whereas the DMSO control had a minimal effect on PHA/PMA induced IL-2 secretion (Figure 1). At 24 hours of treatment, BC12 inhibited IL-2 production to 74% compared to DMSO control at a dose of 1 μM, 15% at 5 μM, and 2% at 10 μM (Figure 1). Cells with the same treatments were analyzed for cell viability by propidium iodide staining and flow cytometry. Compared to cells treated with PHA/PMA/DMSO control, which resulted in 93% of viable cells, BC12 in combination of PHA/PMA moderately reduced cell viability to 85% at 1 μM, 81% at 5 μM, and 65% at 10 μM (Figure 2). Therefore, inhibition on IL-2 production by activated Jurkat cells cannot be attributed to reduced cell viability.

To examine the timing of inhibitory effects on IL-2 production by BC12, Jurkat cells were stimulated by PHA/PMA and/or treated with BC12 simultaneously for various

lengths of time (Figure 3). Following PHA/PMA stimulation, Jurkat cells exhibited a time-dependent secretion of extracellular IL-2 starting from 3-6 hours after stimulation. Treatment with 10 μM of BC12 nearly abolished IL-2 secretion completely from the beginning and the inhibitory effect was maintained over time up to at least 24 hours (Figure 3).

Reduced levels of IL-2 secretion could be due to either decreased endogenous IL-2 protein production or impaired secretion. To examine the endogenous cytokine level, monensin, a Golgi inhibitor was used to block IL-2 secretion in Jurkat cells. Accumulated intracellular IL-2 protein was detected by Western blotting (Figure 4A). As expected, unstimulated or DMSO treated Jurkat cells did not express detectable IL-2. PHA/PMA-stimulated Jurkat cells expressed IL-2 at 12 hours. Incubation with 10 μM of BC12 in addition to PHA/PMA significantly decreased IL-2 expression (Figure 4A). Of note, the effect of monensin to block IL-2 secretion was confirmed by ELISA (Figure 4B). Jurkat cells stimulated by PHA/PMA in the presence of monensin had a significantly lower IL-2 secretion level than in the absence of monensin (Figure 4B).

In summary, we investigated the immunomodulatory effects of BC12 on IL-2 production in activated Jurkat cells and discovered that BC12 inhibited IL-2 protein production in a dose dependent manner. The inhibitory effect started at the beginning of *de novo* protein synthesis and was maintained up to at least 24 hours.

BC12 inhibits IL-2 gene expression in activated Jurkat cells through transcriptional repression

To further evaluate the role of BC12 on IL-2 production, we sought to directly assess relative mRNA levels of *IL-2* in activated Jurkat cells by semi-quantitative reverse transcription PCR (Figure 5). Following PHA/PMA stimulation, *IL-2* mRNA levels started to increase after 1 hour, peaked at approximately 5 hour and then declined. Treatment of Jurkat cells with BC12 simultaneously blocked *IL-2* mRNA expression (Figure 5).

IL-2 mRNA is regulated both at the transcriptional and mRNA degradation levels [123]. Upon stimulation, *IL-2* mRNA is not only upregulated at transcriptional initiation, but also has a prolonged half-life [123]. To further investigate the mechanism of inhibition by BC12 on *IL-2* mRNA level, we performed mRNA stability assays to assess the degradation rate of *IL-2* mRNA (Figure 6). Jurkat cells were stimulated with PHA/PMA for 4 hours to initiate *IL-2* gene transcription. The fold induction of *IL-2* mRNA after 4 hours of stimulation was 1054 compared to unstimulated Jurkat cells. After the initial induction of mRNA expression, cyclosporin A (CsA) was used to inhibit IL-2 transcription [173]. CsA blocks activation of the calcium calmodulin-dependent serine/threonine phosphatase calcineurin, therefore inhibiting NFAT regulated *IL-2* expression [146]. Without CsA, mRNA levels in DMSO treated cells continued to increase for another hour (total 5 hours of stimulation) and then decreased, consistent with the results noted in Figure 5 (Figure 6, DMSO). In the presence of CsA, *IL-2* mRNA levels became a function of degradation rate and time. In the absence of BC12, *IL-2* mRNA levels decreased to about 70% of the starting point after 1 hour, and about 40%

after 2 hours (Figure 6, CsA). Importantly, BC12 did not increase the rate of mRNA turnover beyond that observed for CsA alone (Figure 6, CsA+BC12). Of note, adding BC12 reduced *IL-2* mRNA levels compared to the DMSO control, even when added after *IL-2* mRNA expression has already been induced (Figure 6, BC12).

Taken together, these results indicate that BC12 blocks IL-2 secretion by inhibiting *IL-2* gene transcription, while mRNA degradation rate remains unaffected.

BC12 inhibits IL-2 expressions not through PDE

BC12 was first identified as an *in vitro* PDE7 inhibitor (unpublished data from Hoffman Lab). It has been reported that PDE7A antisense oligonucleotide inhibits cell proliferation and IL-2 production in both Hut78 T cell line and primary $CD4^+$ T lymphocytes [25]. Thus, PDE7 was our original hypothesized *in vivo* target of BC12 in Jurkat cells.

The Hoffman Lab obtained a series of BC12 derivatives that have strong structural similarity to BC12 to study their preliminary structure-activity relationship on PDE7A and 7B (Figure 7). 5-FOA growth assays were performed on *S. pombe* strains expressing human PDE7A or PDE7B enzyme to assess PDE inhibitory capacity of these compounds (Figure 7B and 7C). Compounds with the ability to stimulate 5-FOA resistant growth demonstrate PDE7A or 7B inhibitory activity. BC12 displayed the strongest activity among 7 compounds in both assays (Figure 7B and 7C). BC12-4, which lacks the dimethylamino group at R1 position on A-ring (Figure 7A), is inactive in both assays, demonstrating that this functional group is essential for the PDE7A and 7B inhibitory activity of these compounds. In addition, we also observed that with different substitution

patterns on B-ring (Figure 7A), BC12-1, BC12-2, BC12-5, BC12-6, and BC12-7 are significantly less potent than the parent compound BC12 in both assays, indicating that substitutions on B-ring might not be well tolerated. *In vitro* PDE assays were also performed on the PDE7A catalytic domain (data not shown). BC12 showed the strongest inhibitory capacity among 7 structural analogs with IC_{50} of 0.77 μM. BC12-6 showed similar level of PDE7A inhibitory activity as that of BC12, while BC12-4 did not exhibit measureable PDE7A inhibitory activity when tested at 2 μM (unpublished data from Hoffman Lab).

BC12 and its derivative compounds were then tested for their effects on IL-2 production in activated Jurkat cells (Figure 8A). Among 6 derivative compounds tested, BC12-4, BC12-5, and BC12-7 exhibited similar inhibitory effects on IL-2 production when compared to BC12; BC12-6 showed a minimal effect (Figure 8A). Parallel Jurkat cells were also analyzed for viability (Figure 8B). Many compounds decreased the number of viable cells (BC12-2, BC12-4, BC12-5 and BC12-7). All the others did not reduce the percentage of viable cells to lower than 70% (Figure 8B).

To uncover the correlation between *in vitro* PDE inhibitory activity and IL-2 inhibitory effect, we sought to compare the effects of several key compounds. BC54 is the most potent PDE4 and PDE7 dual inhibitor identified by the Hoffman Lab (personal communication with Dr. Charles Hoffman). BC12 and BC12-6 are the two strongest PDE7 inhibitors among the 7 analogs and BC12-4 has no PDE7 inhibitory activity (Figure 7B and 7C). We compared the effects of BC12, BC12-4, BC12-6 and BC54 on IL-2 secretion in activated Jurkat cells (Figure 9). BC12-4 abolished IL-2 secretion, while BC12-6 and BC54 inhibited IL-2 secretion to about 70%, all at the dose of 10 μM (Figure

9). These results suggest that the inhibitory effects on IL-2 production by BC12 and BC12-4 do not rely on PDE7 inhibitory capacity. Thus, the *in vivo* target of BC12 that leads to IL-2 inhibition is not PDE7.

BC12 augments activation signal towards the AP-1 signaling pathway in T cells

To understand the inhibitory mechanism of BC12 on IL-2 production, we sought to evaluate the activation status of signaling proteins that respond to TCR and CD28 activation and lead to *IL-2* gene transcription. Whole cell extracts were prepared and immunoblotted with antibodies against several signaling proteins. Phosphorylation of signaling proteins was induced by PHA/PMA stimulation for as early as 20 minutes (Figure 10). Phosphorylated Akt was already present in unstimulated cells, which is likely due to deficiency of PTEN in Jurkat cells [174]. Surprisingly, phosphorylation of several signaling proteins was augmented by BC12 treatment in addition to PHA/PMA stimulation, including ERK1/2, MEK1/2, RSK and JNK1/2, all of which are known components of the AP-1 signaling pathway (Figure 10), while the total protein level of ERK2 was not increased by BC12. Of note, BC12 alone did not induce phosphorylation of ERK1/2 or MEK1/2, indicating that BC12 amplifies the activation signal by PHA/PMA but does not initiate it. Although these results do not explain the inhibitory effect of BC12 on IL-2 production, it suggests a possible feedback mechanism that the inhibition of downstream *IL-2* transcription may result in the hyper-activation of upstream AP-1 signaling pathway.

BC12 inhibits IL-2 expression through NFAT and NFκB mediated transcription

To investigate the mechanism of inhibition of BC12 on IL-2 production, we performed microarray analysis of the whole genome expression profile of stimulated Jurkat cells in the presence or absence of BC12. The analysis revealed that 378 genes were found affected by BC12 on PHA/PMA stimulated cells. While most of the genes were inhibited by BC12, including several cytokines and major transcription factors, some were increased in expression levels. Bioinformatic analysis of the microarray data indicated that several pathways were affected by BC12, among which NFκB pathway is related to IL-2 regulation. Interestingly, the expressions of transcription factors c-Fos and c-Jun were increased after BC12 treatment in the presence of stimuli. These results are consistent with our finding that BC12 significantly augments activation of AP-1 signaling pathway by stimuli (Figure 10), which regulates the transcription of both c-Fos and c-Jun [83].

To understand which of these pathways targeted by BC12 may result in inhibition of *IL-2* expression, we analyzed the fold change of target gene expression of five groups of transcription factors: NFATc1/NFATc2, NFκB (p50/p65), c-Fos/FosB, c-Jun/JunB and Oct-1. Of the five major transcription factors known to regulate *IL-2* gene expression, we found that genes regulated by NFκB were most affected by BC12, followed by NFAT regulated genes (Figure 11). Besides *IL-2* gene, several target genes of NFκB had reduced levels of expression, such as *IL-2Rα*, *TNFα* and *TNFβ*. These results suggest that the NFκB pathway, and perhaps NFAT as well, are likely to be inhibited by BC12.

With these results in mind, we sought to examine the protein levels of IκB, which is a key component in the NFκB pathway. In unstimulated T cells, NFκB dimers are sequestered by IκB proteins in cytoplasm. Stimulation induced nuclear translocation of NFκB requires liberation from IκB, which depends on inducible ubiquitination and degradation of IκB [86]. Whole cell extracts were prepared and immunoblotted with anti-IκBα antibody. The protein levels of IκBα decreased in a transient manner when stimulated by PHA/PMA for 20 minutes in comparison to media control; IκBα levels recovered by 90 minutes (Figure 12, IκBα). In contrast to the rapid and transient turnover in stimulated Jurkat cells, BC12 inhibited the degradation of IκBα at 20 and 45 minutes and prevented its recovery at 90 minutes (Figure 12, IκBα). We also evaluated the activation status of IKKα/β, the catalytic dimer that phosphorylates IκB and targets its degradation (Figure 12, p-IKKα/β). The phosphorylation level of IKKα/β was not affected by BC12 at the time points examined. However, the phosphorylation level of IκBα was reduced at 45 and 90 minutes by BC12, even when the total IκBα level was higher in BC12 treated cells (Figure 12, p-IκBα). These results indicate that IκBα degradation is inhibited by BC12, at least partially due to reduced phosphorylation of IκBα. However, upstream kinases IKKα/β that phosphorylate IκB appear to be unaffected by BC12. Other components in the complex such as the regulatory subunit IKKγ may contribute to this effect. Taken together, BC12 inhibits IκB turnover, which is the likely mechanism that inhibit IL-2 expression.

We next examined nuclear translocation of NFκB family transcription factors. Nuclear extracts were prepared and immunoblotted with antibodies against each

individual NFκB family member. Activated NFκB is typically composed of RelA-NFκB1 or c-Rel- NFκB1, the former contributes to early time points and the latter contributes to later [97]. Notably, RelA (p65), NFκB1 (p50), and c-Rel all showed decreased nuclear translocation in the presence of BC12 (Figure 13A). Specifically, NFκB1 was reduced to approximately 50% at all three time-points examined. RelA was decreased to 35% at 2 hours post BC12 treatment. Nuclear protein level of c-Rel was induced by stimulation at 3 hours and inhibited to 50% by BC12 (Figure 13A). Of note, nucleolin is located mainly in nucleolus and β-actin is a cytoplasmic protein. Antibodies against these two proteins were used to confirm the separation of nuclear and cytoplasmic fractions (Figure 13B) [12, 13]. Taken together, BC12 inhibits IκB turnover, leading to impaired nuclear translocation of NFκB family proteins, which is the likely mechanism of IL-2 inhibition.

In addition to NFκB family, nuclear translocation of other key transcription factors was also evaluated. NFATc2 is the major contributor in NFAT family that regulates the early stage of *IL-2* transcription [78]. NFATc2 was detected in isolated nuclei of unstimulated Jurkat cells, consistent with other reports [13, 14]. The protein level of NFATc2 in the nucleus was not significantly changed after BC12 treatment (Figure 14). c-Fos and c-Jun were translocated to the nucleus after stimulation. The nuclear protein levels of c-Fos and c-Jun were not significantly decreased by BC12 treatment (Figure 14). The nuclear protein level of CREB was not induced by stimulation or affected by BC12.

To ensure the inhibitory effect on IL-2 production we observed was not restricted to PHA/PMA stimulation, Jurkat cells were stimulated with 20 ng/ml PMA and 1 μM Ionomycin in the absence or presence of 10 μM of BC12. Ionomycin is a calcium ionophore that is able to raise intracellular level of calcium, which results in activation of NFAT pathway. Ionomycin in combination of PMA can stimulate T cells and induce IL-2 production [179]. Similar levels of inhibition on IL-2 production by BC12 and BC12-4 were observed in ELISA (data not shown). We then sought to examine the ability of transcription factors to bind to the promoter region of *IL-2* gene. Nuclear extracts were prepared and an electrophoresis mobility shift assay (EMSA) was performed. The radiolabeled NFκB-consensus-binding oligonucleotides were bound and shifted by nuclear proteins extracted from Jurkat cells stimulated for 2, 4, and 6 hours, but not control unstimulated Jurkat cells (Figure 15A). Stimulation in the presence of BC12 reduced the amount of bound and shifted DNA probes (Figure 15A). Specificity of the binding was verified by adding increasing amount of the same unlabeled oligonucleotides as cold competitors, which completely competed off the binding of radiolabeled probes when present at 10 fold or more excess (Figure 15B). To examine the binding ability of nuclear NFAT protein to specific DNA regions, two different DNA probes were used, one corresponding to the distal NFAT site of the human *IL-2* promoter (Figure 16A), and the other corresponding to NFAT-consensus-binding motif (Figure 16C). Nuclear extract binding to both probes were increased from 2 hours to 6 hours of stimulation, and inhibited by BC12 (Figure 16A and 16C). Specificity of the binding was also confirmed by competition experiments with inclusion of excess of cold probes (Figure 16B and 16D). In addition, antibody super-shift assay was also performed with anti-NFATc2 and

anti-NFATc1 antibodies using nuclear extracts from 4 hour-stimulated cells (Figure 16B). Anti-NFATc2 antibody reduced the density of the specific band, which indicates prevention of the binding. Anti-NFATc1 antibody super-shifted the specific band, which indicates the formation of an antibody-NFAT-DNA probe complex (Figure 16B). These results suggest that both NFATc1 and NFATc2 are present in nucleus and able to bind to the promoter region after 4 hours of stimulation.

In order to confirm the results we observed in EMSA correlate with the IL-2 inhibitory effect by BC12, analogs BC12-4 and BC12-6 were also used to treat Jurkat cells in addition to PMA/Ionomycin stimulation for 4 hours. BC12-4 and BC12 inhibited the inducible binding of NFκB and NFAT to their specific consensus binding sites, while BC12-6 did not (Figure 17A and 17B). Interestingly, BC12 significantly increased the binding of AP-1 to its specific binding probe (Figure 17C), which is consistent with our findings that BC12 considerably augments activation of pathways upstream of AP-1 (Figure 10). The binding of Oct-1 to its specific probe is not induced by stimulation or inhibited by any of the three compounds (Figure 17D). Taken together, BC12 and BC12-4 inhibit NFκB and NFAT binding to their specific DNA probes, while not inhibiting the binding of AP-1 or Oct-1. BC12-6 does not show inhibitory effects on any transcription factors tested binding to their DNA probes. These results agree with our findings that both BC12 and BC12-4, but not BC12-6 inhibit IL-2 production in activated Jurkat cells, and suggest that inhibition of IL-2 production is through repressing NFκB and NFAT mediated transcription.

BC12 inhibits mouse primary T cell activation and proliferation

To understand whether the results in Jurkat cells are recapitulated in primary T cells, we moved on to investigate the role of BC12 in the activation and proliferation of mouse primary T cells. Mouse primary T cells express and secrete IL-2 in response to TCR engagement and subsequently require IL-2 for proliferation and survival. Total primary T cells were obtained from wild-type BALB/c mouse spleens. Activation of mouse primary T cells was achieved by stimulation with PMA and Ionomycin (Ion). Compounds BC12, BC12-4 and BC12-6 were evaluated in mouse primary T cells as well as the solvent control, DMSO (Figure 18). The combination of PMA/Ionomycin stimulated IL-2 secretion at all three time-points (Figure 18, PMA/Ion/DMSO). BC12-6 did not exhibit significant inhibition at 8 hours, but reduced the level of secreted IL-2 to approximately 80% at 24 hours and 48 hours (Figure 18, PMA/Ion/BC12-6). In the presence of BC12, IL-2 secretion was reduced to about 20% at all three time-points (Figure 18, PMA/Ion/BC12), which was less potent compared to the effect on Jurkat cells (inhibited to 2%) (refer to Figure 8A and 9). BC12-4, however, abolished IL-2 secretion to a level that was undetectable by the method (Figure 18, PMA/Ion/BC12-4). Overall, BC12 and its two derivatives showed similar effects on IL-2 secretion in stimulated mouse primary T cells as in Jurkat cells, which suggests a possibly similar off-target mechanism.

We then evaluated the effect of BC12 and its derivatives on mouse primary T cell viability (Figure 19). In addition to PMA/Ionomycin stimulation, BC12 and BC12-4 did not decrease cell viability at the dose of 10 μM. BC12-6 slightly increased cell viability in addition to stimulation. In the absence of PMA/Ionomycin, mouse primary T cells

remained above 90% viable after 24 hour-treatment with BC12 (Figure 19). These results confirmed that the inhibitory effect on IL-2 production was not attributable to cell death.

Because IL-2 is required for primary T cells to proliferate, we next evaluated the effect of BC12 on mouse primary T cell proliferation induced by PMA/Ionomycin. We analyzed cell cycle entry and progression in mouse T cells by propidium iodide staining and flow cytometry. Mouse primary T cells did not enter the cell cycle or proliferate without stimulation (Figure 20A, Media). Approximately 30% of cells entering $S+G_2/M$-phase of cell cycle after treating cells with PMA/Ionomycin for 48 hours (Figure 20A and 20B, PMA/Ion 48hrs). DMSO or BC12-6 treated cells exhibit minimal effect on the percentage of $S+G_2/M$-phase cells in comparison to PMA/Ionomycin stimulated cells (Figure 20A, PMA/Ion+DMSO and PMA/Ion+BC12-6). In contrast, treatment of stimulated T cells with BC12 or BC12-4 resulted in inhibition of cell cycle entry (Figure 20A and 20B), as the percentage of $S+G_2/M$-phase cells were decreased to the basal level compared to untreated cells. These results agree with the effect of BC12 and its derivatives on IL-2 secretion in activated mouse primary T cells (Figure 18) and indicate that the inhibition of cell cycle entry by BC12 and BC12-4 is a result of inhibited IL-2 production. To note, hypodiploid DNA indicates cells undergoing apoptosis. Stimulated mouse primary T cells treated with BC12-6 did not increase the percentage of hypodiploid DNA. Treating cells with BC12 resulted in approximately 10% increase in the percentage of hypodiploid DNA at 24 hours and 20% increase at 48 hours (Figure 21). The inhibition of IL-2 production and cell cycle entry in mouse primary T cells may lead to apoptosis.

We then evaluated signaling pathways in activated mouse primary T cells in the presence of BC12. Whole cell extracts were prepared and immunoblotted for signaling proteins that lead to *IL-2* expression. Similar to Jurkat cells, phosphorylation levels of ERK1/2 and RSK were increased by BC12 in stimulated mouse primary T cells, while BC12 alone did not induce phosphorylation of any proteins tested (Figure 22).

Taken together, BC12 and BC12-4 inhibit IL-2 production in mouse primary T cells without measurably affecting cell viability within 24 hours, leading to prevention of cell cycle entry and apoptosis after prolonged treatment. Similar to Jurkat cells, hyper-activation of some signaling proteins by BC12 was observed in mouse primary T cells.

BC12 inhibits IL-2 transcription in activated human primary T cells

After investigating the impact of BC12 on human Jurkat cells and mouse primary T cell activation, we sought to evaluate its efficacy in human primary T cells. Human primary T cells were obtained from healthy donors' blood. We first sought to examine IL-2 secretion from stimulated human primary T cells in the presence of BC12 by ELISA. IL-2 secretion was induced when T cells were stimulated with PMA and Ionomycin (Figure 23A), or with physiological ligands anti-CD3 and anti-CD28 antibodies (Figure 23B) for 24 hours and 48 hours. The presence of BC12 inhibited IL-2 secretion in stimulated human primary T cells at both 24 and 48 hours (Figure 23A and B).

We then examined the effect of BC12 on human primary T cell viability. BC12, at a dose of 10 μM, reduced the percentage of viable cells from about 72% of PMA and Ionomycin stimulated cells to 58% (Figure 24A), which indicates that the complete inhibition of IL-2 secretion by BC12 cannot be attributed to cell death. We also evaluated

the effect of BC12 on cell viability in the absence of stimuli. BC12 at 10 μM increased the percentage of cell death from 16% to 37%, averaging data from both 24 and 48 hours of treatment (Figure 24B). Increasing dose of BC12 resulted in increased cell death, with a maximum of 75% cell death when treated at a dose of 50 μM or higher (Figure 24B).

We also examined the effects of derivatives BC12-4 and BC12-6 on activated human primary T cells (Figure 25). Similarly to Jurkat cells (Figure 9) and mouse primary T cells (Figure 18), BC12-4 inhibited IL-2 secretion while BC12-6 did not, indicating a probably similar inhibition mechanism of these compounds on T cells from different origins.

Next, we sought to determine the mRNA level of *IL-2* gene in activated human primary T cells in the presence or absence of BC12. After stimulation with PMA/Ionomycin for 4 hours, *IL-2* mRNA level was increased by about 22000 fold. In the presence of 10 μM of BC12 in addition to stimuli, *IL-2* mRNA level was induced to about 2200 fold compared to untreated human T cells, which was 90% reduction compared to PMA/Ionomycin stimulated cells (Figure 26). This result suggests that BC12 inhibits *IL-2* gene transcription in activated human primary T cells similarly as in Jurkat cells. Taken together, BC12 and its derivatives exhibit similar effects on IL-2 production in activated human primary T cells as in Jurkat cells and mouse primary T cells, indicating the same off-target inhibitory mechanism. IL-2 production is inhibited at mRNA level, and the inhibitory effect is not a result of loss of cells from cell death.

Finally, we sought to investigate the effect of BC12 on other cytokine secretion from activated human $CD4^+$ T cells. Eleven cytokines were tested, including three Th1 specific, four Th2 specific and four Th17 specific cytokines (Figure 27 and Table 1).

Among the eleven cytokines, TGFβ1 exhibited a high level of secretion in untreated cells, and nine cytokines were induced to a detectable level after PMA/Ionomycin stimulation for 24 hours, with the exception of IL-12 and G-CSF (Table 1). Interestingly, in the presence of 10 μM of BC12, secretion levels of six cytokines were significantly decreased, including all four Th2 specific cytokines, IL-4, IL-5, IL-10, and IL-13, but no Th1 specific cytokines (Figure 27 and Table 1). Secretion of three cytokines were not affected or mildly inhibited, including two Th1 specific cytokines, IFNγ and TNFα (Figure 27 and Table 1). These data indicate that BC12 selectively inhibits Th2 specific cytokines over Th1 cytokines, suggesting a possible Th1 polarization effect of BC12 on human primary $CD4^+$ T cells.

FIGURES AND LEGENDS

Figure 1. BC12 inhibits IL-2 secretion in activated Jurkat cells in a dose-dependent manner. Jurkat cells were cultured in media alone, treated with DMSO, or stimulated by the combination of 0.5 μg/ml PHA and 50 ng/ml PMA. Stimulated Jurkat cells were simultaneously treated with increasing dose of BC12 (1 μM, 5 μM and 10 μM) or DMSO for 24 hours. Supernatants were collected and analyzed by ELISA as described in *Material and Methods* to examine the concentration of IL-2 secreted. The data are representative of two independent experiments, each conducted in duplicates. Error bars reflect standard deviation from the mean of duplicate measurements.

Figure 1.

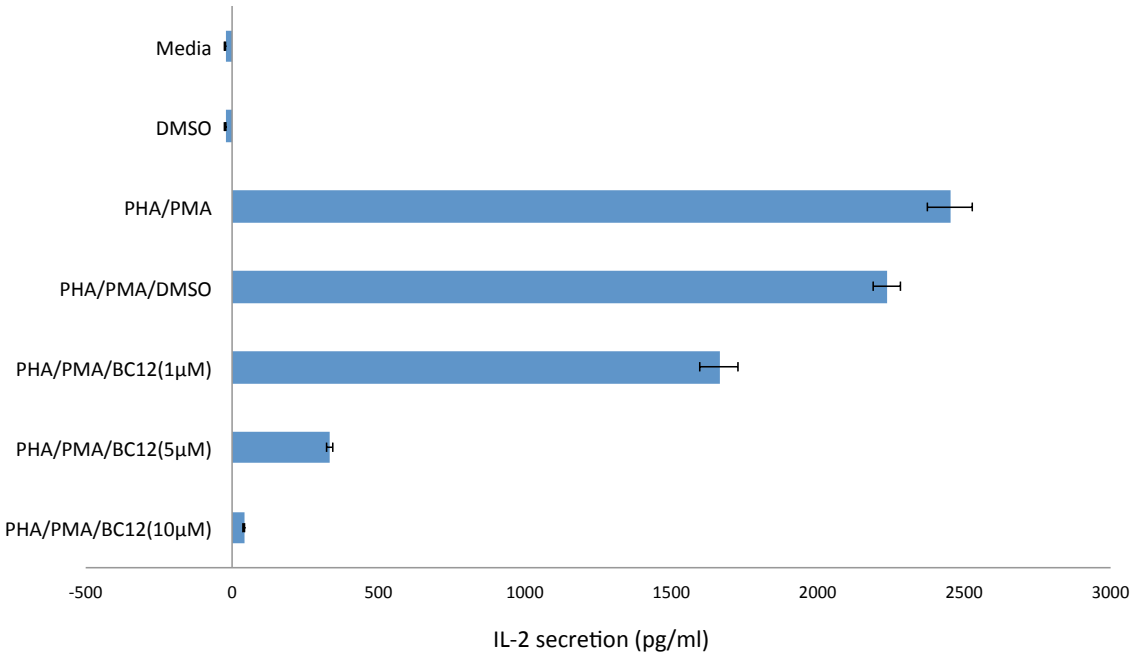
Media
DMSO
PHA/PMA
PHA/PMA/DMSO
PHA/PMA/BC12(1µM)
PHA/PMA/BC12(5µM)
PHA/PMA/BC12(10µM)
-500
0
500
1000
1500
2000
2500
3000
IL-2 secretion (pg/ml)

Figure 2. BC12 does not severely reduce cell viability. Jurkat cells were cultured in media alone or treated with 10 μM of BC12 with increasing doses along with 0.5 μg/ml PHA and 50 ng/ml PMA stimulation for 24 hours. The viability of cells was determined by propidium iodide staining. Samples were analyzed by flow cytometry as described in *Material and Methods*. The data are represented as the percentage of Jurkat cells that are negative for propidium iodide staining. The data are representative of 10,000 cells and two independent experiments.

Figure 2

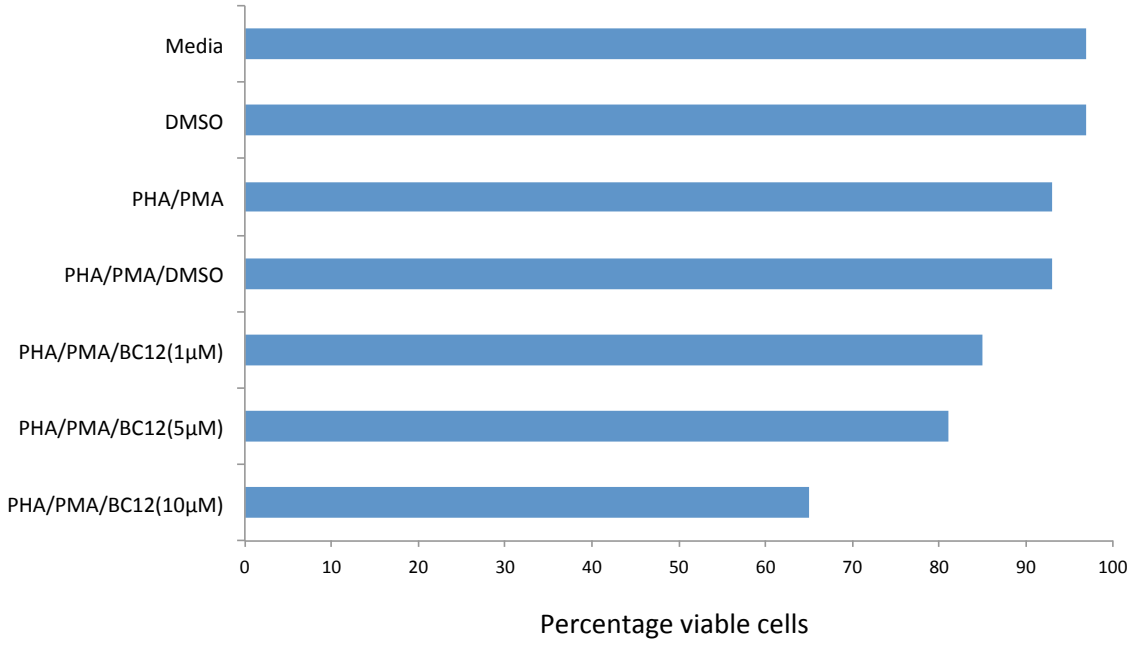
Media
DMSO
PHA/PMA
PHA/PMA/DMSO
PHA/PMA/BC12(1µM)
PHA/PMA/BC12(5µM)
PHA/PMA/BC12(10µM)
0
10
20
30
40
50
60
70
80
90
100
Percentage viable cells

Figure 3. Time course of IL-2 inhibition by BC12. Jurkat cells were stimulated with a combination of 0.5 μg/ml PHA and 50 ng/ml PMA, or treated with 10 μM of BC12 simultaneously with stimulation up to 24 hours. Supernatant samples were taken at indicated time points and were analyzed by ELISA as described in *Material and Methods* to examine the concentration of IL-2 secreted. The data are representative of two independent experiments, each conducted in duplicates. Error bars reflect standard deviation from the mean of duplicate measurements.

Figure 3

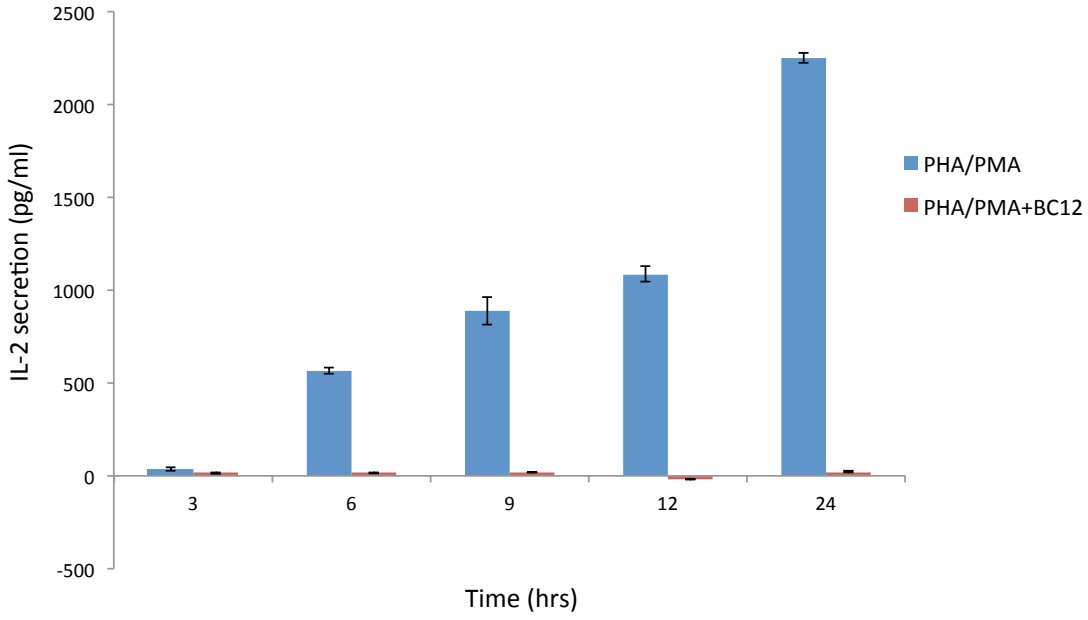
2500
2000
1500
1000
500
0
-500
IL-2 secretion (pg/ml)
3
6
9
12
24
Time (hrs)
PHA/PMA
PHA/PMA+BC12

Figure 4. BC12 inhibits endogenous IL-2 protein production. *A,* Jurkat cells were cultured in media alone, treated with DMSO, 0.5 μg/ml PHA and 50 ng/ml PMA or PHA and PMA plus 10 μM of BC12, all in the presence of monensin, a Golgi inhibitor to block IL-2 secretion. Whole cell extracts were prepared from Jurkat cells treated for 12 hours, and Western blotting was performed with an anti-human IL-2 antibody. The blot was stripped and reprobed with an anti-β-actin antibody to ensure equal loading. Quantification of the Western blotting bands was obtained with ImageJ software (v1.45s). Band densities are listed as fold increase above first detected band relative to β-actin loading control. The data are representative of two independent experiments. *B,* Jurkat cells were cultured in media alone, treated with 0.5 μg/ml PHA and 50 ng/ml PMA in the presence or absence of monensin for 24 hours. Supernatant samples were taken and analyzed by ELISA as described in *Material and Methods*. The data are representative of two independent experiments, each conducted in duplicates. Error bars reflect standard deviation from the mean of duplicate measurements.

Figure 4

A

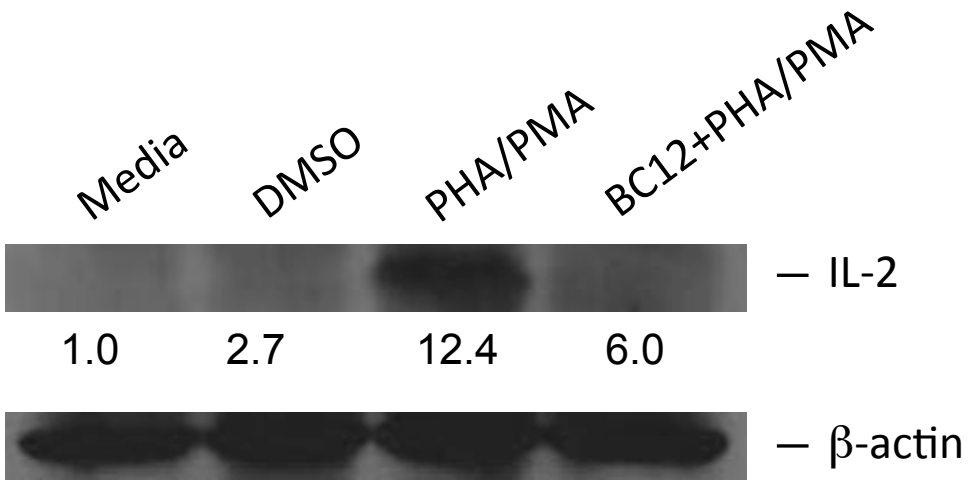
Media
DMSO
PHA/PMA
BC12+PHA/PMA
— IL-2
1.0
2.7
12.4
6.0
— β-actin

B

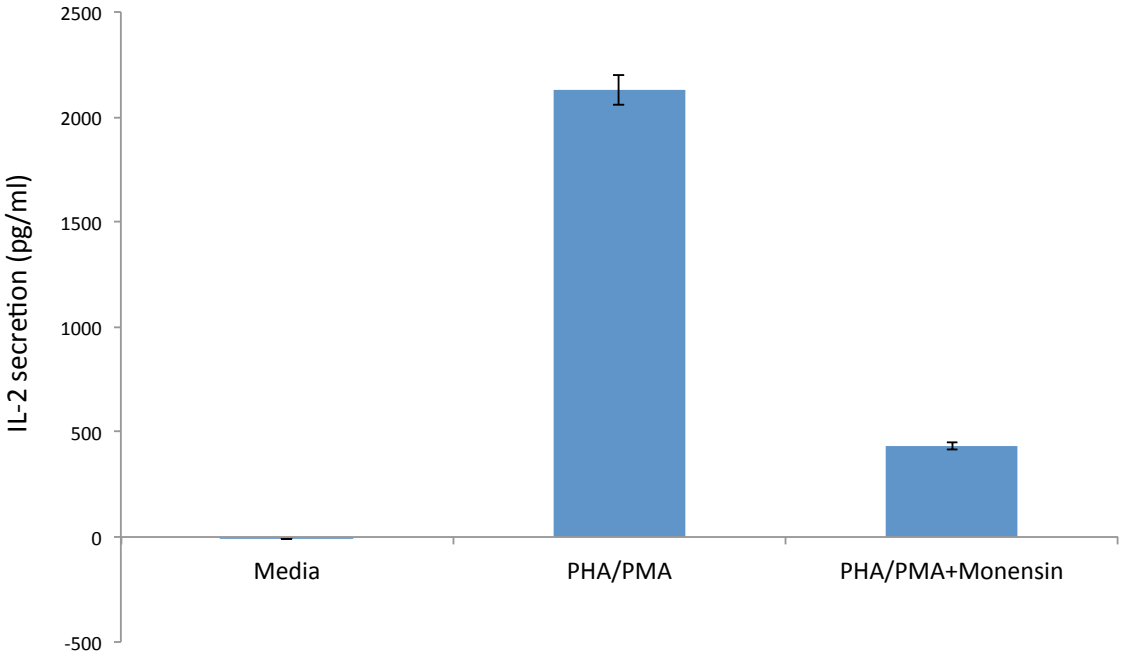
2500
2000
1500
1000
500
0
-500
IL-2 secretion (pg/ml)
Media
PHA/PMA
PHA/PMA+Monensin

Figure 5. BC12 decreases *IL-2* mRNA level in activated Jurkat cells. Jurkat cells were stimulated with 0.5 μg/ml PHA and 50 ng/ml PMA in the presence or absence of 10 μM of BC12. RNA was extracted at the indicated times as described in *Material and Methods*. *IL-2* mRNA was analyzed by semi-quantitative reverse transcription-PCR following normalization to *β-actin* as described in *Material and Methods*. The data are average from two independent experiments and error bars reflect standard deviation from the mean of two independent experiments.

Figure 5

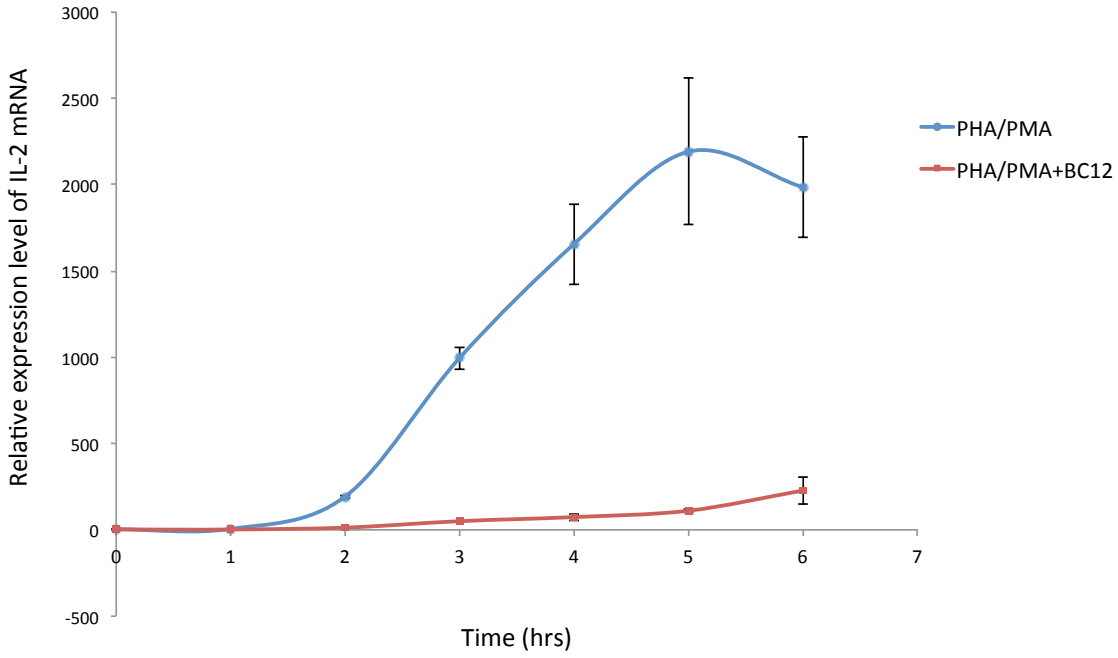
Relative expression level of IL-2 mRNA
3000
2500
2000
1500
1000
500
0
-500
0
1
2
3
4
5
6
7
Time (hrs)
PHA/PMA
PHA/PMA+BC12

Figure 6. BC12 does not affect *IL-2* mRNA stability. Jurkat cells were previously stimulated with 0.5 μg/ml PHA and 50 ng/ml PMA for 4 hours. DMSO or 10 μM BC12 or 1 μg/ml Cyclosporin A (CsA) or CsA+BC12 were then added. Levels of mRNA are shown as a percentage of *IL-2* mRNA after the initial stimulation. The fold induction of IL-2 mRNA after the initial 4 hours of stimulation was 1054 compared to unstimulated cells. The data are representative of three independent experiments and error bars reflect standard deviation from the mean of three independent experiments.

Figure 6

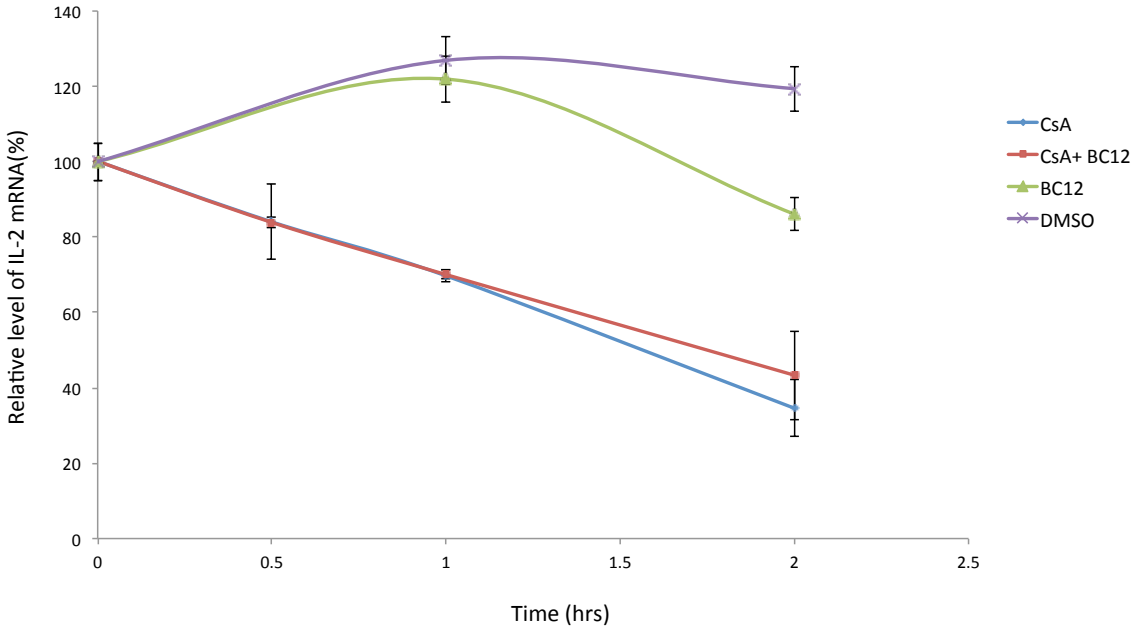
Relative level of IL-2 mRNA(%)
140
120
100
80
60
40
20
0
0
0.5
1
1.5
2
2.5
Time (hrs)
CsA
CsA+ BC12
BC12
DMSO

Figure 7. BC12 and its derivatives have different PDE7A and 7B inhibitory activity. *A,* Structures of BC12 and its derivative compounds. *B,* BC12 and its derivative compounds BC12-1, BC12-2, BC12-4, BC12-5, BC12-6 and BC12-7 were used to treat a human-PDE7A-expressing strain with increasing doses (0, 0.21, 0.31, 0.46, 0.69, 1.03, 1.54, 2.31, 3.47, 5.20, 7.81, 11.71 and 17.6 μM). *C,* BC12 and its derivative compounds BC12-1, BC12-2, BC12-4, BC12-5, BC12-6 and BC12-7 were used to treat a human-PDE7B-expressing strain with increasing doses (0, 0.21, 0.31, 0.46, 0.69, 1.03, 1.54, 2.31, 3.47, 5.20, 7.81, 11.71, 17.6, 26.4, 39.5, 59.3 and 88.9 μM). Optical densities (OD_{600}) of the cultures were determined after 48 hours incubation at 30 ^{o}C, using a microplate reader to measure growth. Each value represents the average reading of four wells. These assays were conducted by Dr. Arlene Wyman.

Figure 7

A

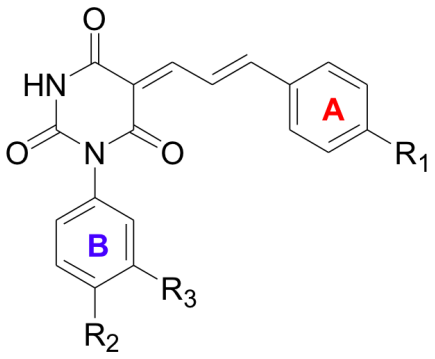

Compound	R_1	R_2	R_3
BC12	$N(CH_3)_2$	H	H
BC12-1	$N(CH_3)_2$	CH_3	H
BC12-2	$N(CH_3)_2$	Br	H
BC12-4	H	H	H
BC12-5	$N(CH_3)_2$	Cl	H
BC12-6	$N(CH_3)_2$	F	H
BC12-7	$N(CH_3)_2$	H	CH_3

B **Inhibition of PDE7A by BC12 series**

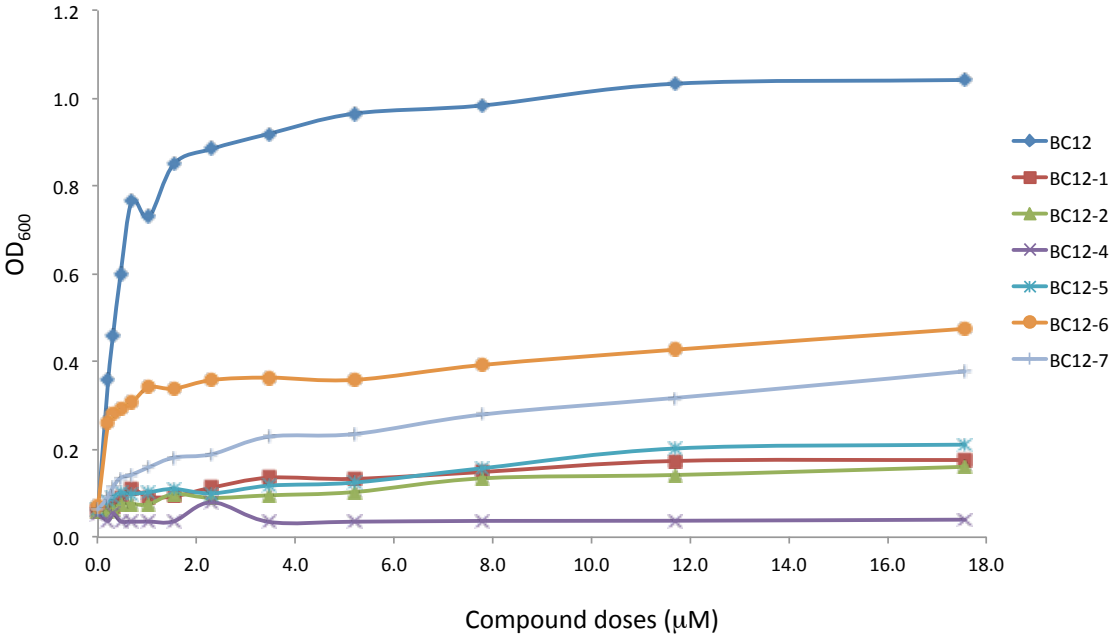

C **Inhibition of PDE7B by BC12 series**

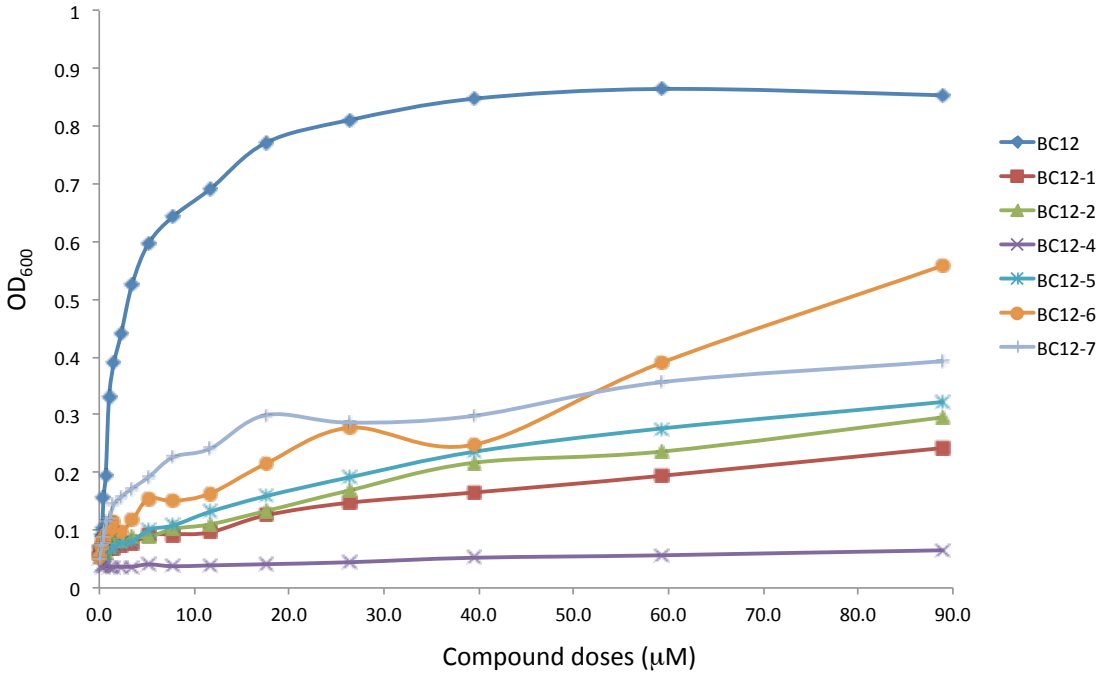

Figure 8. BC12 and its derivatives have various effects on IL-2 secretion. Jurkat cells were cultured in media alone, or treated with DMSO, or stimulated with 0.5 μg/ml PHA and 50 ng/ml PMA in the presence of DMSO, 10 μM of BC12 (indicated as 12) or compounds of similar structure with that of BC12 (indicated as 12-1 to 12-7) for 15 hours. *A,* Supernatant samples were collected and analyzed by ELISA as described in *Material and Methods*. The data are representative of two independent experiments, each conducted in duplicates. Error bars reflect standard deviation from the mean of duplicate measurements. *B,* The viability of cells was determined by propidium iodide staining. Samples were analyzed by flow cytometry as described in *Material and Methods*. The data are represented as the percentage of Jurkat cells that are negative for propidium iodide staining. The data are representative of 10,000 cells and two independent experiments.

Figure 8

A

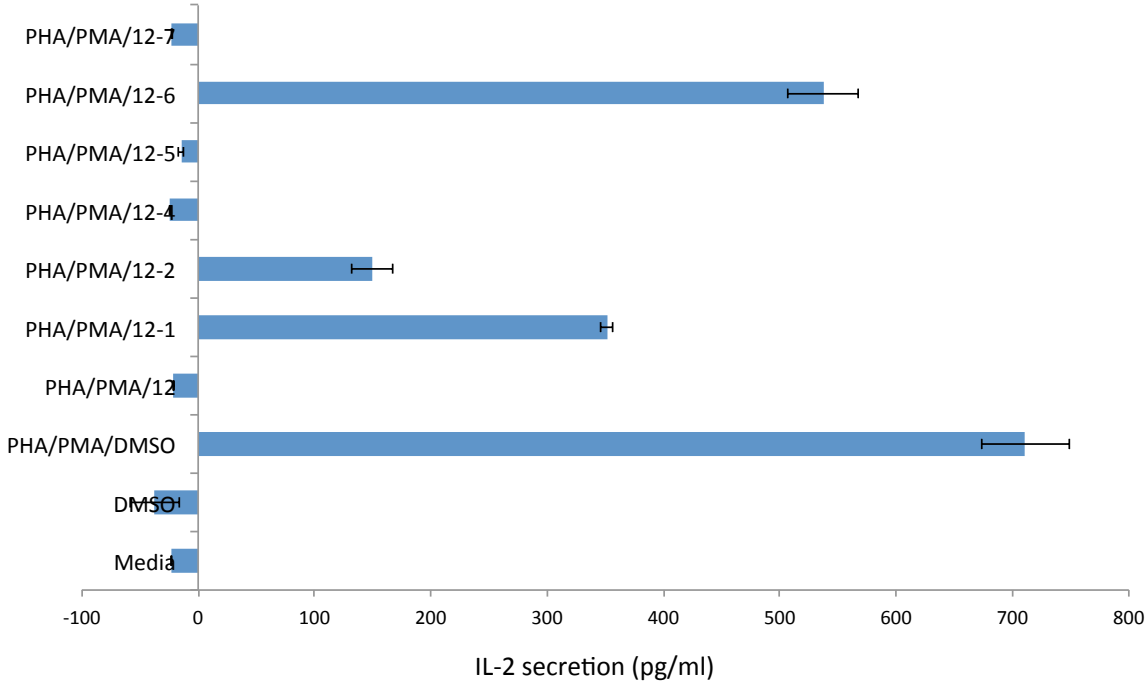
PHA/PMA/12-7
PHA/PMA/12-6
PHA/PMA/12-5
PHA/PMA/12-4
PHA/PMA/12-2
PHA/PMA/12-1
PHA/PMA/12
PHA/PMA/DMSO
DMSO
Media
-100
0
100
200
300
400
500
600
700
800
IL-2 secretion (pg/ml)

B

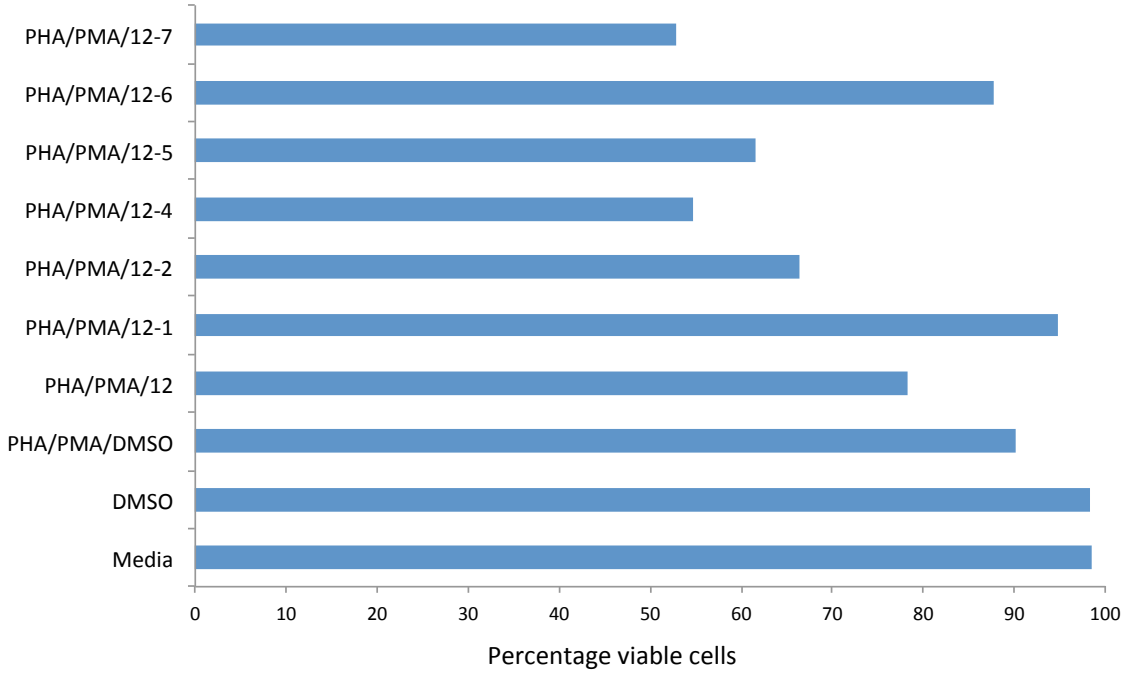
PHA/PMA/12-7
PHA/PMA/12-6
PHA/PMA/12-5
PHA/PMA/12-4
PHA/PMA/12-2
PHA/PMA/12-1
PHA/PMA/12
PHA/PMA/DMSO
DMSO
Media
0
10
20
30
40
50
60
70
80
90
100
Percentage viable cells

Figure 9. BC12 inhibits IL-2 expression not through PDE7. Jurkat cells were cultured in media alone, or treated with DMSO, or stimulated with 0.5 μg/ml PHA and 50 ng/ml PMA in the presence of DMSO, 10 μM of BC12, BC12-4, BC12-6 or BC54 for 15 hours. Supernatant samples were collected and analyzed by ELISA as described in *Material and Methods*. The data are representative of two independent experiments, each conducted in duplicates. Error bars reflect standard deviation from the mean of duplicate measurements.

Figure 9

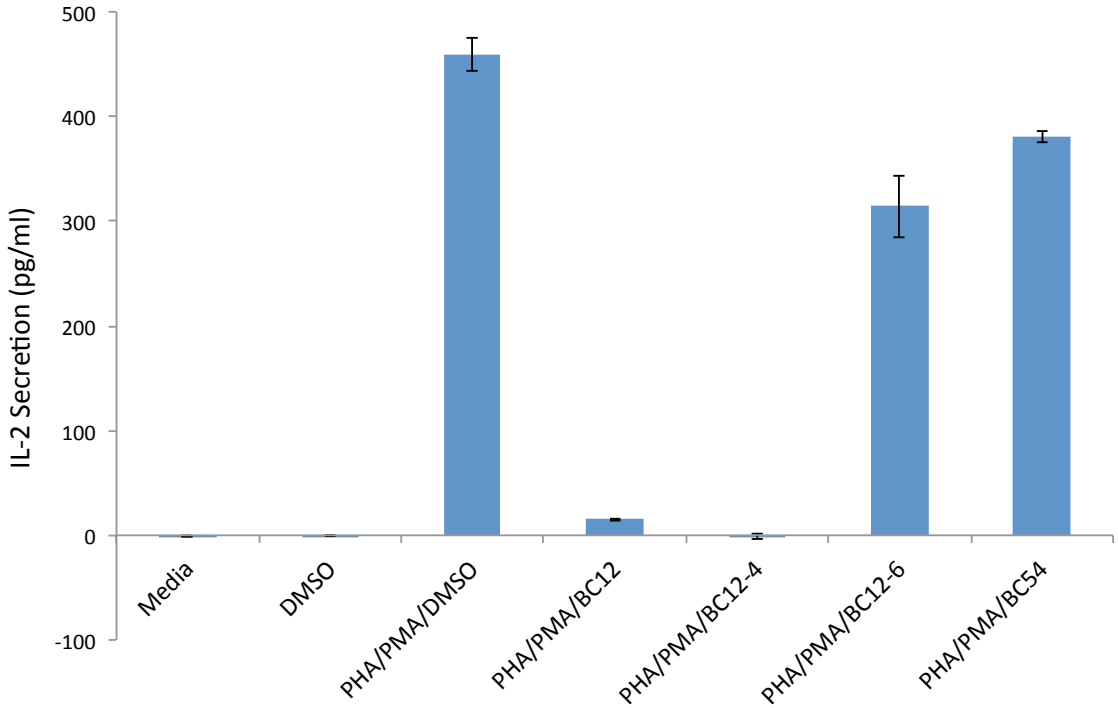
IL-2 Secretion (pg/ml)
500
400
300
200
100
0
-100
Media
DMSO
PHA/PMA/DMSO
PHA/PMA/BC12
PHA/PMA/BC12-4
PHA/PMA/BC12-6
PHA/PMA/BC54

Figure 10. BC12 augments activation signal towards AP-1 pathway. Jurkat cells were cultured in media, treated with DMSO, stimulated with a combination of PHA/PMA, or pre-treated with 10 μM of BC12 for 20 minutes before incubating with BC12 plus PHA/PMA or DMSO for various lengths of time. Whole cell extracts were prepared and Western blotting was performed with antibodies against various signaling proteins as described in *Material and Methods*. The blot was stripped and reprobed for anti-HSP90 antibody to ensure equal loading of each sample. Quantification of the Western blotting bands was obtained with ImageJ software (v1.45s). Both top and bottom band densities are listed as fold increase above first detected band. The data are representative of three independent experiments.

Figure 10

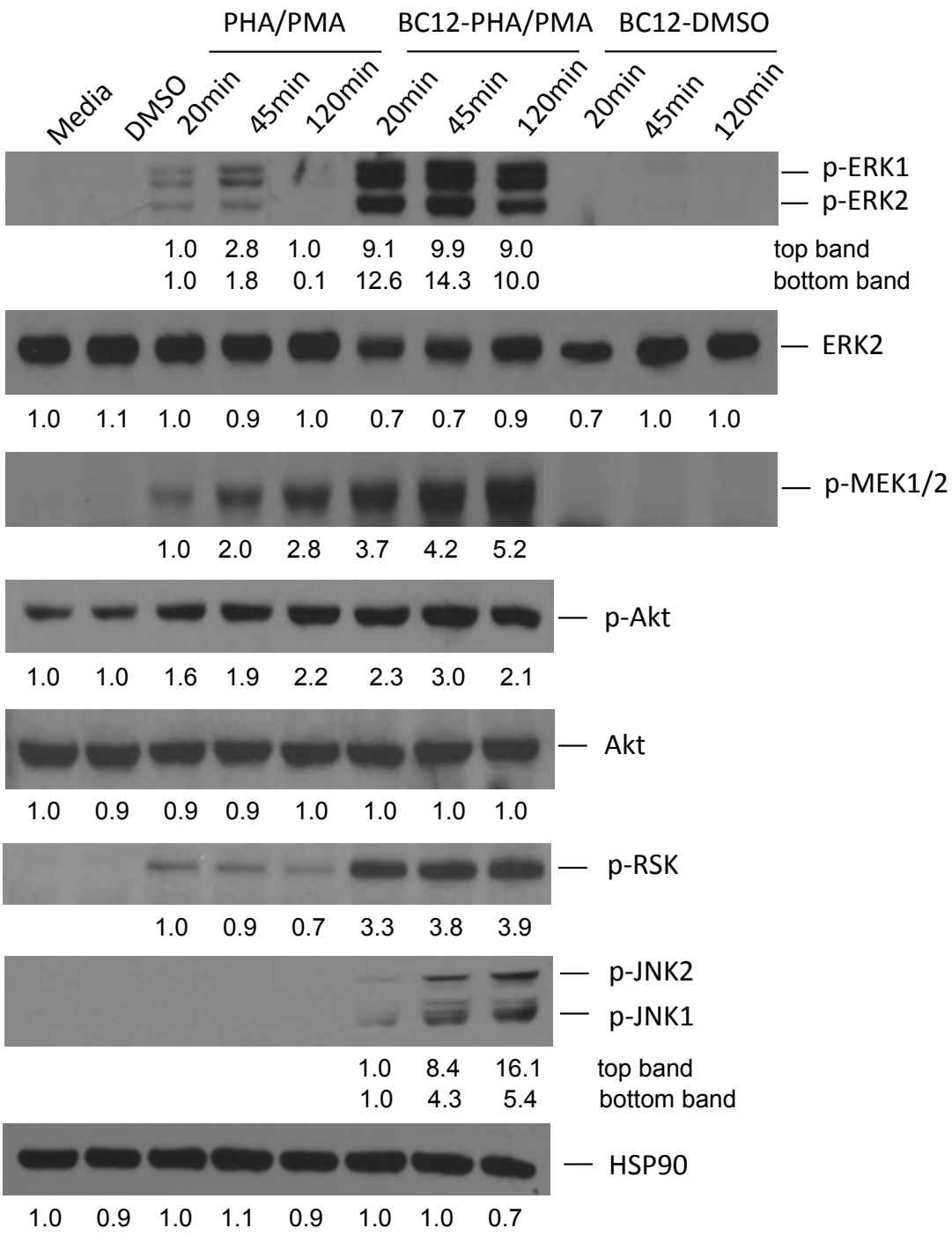
PHA/PMA
BC12-PHA/PMA
BC12-DMSO
Media
DMSO
20min
45min
120min
20min
45min
120min
20min
45min
120min
p-ERK1
p-ERK2
1.0 2.8 1.0 9.1 9.9 9.0 top band
1.0 1.8 0.1 12.6 14.3 10.0 bottom band
ERK2
1.0 1.1 1.0 0.9 1.0 0.7 0.7 0.9 0.7 1.0 1.0
p-MEK1/2
1.0 2.0 2.8 3.7 4.2 5.2
p-Akt
1.0 1.0 1.6 1.9 2.2 2.3 3.0 2.1
Akt
1.0 0.9 0.9 0.9 1.0 1.0 1.0 1.0
p-RSK
1.0 0.9 0.7 3.3 3.8 3.9
p-JNK2
p-JNK1
1.0 8.4 16.1 top band
1.0 4.3 5.4 bottom band
HSP90
1.0 0.9 1.0 1.1 0.9 1.0 1.0 0.7

Figure 11. Microarray analysis of *IL-2* gene regulators suggests NFκB the most likely transcription factor responsible for down-regulation of *IL-2* gene. Jurkat cells were treated with media, stimulated with 0.5 μg/ml PHA and 50ng/ml PMA in the presence or absence of 10 μM of BC12. Each treatment was prepared in quadruplicates. RNA was extracted after 3 hours of treatment as described in *Material and Methods*, and was tested by the Affymetrix facility at Boston University for whole genome expression profile. Microarray expression data were analyzed based on *IL-2* gene regulators. Five groups of transcription factors were analyzed: NFATc1/NFATc2, NFκB (p50/p65), c-Fos/FosB, c-Jun/JunB and Oct-1, as candidates responsible for down-regulation of the *IL-2* gene. Target genes of these transcription factors were obtained from TRANSFAC database and their expression levels were analyzed. The fold changes of target gene expression for five groups of transcription factors were illustrated on a color scale. The value was calculated by (stimuli with BC12 treatment - stimuli treatment)/ untreated control. White color represents that the gene is not a target of the transcription factors at corresponding column. Blue color indicates the gene expression is reduced, whereas orange color indicates the gene expression is increased when treated with BC12. This analysis was conducted by Dr. Lu Zhang.

Figure 11


X: 2 Y: 1
Index: -5.493
RGB: 0, 0, 0.562
X: 5 Y: 2
Index: -4.675
RGB: 0, 0, 0.625
X: 4 Y: 6
Index: -1.791
RGB: 0, 0, 0.938
X: 1 Y: 8
Index: -0.6946
RGB: 0, 0.0625, 1
X: 2 Y: 7
Index: -1.624
RGB: 0, 0, 0.938
X: 4 Y: 55
Index: 0.9079
RGB: 0, 0.25, 1
X: 3 Y: 58
Index: 19.87
RGB: 1, 0.625, 0
IL2RA
IL3
IL2
LTA
IFNG
PLAU
TNF
CSF2
FASLG
MYC
MT2A
BCL2A1
NFKB1
ICAM1
CCND1
MSH2
FAS
HIST1H2BJ
WEE1
CCL2
VIP
IFNB1
IGHA1
HLA-DRA
IL4
IVL
CXCL1
LPL
SELE
HBG1
COL1A2
HLA-DPB1
IL6
HBB
IL5
KRT16
PENK
EDN1
TSHB
ITGAX
F8
CXCL2
PTGS2
FOSL1
PTK2
CCL5
TP53
MMP1
FN1
CSNK1A1
LYN
GJA1
CXCL3
NPPA
SLC3A2
IL8
JUN
FOS
NFAT
NFkB
Fos
Jun
Oct
5
4
3
2
1
0
-1
-2
-3
-4
-5

Figure 12. BC12 inhibits IκBα turnover at early time points. Jurkat cells were cultured in media, stimulated with 0.5 μg/ml PHA and 50ng/ml PMA, or pre-treated with10 μM of BC12 for 20 minutes before incubating with PHA/PMA plus BC12 for various lengths of time. Whole cell extracts were prepared and Western blotting was performed with anti-IκBα, p-IκBα, or p-IKKα/β antibody as described in *Material and Methods*. The blot was stripped and reprobed for anti-HSP90 antibody to ensure equal loading of each sample. Quantification of the Western blotting bands was obtained with ImageJ software (v1.45s). Band densities are listed as fold increase above first detected. The data are representative of two independent experiments.

Figure 12

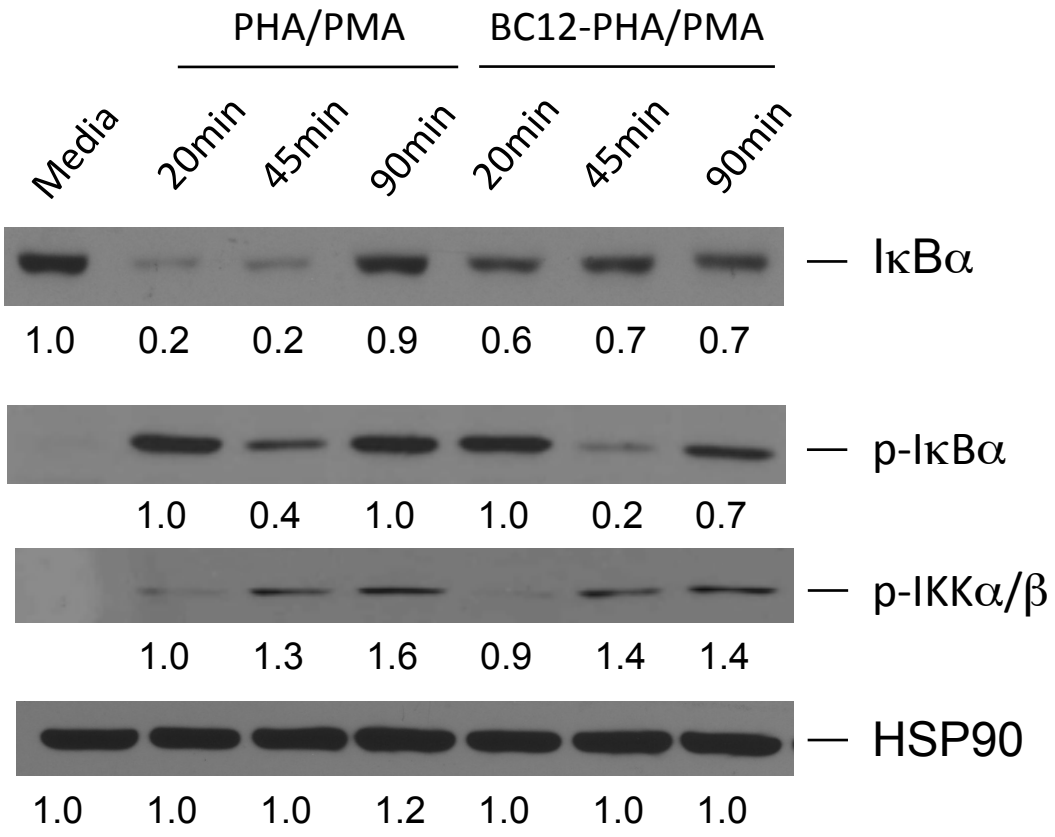
PHA/PMA
BC12-PHA/PMA
Media
20min
45min
90min
20min
45min
90min
IκBα
1.0 0.2 0.2 0.9 0.6 0.7 0.7
p-IκBα
1.0 0.4 1.0 1.0 0.2 0.7
p-IKKα/β
1.0 1.3 1.6 0.9 1.4 1.4
HSP90
1.0 1.0 1.0 1.2 1.0 1.0 1.0

Figure 13. BC12 inhibits nuclear translocation of some NFκB family proteins. *A,* Jurkat cells were cultured in media, stimulated with 0.5 μg/ml PHA and 50ng/ml PMA, or pre-treated with 10 μM of BC12 for 20 minutes before incubating with PHA/PMA plus BC12 for various lengths of time. Nuclear extracts were prepared and Western blotting was performed with anti-NFκB1, anti-RelA or anti-c-Rel antibody as described in *Material and Methods*. The blot was stripped and reprobed for anti-nucleolin to verify equal loading of each nuclear extract sample. Quantification of the Western blotting bands was obtained with ImageJ software (v1.45s). Band densities are listed as fold increase above first detected band relative to nucleolin loading control. The data are representative of two independent experiments. *B,* The nuclear and cytosolic extracts were prepared from Jurkat cells stimulated with PHA/PMA for 2 hours. Anti-nucleolin or anti-β-actin antibodies were used to verify complete separation of nuclear and cytosolic proteins.

Figure 13

A

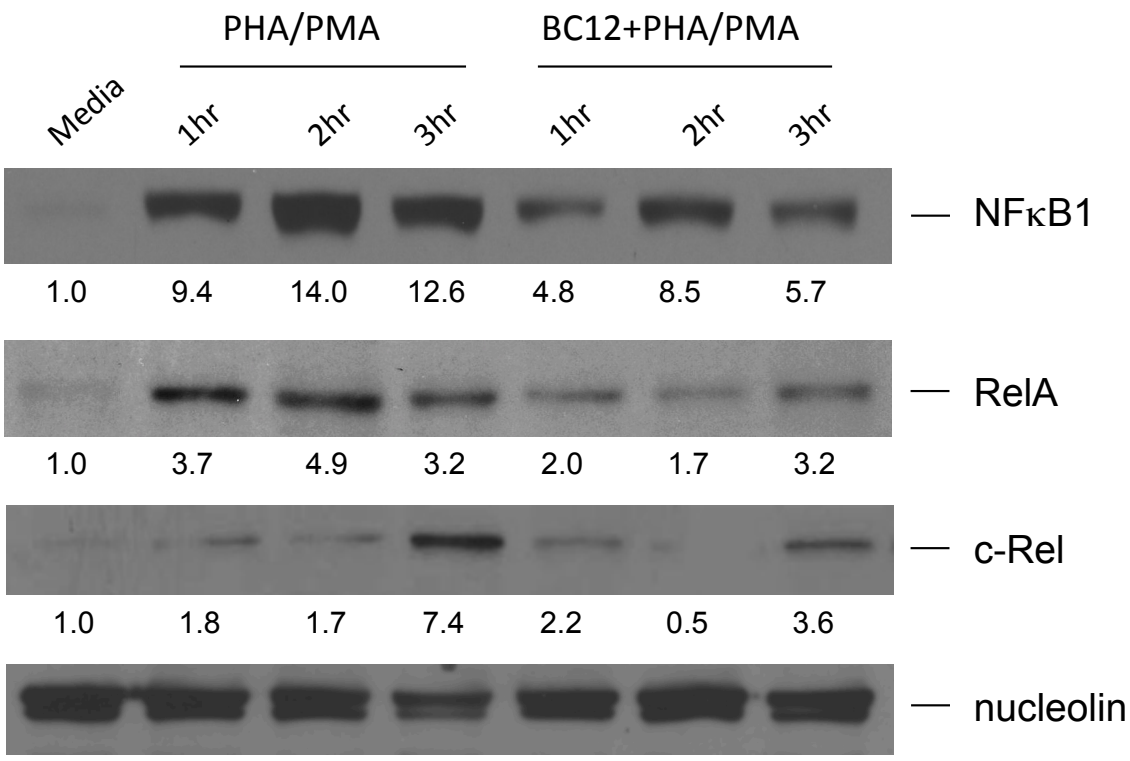
PHA/PMA
BC12+PHA/PMA
Media
1hr
2hr
3hr
1hr
2hr
3hr
NFκB1
1.0
9.4
14.0
12.6
4.8
8.5
5.7
RelA
1.0
3.7
4.9
3.2
2.0
1.7
3.2
c-Rel
1.0
1.8
1.7
7.4
2.2
0.5
3.6
nucleolin

B

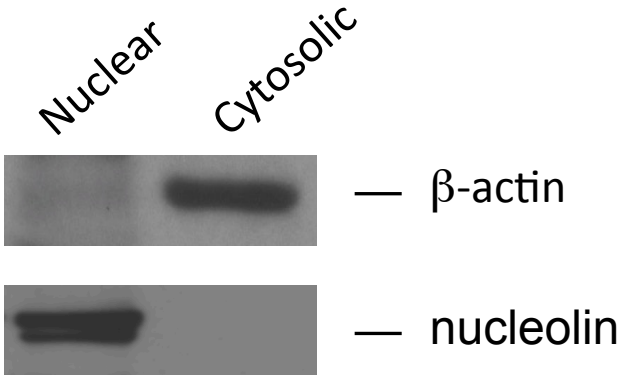
Nuclear
Cytosolic
β-actin
nucleolin

Figure 14. BC12 does not affect nuclear translocation of NFAT, AP-1 or CREB. *A,* Jurkat cells were cultured in media, stimulated with 0.5 μg/ml PHA and 50ng/ml PMA, or pre-treated with 10 μM of BC12 for 20 minutes before incubating with PHA/PMA plus BC12 for various lengths of time. Nuclear extracts and cytosolic extracts were prepared and Western blotting was performed with anti-NFATc2, anti-c-Fos or anti-c-Jun antibody as described in *Material and Methods*. The blot was stripped and reprobed for anti-nucleolin to verify equal loading of each nuclear extract sample. Quantification of the Western blotting bands was obtained with ImageJ software (v1.45s). Band densities are listed as fold increase above first detected band. The data are representative of two independent experiments. *B,* The nuclear and cytosolic extracts were prepared from Jurkat cells stimulated with PHA/PMA for 2 hours. Anti-nucleolin or anti-β-actin antibodies were used to verify complete separation of nuclear and cytosolic proteins.

Figure 14

A

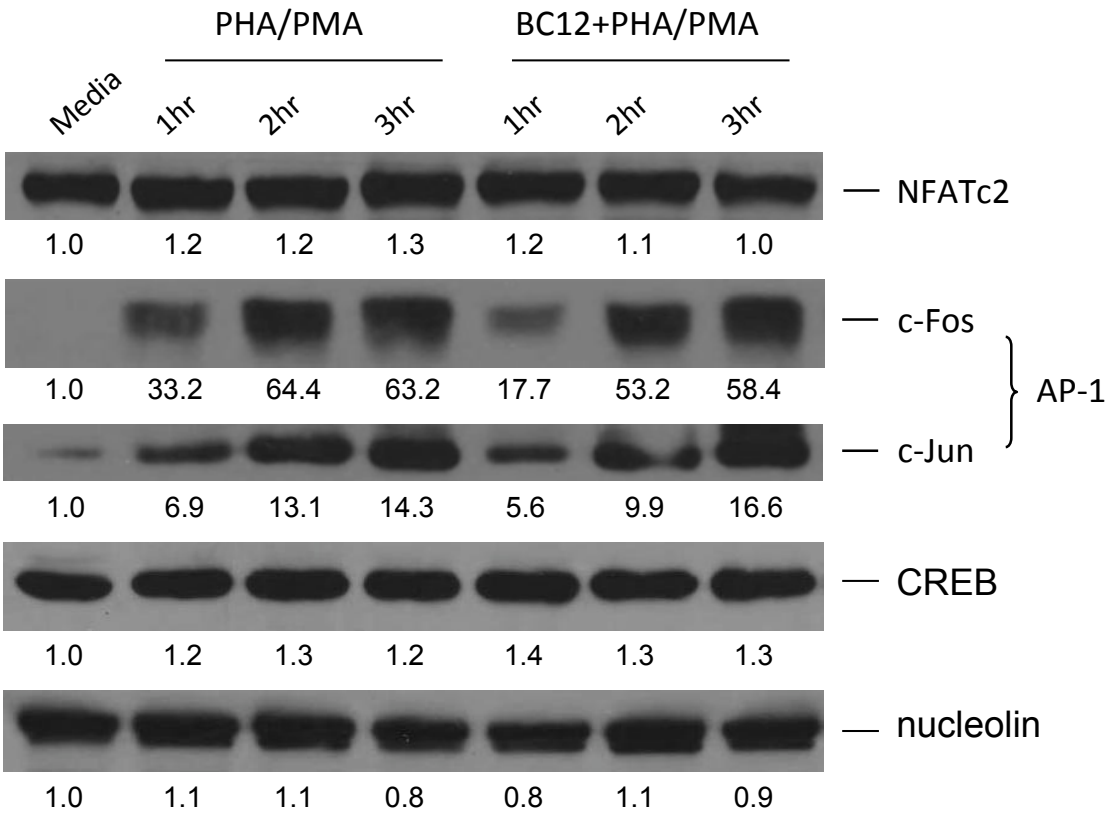
PHA/PMA
BC12+PHA/PMA
Media
1hr
2hr
3hr
1hr
2hr
3hr
NFATc2
1.0 1.2 1.2 1.3 1.2 1.1 1.0
c-Fos
1.0 33.2 64.4 63.2 17.7 53.2 58.4
AP-1
c-Jun
1.0 6.9 13.1 14.3 5.6 9.9 16.6
CREB
1.0 1.2 1.3 1.2 1.4 1.3 1.3
nucleolin
1.0 1.1 1.1 0.8 0.8 1.1 0.9

B

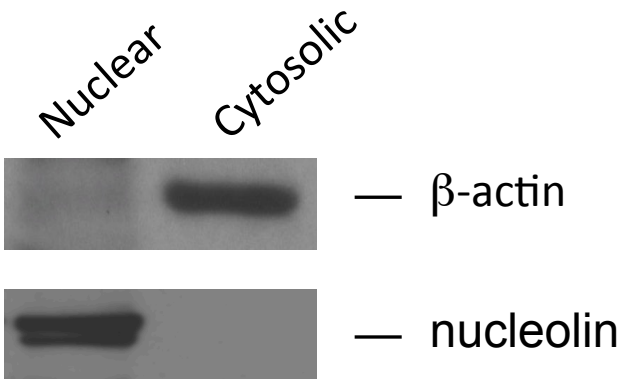
Nuclear
Cytosolic
β-actin
nucleolin

Figure 15. BC12 inhibits the binding of NFκB to the consensus NFκB-binding probe. *A,* Jurkat cells were cultured in media alone, or stimulated with 20 ng/ml PMA and 1 μM Ionomycin in the absence or presence of 10 μM of BC12. Nuclear extracts of Jurkat cells were prepared at indicated times and analyzed by EMSA using radiolabeled probes corresponding to the NFκB-consensus-binding site as described in *Material and Methods*. *B,* Jurkat cells were cultured in media alone, or stimulated with 20 ng/ml PMA and 1 μM Ionomycin for 4hours. Nuclear extracts of Jurkat cells were prepared and analyzed by EMSA using radiolabeled probes corresponding to the NFκB-consensus-binding site as described in *Material and Methods*. Competition experiments were performed by adding 1, 10, or 25 fold molar excess of the same unlabelled NFκB-consensus-binding oligonucleotide to the reaction mixtures as indicated in the figure. The specific shifted bands are indicated by red arrows. Quantification of the specific bands was obtained with ImageJ software (v1.45s). Band densities are listed as fold increase above first detected band. The data are representative of two independent experiments.

Figure 15

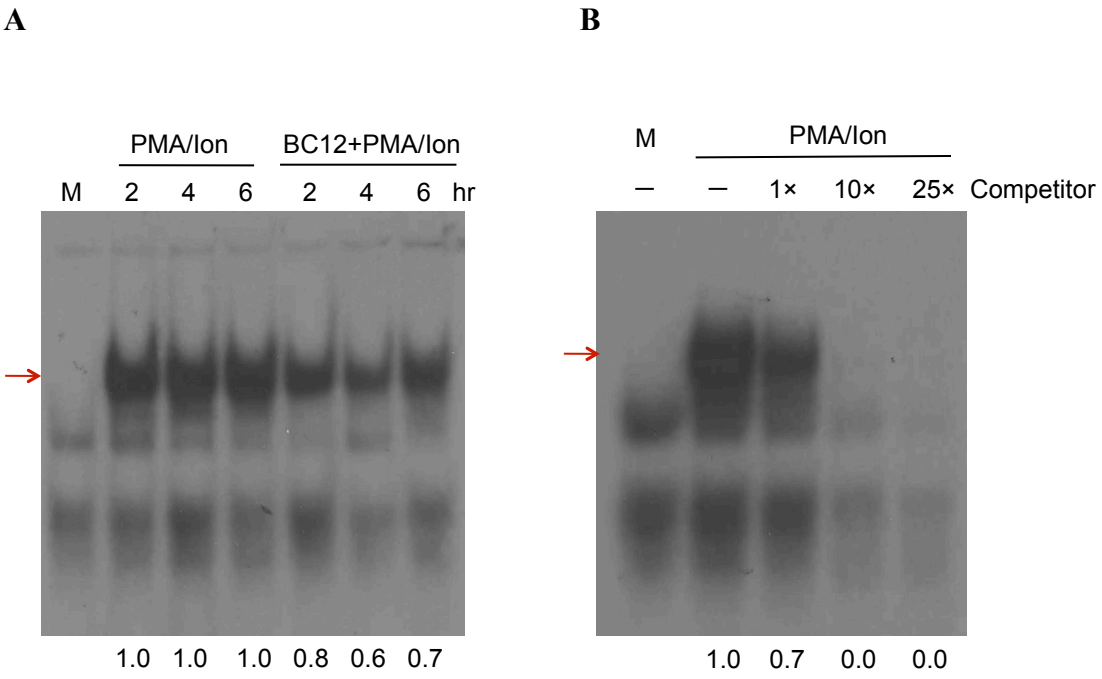
A
PMA/Ion
BC12+PMA/Ion
M 2 4 6 2 4 6 hr
1.0 1.0 1.0 0.8 0.6 0.7
B
M
PMA/Ion
– – 1× 10× 25× Competitor
1.0 0.7 0.0 0.0

Figure 16. BC12 inhibits the binding of NFAT to the NFAT-binding probes. *A,* Jurkat cells were cultured in media alone, or stimulated with 20 ng/ml PMA and 1 μM Ionomycin in the absence or presence of 10 μM of BC12. Nuclear extracts of Jurkat cells were prepared at indicated times and analyzed by EMSA using radiolabeled probes corresponding to the distal NFAT site of the human IL-2 promoter as described in *Material and Methods*. *B,* Jurkat cells were cultured in media alone, or stimulated with 20 ng/ml PMA and 1 μM Ionomycin for 4hours. Nuclear extracts of Jurkat cells were prepared and analyzed by EMSA using radiolabeled probes corresponding to the distal NFAT site of the human *IL-2* promoter. Competition experiments were performed by adding 1, 10, or 25 fold molar excess of the same unlabelled NFAT-binding oligonucleotide to the reaction mixtures as indicated in the figure. Supershift assay was performed by adding 4 μg anti-NFATc1 or anti-NFATc2 antibodies to the reaction mixtures. *C,* Jurkat cells were cultured in media alone, or stimulated with 20 ng/ml PMA and 1 μM Ionomycin in the absence or presence of 10 μM of BC12. Nuclear extracts of Jurkat cells were prepared at indicated times and analyzed by EMSA using radiolabeled probes corresponding to the NFAT-consensus-binding site as described in *Material and Methods*. *D,* Jurkat cells were cultured in media alone, or stimulated with 20 ng/ml PMA and 1 μM Ionomycin for 4hours. Nuclear extracts of Jurkat cells were prepared and analyzed by EMSA using radiolabeled probes corresponding to the NFAT-consensus-binding site. Competition experiments were performed by adding 1, 10, or 25 fold molar excess of the same unlabelled NFAT-consensus-binding oligonucleotide to the reaction mixtures as indicated in the figure. The specific shifted bands are indicated by red arrows. The super-shifted band is indicated by blue arrow. Quantification of the specific bands

was obtained with ImageJ software (v1.45s). Band densities are listed as fold increase above first detected band. The data are representative of two independent experiments.

Figure 16

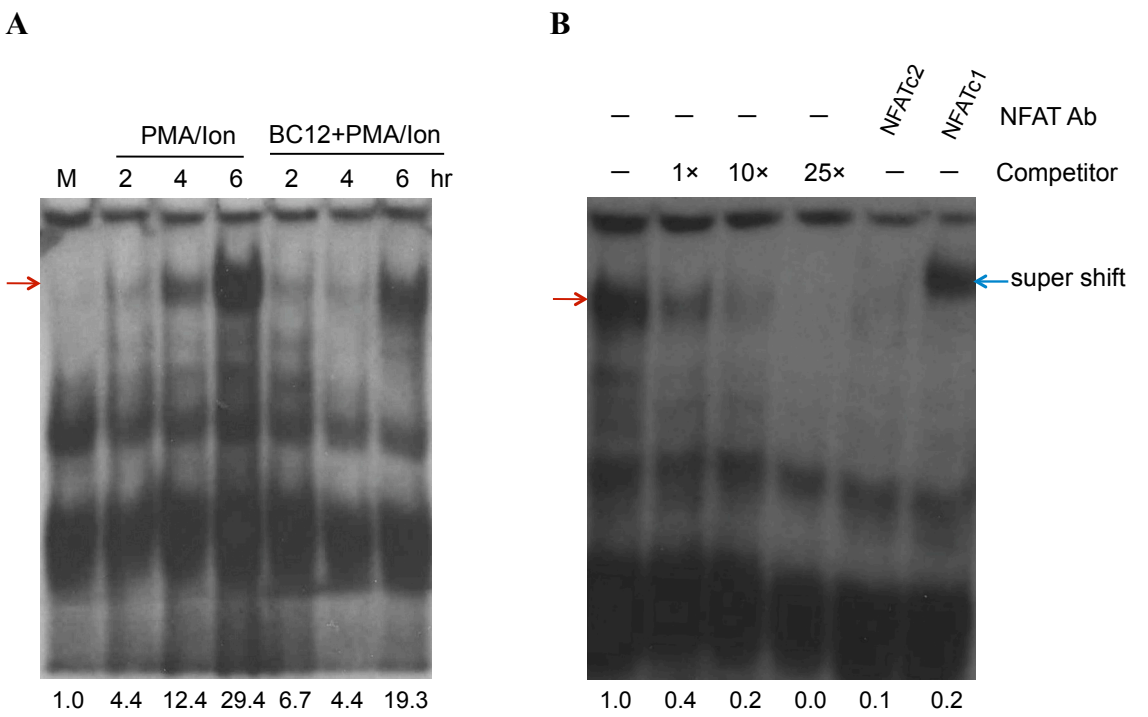

The distal NFAT site of the human *IL-2* promoter

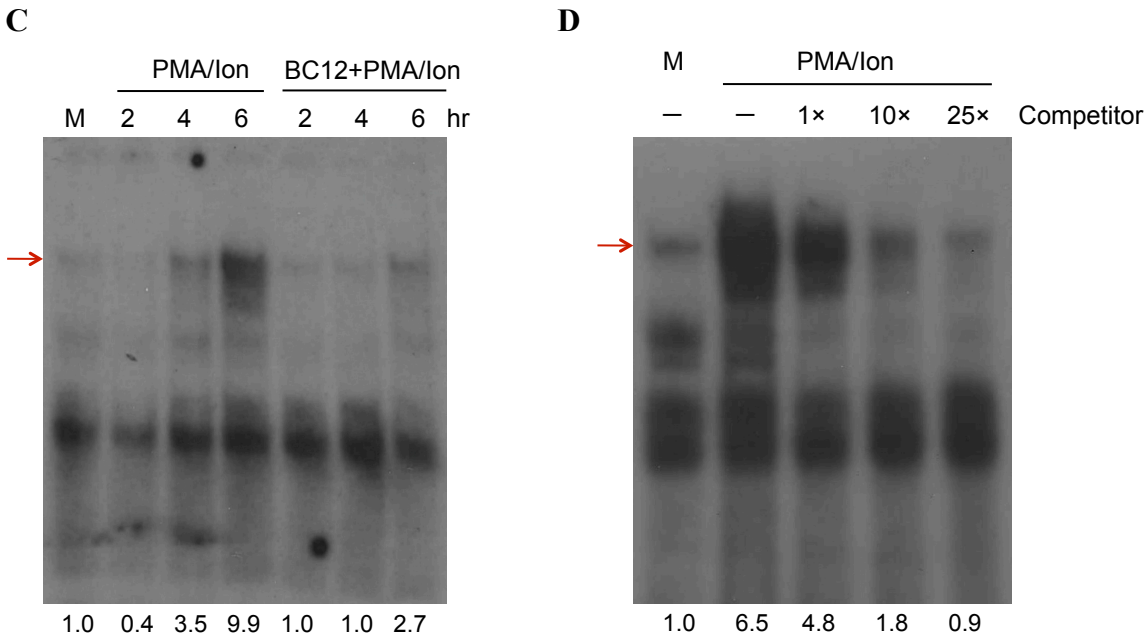

The NFAT-consensus-binding site

Figure 17. BC12 and its analogs have different effects on Transcription factor binding activity. Jurkat cells were cultured in media alone, or stimulated with 20 ng/ml PMA and 1 μM Ionomycin in the absence or presence of 10 μM of indicated compound for 4 hours. Nuclear extracts of Jurkat cells were prepared as described in *Material and Methods*. *A,* Nuclear extracts were analyzed by EMSA using radiolabeled probes corresponding to the NFκB-consensus-binding site as described in *Material and Methods*. *B,* Nuclear extracts were analyzed by EMSA using radiolabeled probes corresponding to the distal NFAT site of the human *IL-2* promoter. *C,* Nuclear extracts were analyzed by EMSA using radiolabeled probes corresponding to the AP-1-consensus-binding site. *D,* Nuclear extracts were analyzed by EMSA using radiolabeled probes corresponding to the Oct-1-consensus-binding site. The specific shifted bands are indicated by red arrows. Quantification of the specific bands was obtained with ImageJ software (v1.45s). Band densities are listed as fold increase above first detected band. The data are representative of two independent experiments.

Figure 17

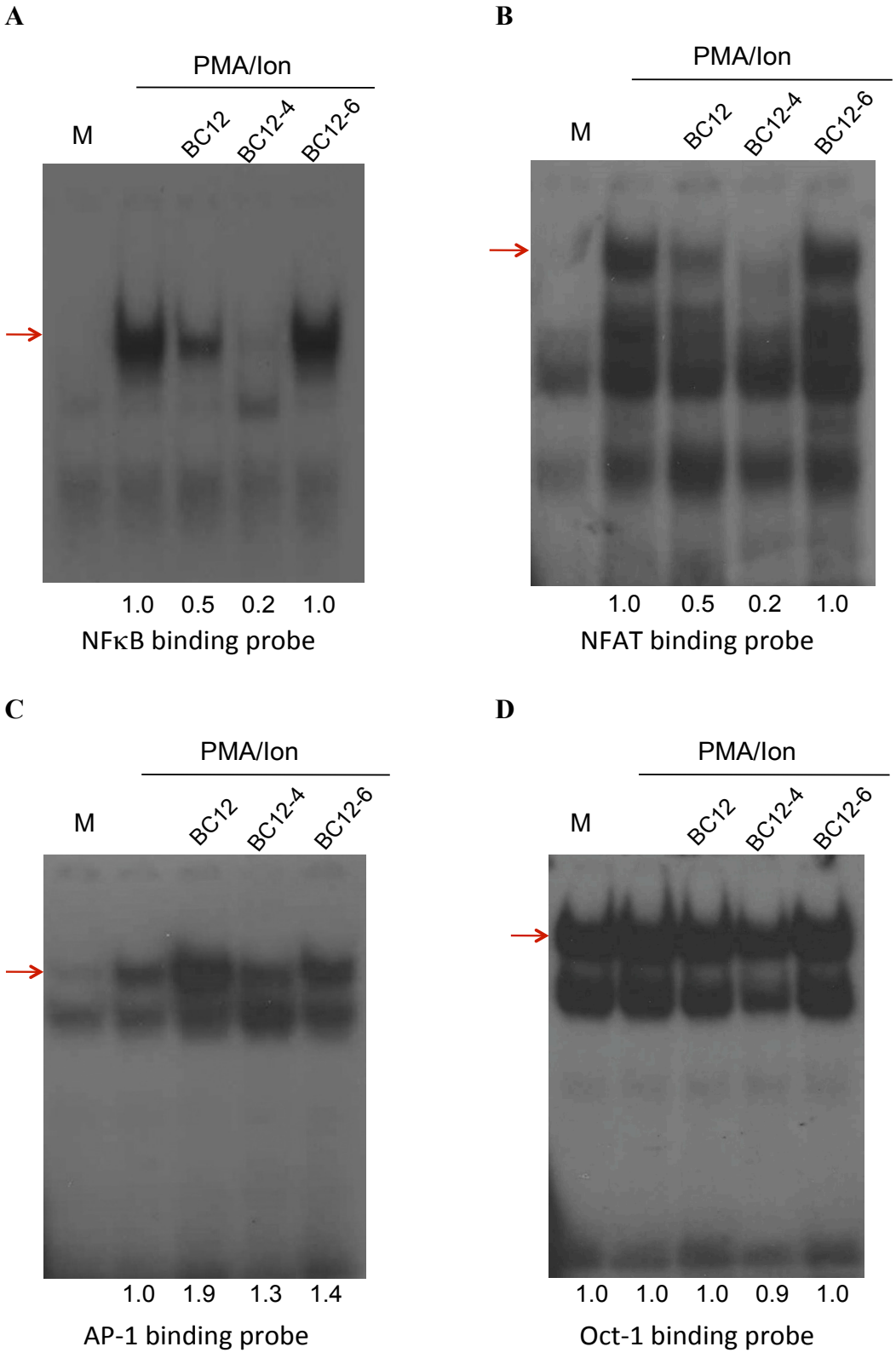
A
PMA/Ion
M
BC12
BC12-4
BC12-6
1.0 0.5 0.2 1.0
NFκB binding probe
B
PMA/Ion
M
BC12
BC12-4
BC12-6
1.0 0.5 0.2 1.0
NFAT binding probe
C
PMA/Ion
M
BC12
BC12-4
BC12-6
1.0 1.9 1.3 1.4
AP-1 binding probe
D
PMA/Ion
M
BC12
BC12-4
BC12-6
1.0 1.0 1.0 0.9 1.0
Oct-1 binding probe

Figure 18. BC12 and BC12-4 inhibit IL-2 secretion in activated mouse primary T cells. Mouse primary T cells were isolated from mouse spleens and cultured in media alone, or stimulated with 20 ng/ml PMA and 1 μM Ionomycin in the presence of DMSO or 10 μM of indicated compound. Supernatant from media sample served as time point 0. Supernatant from other samples were taken at 8, 24, and 48 hours. All supernatant samples were analyzed by ELISA to examine mouse IL-2 concentration as described in *Material and Methods*. The data are representative of two independent experiments, each conducted in duplicates. Error bars reflect standard deviation from the mean of duplicate measurements.

Figure 18

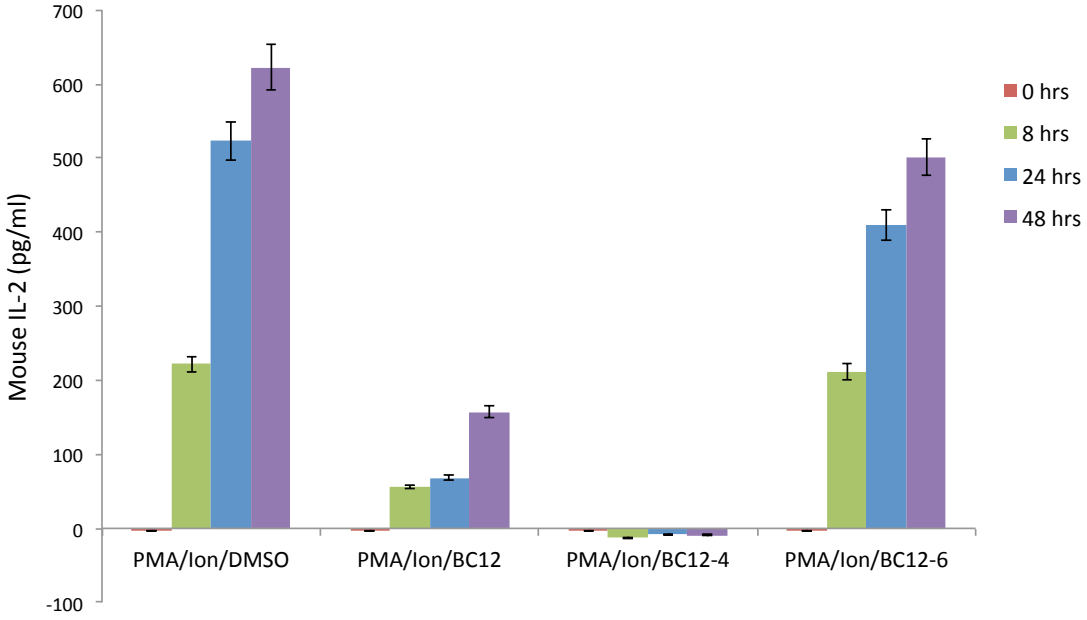
700
600
500
400
300
200
100
0
-100
Mouse IL-2 (pg/ml)
PMA/Ion/DMSO
PMA/Ion/BC12
PMA/Ion/BC12-4
PMA/Ion/BC12-6
0 hrs
8 hrs
24 hrs
48 hrs

Figure 19. BC12, BC12-4 and BC12-6 do not significantly reduce mouse primary T cell viability. Mouse primary T cells were isolated from mouse spleens and cultured in media alone, or stimulated with 20 ng/ml PMA and 1 μM Ionomycin in the presence of DMSO or 10 μM of indicated compound, or in the presence 10 μM of BC12 for 24 hours. The viability of cells was determined by propidium iodide staining. Samples were analyzed by flow cytometry as described in *Material and Methods*. The data are represented as the percentage of mouse primary T cells that are negative for propidium iodide staining. The data are representative of 10,000 cells and two independent experiments.

Figure 19

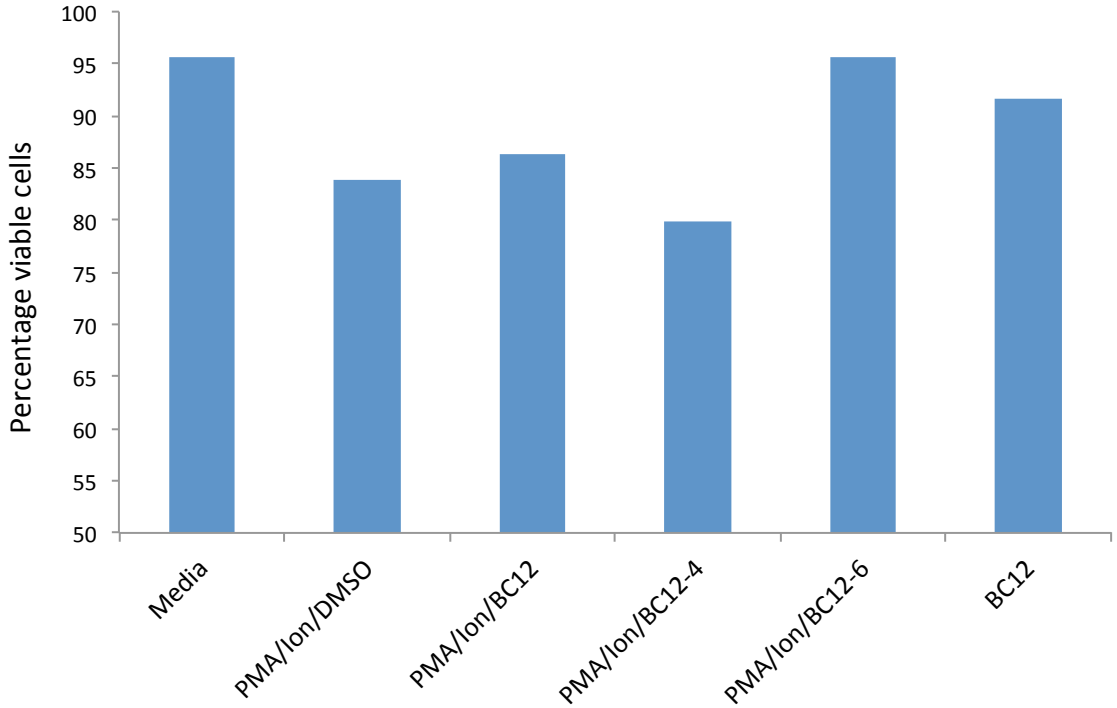
Percentage viable cells
100
95
90
85
80
75
70
65
60
55
50
Media
PMA/Ion/DMSO
PMA/Ion/BC12
PMA/Ion/BC12-4
PMA/Ion/BC12-6
BC12

Figure 20. BC12 inhibits mouse primary T cell proliferation. Mouse primary T cells were isolated from mouse spleens and cultured in media alone, or with 20 ng/ml PMA and 1 μM Ionomycin in the absence or presence of DMSO or 10 μM of indicated compound. At the indicated times, mouse T cells were stained with propidium iodide and cell cycle analyzed by flow cytometry as described in *Materials and Methods*. *A,* The data are represented as the percentage of mouse T cells in the S+G_2/M-phase of the cell cycle. The data are representative of 10,000 cells. *B,* Example flow cytometry data at 48 hours with indicated treatments.

Figure 20

A

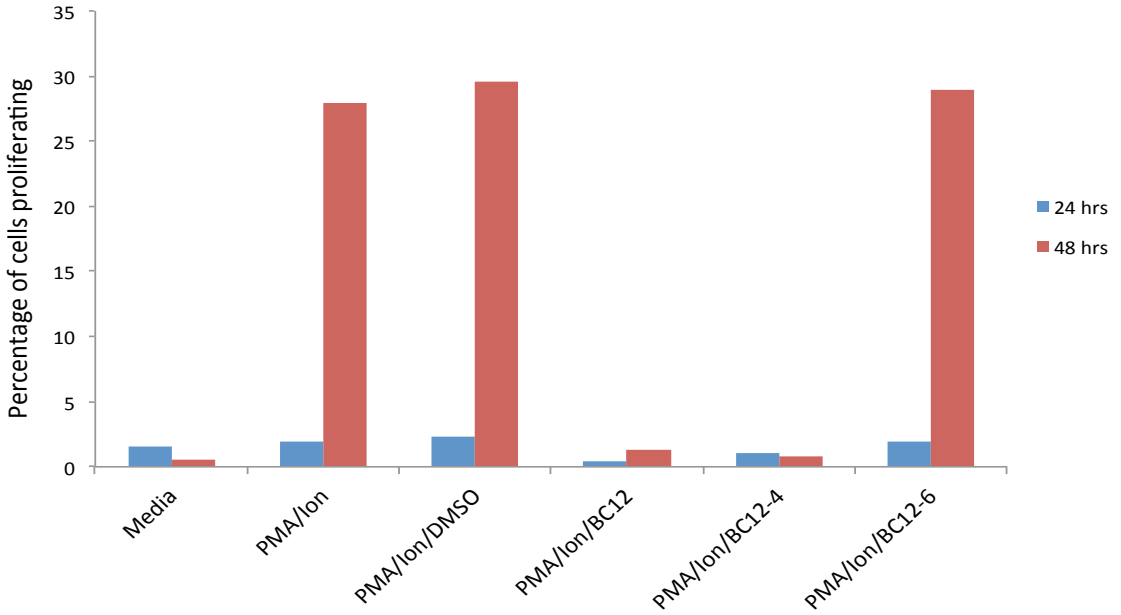
Percentage of cells proliferating
35
30
25
20
15
10
5
0
Media
PMA/Ion
PMA/Ion/DMSO
PMA/Ion/BC12
PMA/Ion/BC12-4
PMA/Ion/BC12-6
24 hrs
48 hrs

B

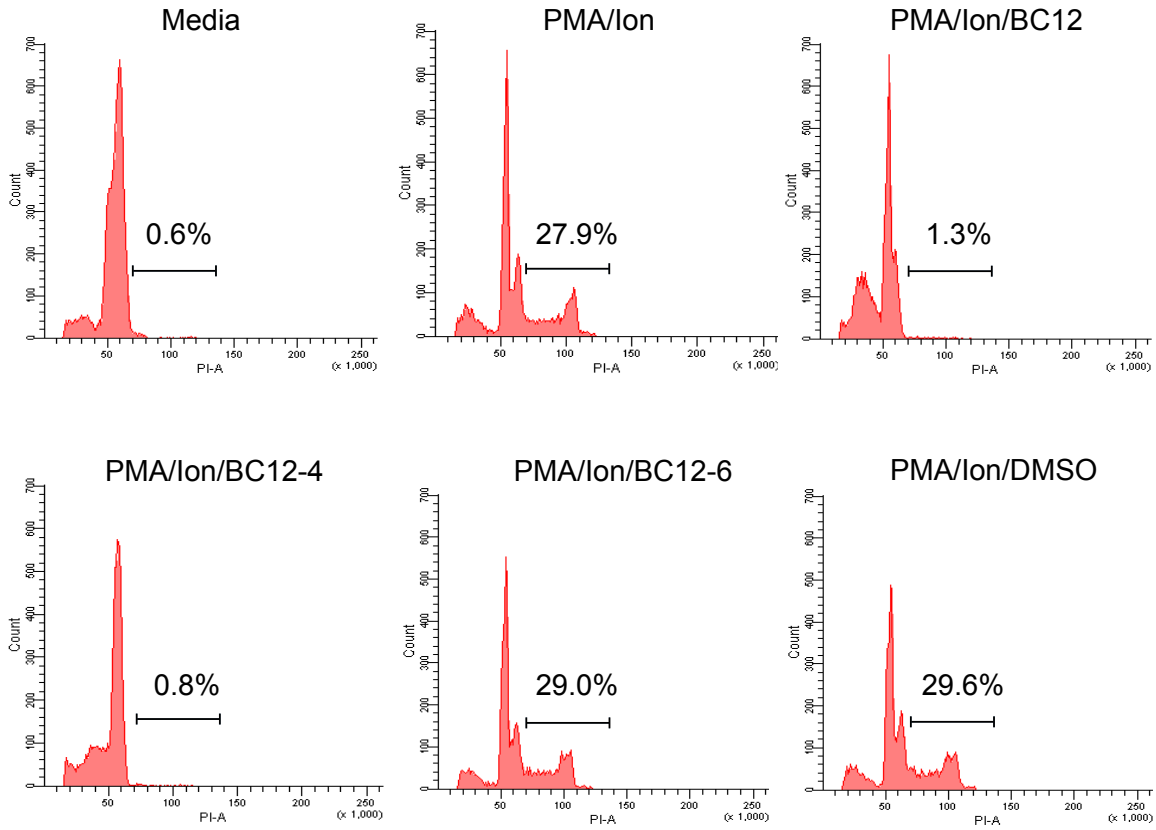
Media
0.6%
PMA/Ion
27.9%
PMA/Ion/BC12
1.3%
PMA/Ion/BC12-4
0.8%
PMA/Ion/BC12-6
29.0%
PMA/Ion/DMSO
29.6%
Count
PI-A
(x 1,000)

Figure 21. BC12 induces a moderate level of increase in hypodiploid DNA resulting in apoptosis in mouse primary T cells. Mouse primary T cells were isolated from mouse spleens and cultured in media alone, or with 20 ng/ml PMA and 1 μM Ionomycin in the absence or presence of DMSO or 10 μM of indicated compound. *A,* At the indicated times, mouse primary T cells were stained with propidium iodide and cell cycle analyzed by flow cytometry as described in *Materials and Methods*. The data are represented as the percentage of mouse T cells in the sub-G_0/G_1-phase of the cell cycle. The data are representative of 10,000 cells.

Figure 21

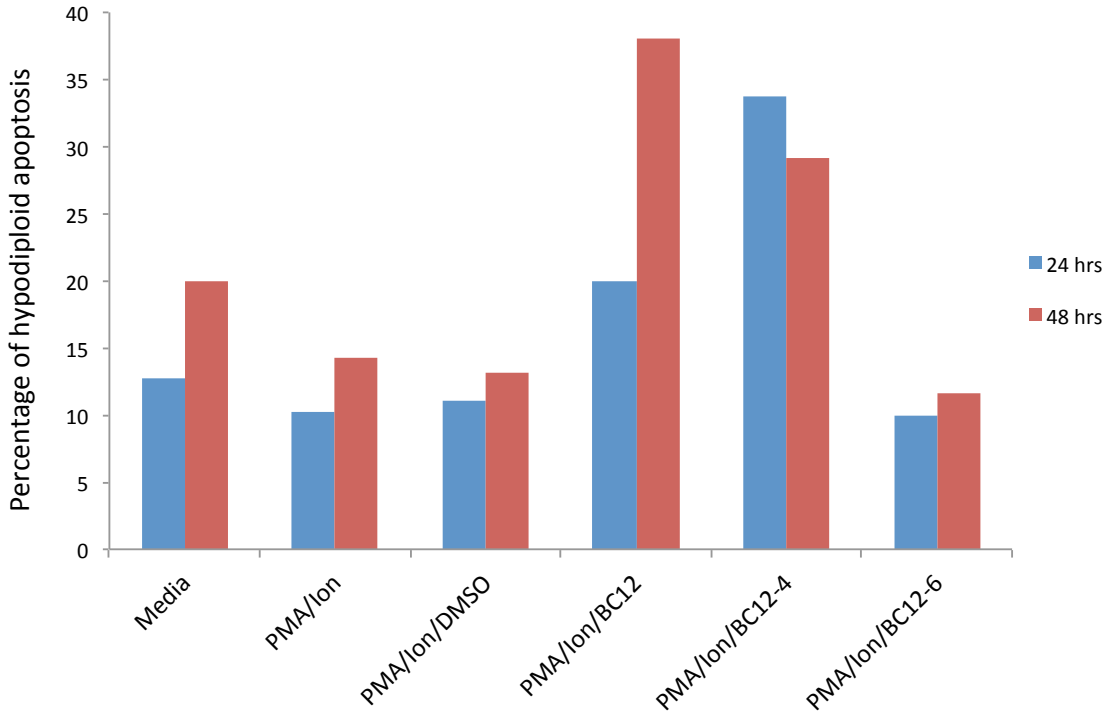
Percentage of hypodiploid apoptosis
40
35
30
25
20
15
10
5
0
Media
PMA/Ion
PMA/Ion/DMSO
PMA/Ion/BC12
PMA/Ion/BC12-4
PMA/Ion/BC12-6
24 hrs
48 hrs

Figure 22. BC12 augments activation signals in activated mouse primary T cells. Mouse primary T cells were cultured in media, pre-treated with 10 μM of BC12 or DMSO for 20 minutes before stimulating with 20 ng/ml PMA and 1 μM Ionomycin for various lengths of time, or treated with 10 μM of BC12 for 45 minutes. Whole cell extracts were prepared and Western blotting was performed with anti-phospho-ERK, anti-phospho-RSK90 and anti-phospho-IKKα/β antibodies as described in *Material and Methods*. The blot was stripped and reprobed for anti-β-actin antibody to ensure equal loading of each sample. Quantification of the Western blotting bands was obtained with ImageJ software (v1.45s). Both top and bottom band densities are listed as fold increase above first detected band relative to β-actin loading control. The data are representative of two independent experiments.

Figure 22

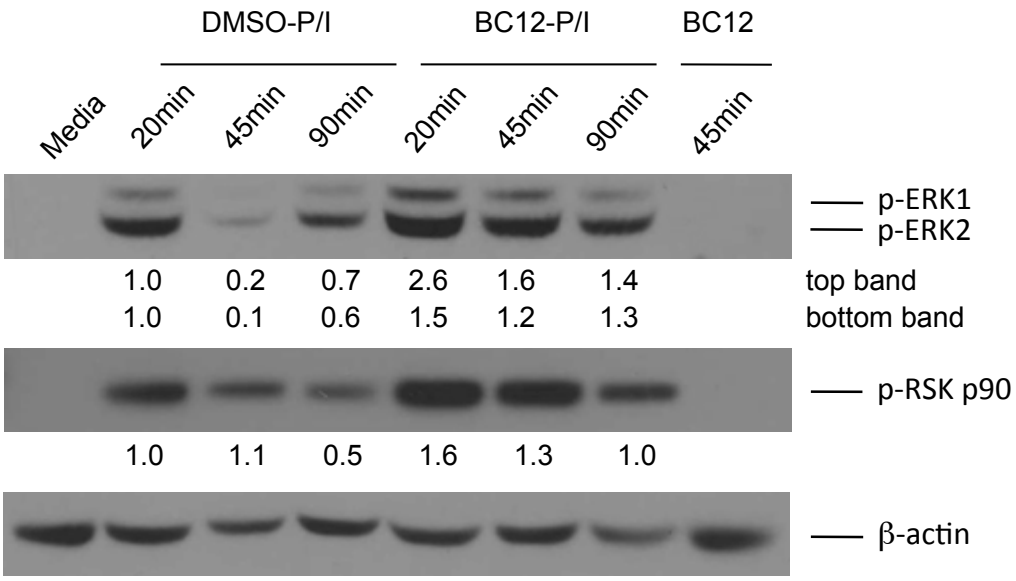
DMSO-P/I
BC12-P/I
BC12
Media
20min
45min
90min
20min
45min
90min
45min
p-ERK1
p-ERK2
1.0 0.2 0.7 2.6 1.6 1.4
top band
1.0 0.1 0.6 1.5 1.2 1.3
bottom band
p-RSK p90
1.0 1.1 0.5 1.6 1.3 1.0
β-actin

Figure 23. BC12 inhibits IL-2 secretion in activated human primary T cells. Human primary T cells were isolated from donor's blood as described in *Material and Methods*. *A,* Human primary T cells were stimulated with 20 ng/ml PMA and 1 μM Ionomycin in the presence or absence of 10 μM of BC12. The data are representative of two independent experiments, each conducted in duplicates. Error bars reflect standard deviation from the mean of duplicate measurements. *B,* Human primary T cells were stimulated with anti-CD3/anti-CD28 antibodies as described in *Material and Methods*, in the presence or absence of 10 μM of BC12. Supernatant samples were taken at indicated times and analyzed by ELISA to examine human IL-2 concentration as described in *Material and Methods*. The data are representative of two independent experiments, each conducted in duplicates. Error bars reflect standard deviation from the mean of duplicate measurements.

Figure 23

A

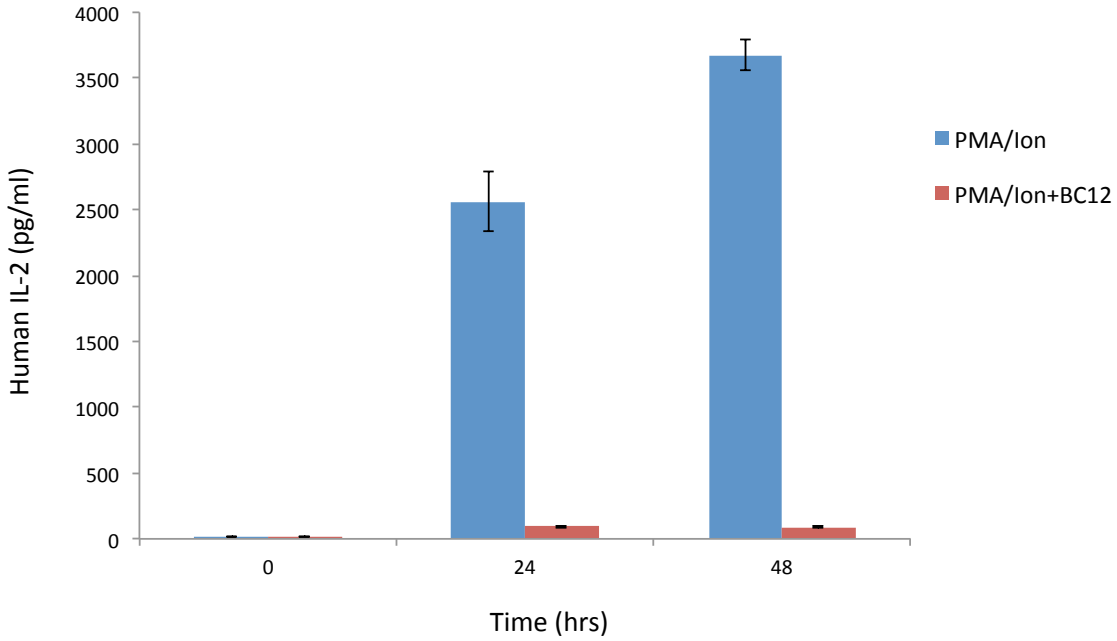
4000
3500
3000
2500
2000
1500
1000
500
0
Human IL-2 (pg/ml)
0
24
48
Time (hrs)
PMA/Ion
PMA/Ion+BC12

B

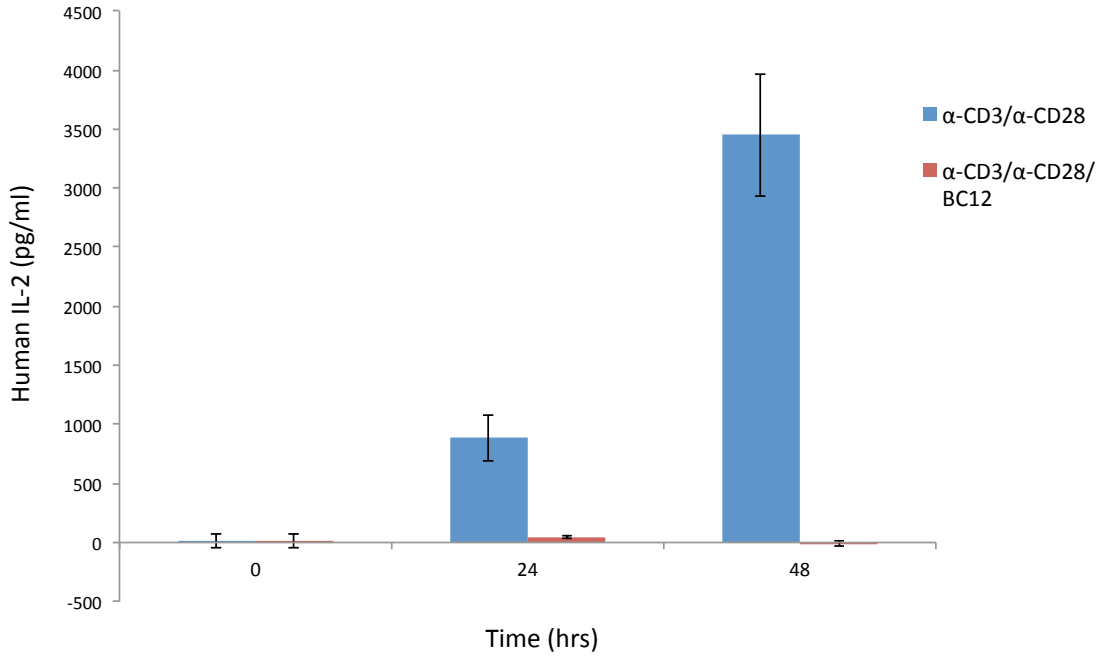
4500
4000
3500
3000
2500
2000
1500
1000
500
0
-500
Human IL-2 (pg/ml)
0
24
48
Time (hrs)
α-CD3/α-CD28
α-CD3/α-CD28/
BC12

Figure 24. BC12 induces cell death in human primary T cells. *A,* Human primary T cells were isolated from donor's blood as described in *Material and Methods*. *A,* Cells were cultured in media alone, or stimulated with 20 ng/ml PMA and 1 μM Ionomycin in the presence or absence of 10 μM of BC12 for 24 hours. Cell viability was determined by propidium iodide staining. Samples were analyzed by flow cytometry as described in *Material and Methods*. The data are represented as the percentage of cells that are negative for propidium iodide staining. *B,* Human primary T cells were cultured in media or treated with increasing doses of BC12 (0.05 μM, 0.5 μM, 2.5 μM, 5 μM, 10 μM, 25 μM, 50 μM and 100 μM) for 24 hours or 48 hours. Cell viability was determined by propidium iodide staining. Samples were analyzed by flow cytometry as described in *Material and Methods*. The data are represented as the percentage of cells that are positive for propidium iodide staining. The data are representative of 10,000 cells. Titration of BC12 was repeated at doses 5 μM, 10 μM, 20 μM, 50 μM and 100 μM. The same trend was observed in two independent experiments.

Figure 24

A

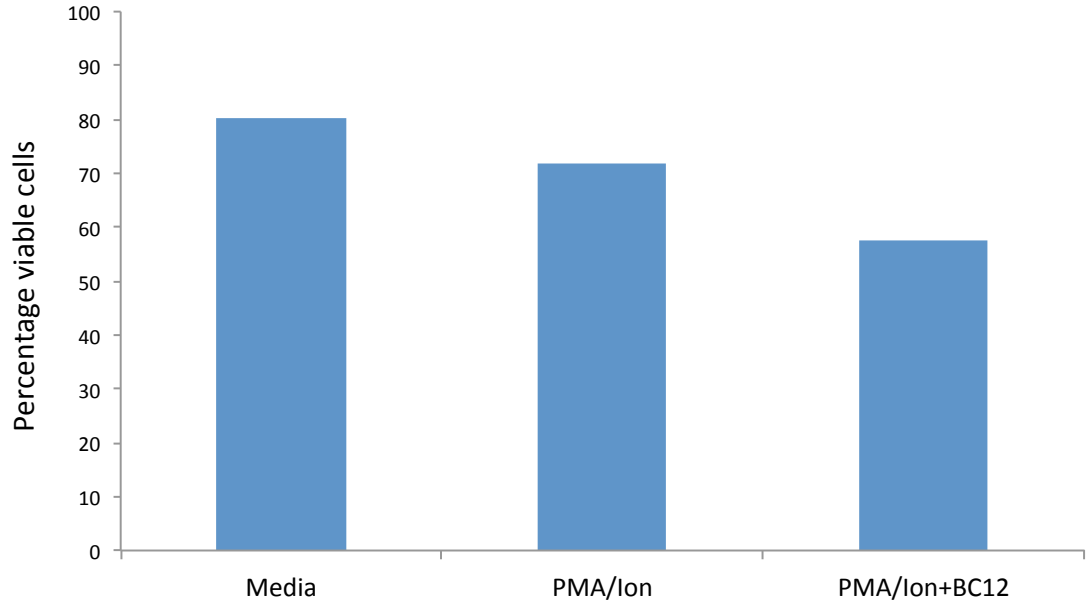
Percentage viable cells
100
90
80
70
60
50
40
30
20
10
0
Media
PMA/Ion
PMA/Ion+BC12

B

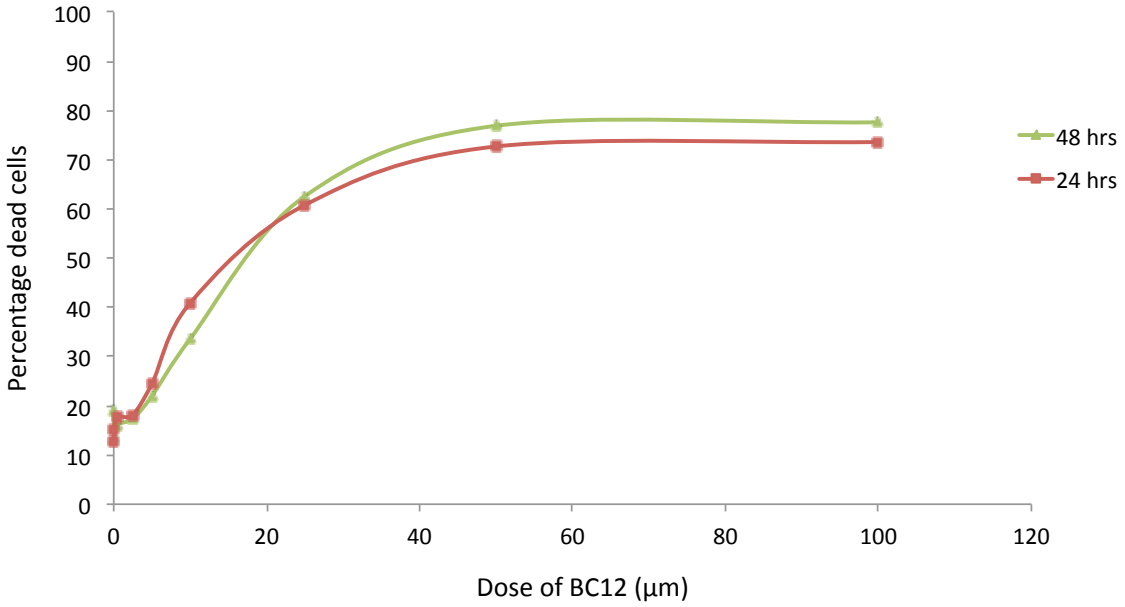
Percentage dead cells
100
90
80
70
60
50
40
30
20
10
0
0
20
40
60
80
100
120
Dose of BC12 (µm)
48 hrs
24 hrs

Figure 25. BC12 and BC12-4, but not BC12-6, inhibit IL-2 secretion in activated human primary T cells. Human primary T cells were stimulated with anti-CD3/anti-CD28 antibodies as described in *Material and Methods*, in the presence or absence of 10 μM of BC12, BC12-4 or BC12-6 for 24 hours. Supernatant samples were collected and analyzed by ELISA to examine human IL-2 concentration as described in *Material and Methods*. The data are representative of two independent experiments, each conducted in duplicates. Error bars reflect standard deviation from the mean of duplicate measurements.

Figure 25

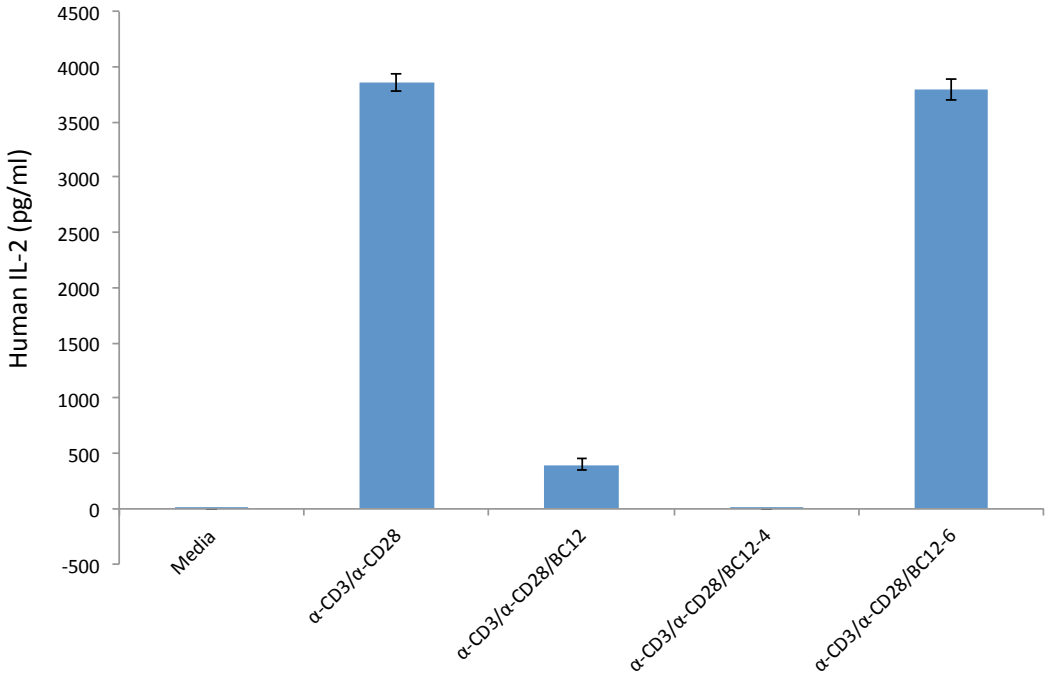
Human IL-2 (pg/ml)
4500
4000
3500
3000
2500
2000
1500
1000
500
0
-500
Media
α-CD3/α-CD28
α-CD3/α-CD28/BC12
α-CD3/α-CD28/BC12-4
α-CD3/α-CD28/BC12-6

Figure 26. BC12 decreases the IL-2 mRNA level in activated human primary T cells. Human primary T cells were isolated from donor's blood and stimulated with 20 ng/ml PMA and 1 μM Ionomycin in the presence or absence of 10 μM of BC12 for 4 hours. *IL-2* mRNA was analyzed by semi-quantitative RT-PCR following normalization to *β-actin* as described in *Material and Methods*. Error bars reflect standard deviation from the mean of triplicate measurements.

Figure 26

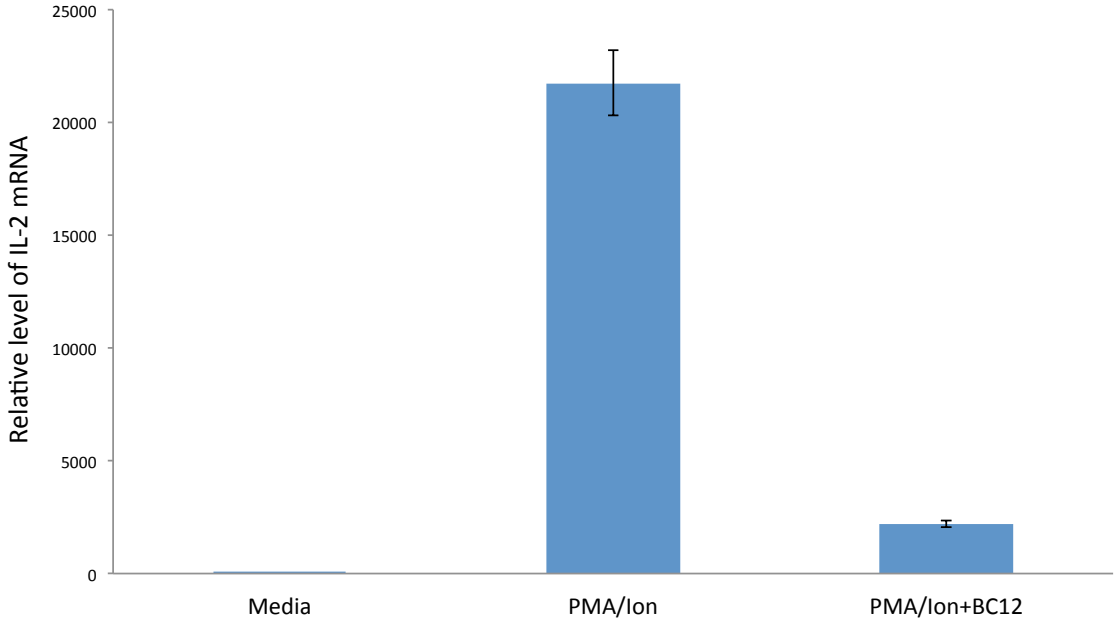
Relative level of IL-2 mRNA
25000
20000
15000
10000
5000
0
Media
PMA/Ion
PMA/Ion+BC12

Figure 27. BC12 selectively inhibits Th2 cytokines over Th1. Human $CD4^+$ T cells were cultured in media alone, or stimulated with 20 ng/ml PMA and 1 μM Ionomycin in the presence or absence of 10 μM of BC12. Supernatant samples were collected at 24 hours and analyzed by multi-cytokine ELISA as described in *Material and Methods*. The same trend was observed in two independent experiments.

Figure 27

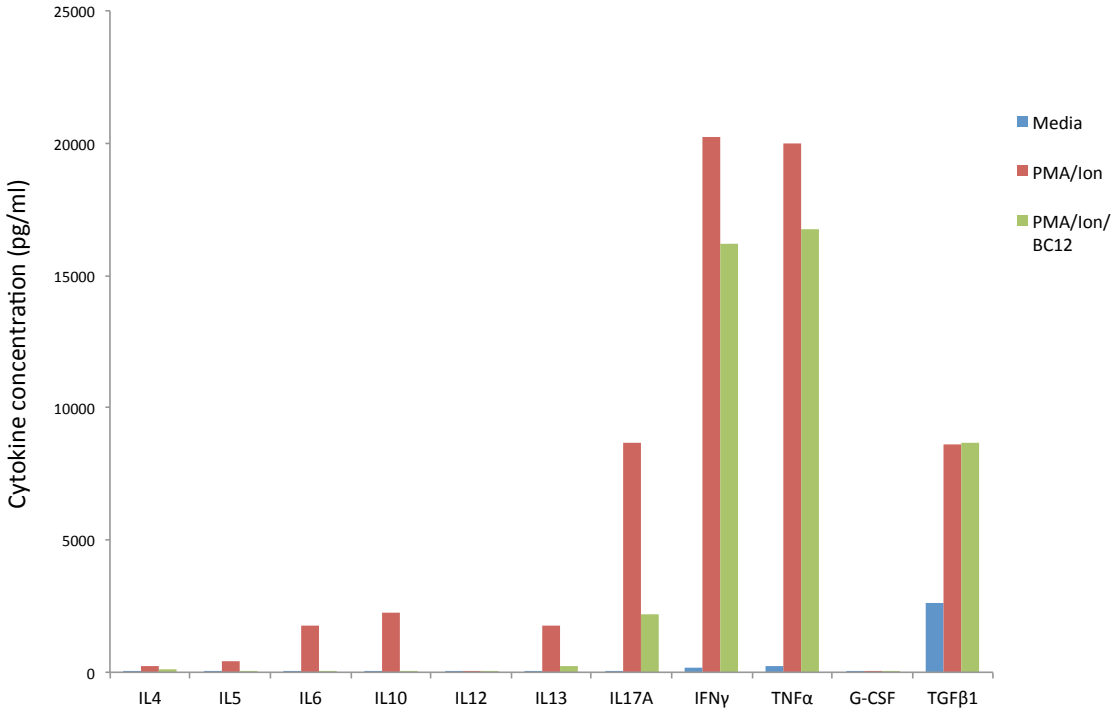
25000
20000
15000
10000
5000
0
Cytokine concentration (pg/ml)
IL4
IL5
IL6
IL10
IL12
IL13
IL17A
IFNγ
TNFα
G-CSF
TGFβ1
Media
PMA/Ion
PMA/Ion/ BC12

Table 1. BC12 selectively inhibits Th2 cytokines over Th1. Cytokines tested in Figure 25 were sorted by cell types that secret them by color (Th1 as red, Th2 as blue, Th17 as yellow and Treg as purple), or by secretion response to BC12 into inhibited, not affected, and inconclusive.

Table 1.

Inhibited	Not affected	Inconclusive	
IL4	IFNγ	IL12	Th1
IL5	TNFα	G-CSF	Th2
IL6	TGFβ1		Th17
IL10			Treg
IL13			
IL17A			

Chapter Two

BC12 induces apoptosis in LY18, U937 cells and primary B cells

RESULTS

BC12 induces apoptosis in LY18 cells and human primary B cells

It has been reported that PDE4 inhibitors induce apoptosis in malignant lymphoid cells [6–10]. Theophylline and PDE4 inhibitors were reported to augment glucocorticoid-mediated apoptotic effects in B cell chronic lymphocytic leukemia (B-CLL) [9]. Our collaborator, Dr. Hoffman and his laboratory at Boston College, also tested several novel *in vitro* PDE4 and PDE7 inhibitors on B-CLL cells. Some of these compounds exhibited potent activity in inducing apoptosis in B-CLL cells (unpublished data). LY18 is a human Diffuse Large B Cell Lymphoma (DLBCL) cell line [159], and my study sought to use LY18 cell line as a model system for malignant human B cells.

To begin to evaluate the effect of PDE inhibitors on human LY18 cells, we tested a series of *in vitro* PDE4 and PDE7 inhibitors identified from high-throughput fission-yeast-based screen (HTS) by Hoffman Lab. Among the 5 compounds we tested, BC54 was the most potent PDE4 and PDE7 dual inhibitor identified in both HTS and *in vitro* PDE assays, which also induced a higher percentage of apoptosis in B-CLL cells than a combination of rolipram and BRL50481 (unpublished data). BC12 is one of the best PDE7A inhibitors in both HTS and *in vitro* assays. BC38 is a moderate inhibitor of PDE7A and 7B in cell-based assays. BC51 is an *in vitro* PDE4A and 7A inhibitor. BC58 is a potent *in vitro* inhibitor of both PDE4B and 4D (unpublished data). Surprisingly, the effects on LY18 cell viability were not correlated to the PDE inhibitory activity of the compounds (Figure 28). Specifically, BC12 exhibited the most significant effect on LY18 cell viability after 48 hours of treatment, while the most potent and broad-spectrum

inhibitor BC54 did not display a measurable effect up to a dose of 100 μM compared to the DMSO control (Figure 28A). We then compared the effects of BC12, BC38 and rolipram at a dose of 20 μM; BC12 was the only compound that significantly decreased cell viability at this dose (Figure 28B).

To further confirm the effect of BC12 on LY18 cell viability, we performed a more detailed dose-titration of BC12 and analyzed cell viability at 24, 48 and 72 hours post treatment by propidium iodide staining followed by flow cytometric analysis. BC12 induced LY18 cell death in a dose-dependent manner (Figure 29). At a dose of 20 μM, BC12 resulted in about 95% of cell death at 24 hours (Figure 29).

We next sought to determine whether LY18 cells were undergoing apoptosis after BC12 treatment. The presence of apoptotic cells was detected by TUNEL assay, which labels the terminal end of DNA to indicate DNA fragmentation. BC12 induced approximately 35% of apoptosis at 10 μM, and 75% at 20 μM at both 24 and 48 hours (Figure 30).

To obtain further evidence of the pathway underlying the apoptotic effect induced by BC12 on LY18 cells, we analyzed caspase pathway activation by Western blotting. Following treatment with 20 μM of BC12, LY18 cells displayed a time-dependent increase in active caspase 8 and caspase 3 levels (Figure 31A, BC12). Specifically, caspase 8 cleavage and activation was observed at 3 hours post treatment and peaked at 12 hours. Full-length caspase 3 levels showed a decrease at 12 hours to about 60% and cleaved caspase 3 was observed at 24 hours (Figure 31A, BC12). Note that both antibodies detect full-length caspases and the large fragment of capases but not small ones. Due to the limited sensitivity of Western blotting, an alternative approach was also

employed. After treating with 20 μM of BC12 for indicated length of time, LY18 cells were stained for active caspase 3 and analyzed by flow cytometry. From 12 to 48 hours, approximately 90% of the cells were stained positive for active caspase 3 (Figure 31B). Of note, the flow cytometric analysis is more sensitive and quantitative insofar as it detects individual cells for the presence of cleaved and active caspase 3, while Western blotting analyzes the cell population as a whole. These results indicate that most of the cells activate caspase pathway by 12 hours post BC12 treatment and that in apoptotic LY18 cells, only a small portion of caspase 8 and caspase 3 protein are cleaved and activated, while the majority remain inactive pro-enzymes.

Active caspase 3 proteolytically cleaves and activates other targets relevant to apoptosis, including Poly ADP Ribose Polymerase (PARP) [180]. We therefore examined the activation of PARP enzyme following BC12 treatment. PARP cleavage was observed after 6 hours post treatment by Western blotting (Figure 32). Taken together, these data confirm that LY18 cells undergo apoptosis through activation of caspase 8 and caspase 3, following BC12 treatment.

We then sought to test BC12 derivatives on LY18 cell viability. Among the six compounds tested, BC12-7 and BC12-4 showed strong effects in inducing cell death. BC12-1, BC12-2 and BC12-6 had minimal effects on LY18 viability (Figure 33B). Comparing the structures of BC12, BC12-7 and BC12-4, we can speculate that substitutions of R3 and R1 are well tolerated in eliciting the effects. In contrast, substitution of R2 affects *in vivo* activity (Figure 33A). To note that BC12-6 is the best PDE7A inhibitor based on *in vitro* kinase assay among the seven derivatives and BC12-4 does not have any PDE inhibitory activity (refer to Chapter One Figure 7). Thus, the

effectiveness in inducing cell death was not correlated to the PDE inhibitory activity of the compounds, which suggests that the effect of inducing apoptosis in LY18 cells is probably not attributable to PDE inhibition.

Next, we sought to examine cell cycle progression in LY18 cells treated with BC12. The overlay graphs represent total cell counts (Figure 34A), while the bar graphs represent the percentage of cells in each phase of cell cycle (Figure 34B and C). At 24 hours post treatment, 10 μM of BC12 did not significantly alter cell cycle progression, except for a small decrease in S+G_2/M-phase and increase in sub-G_0/G_1-phase, which indicates apoptotic cells (Figure 34A, 34B and 34C, 24hrs). At 48 hours, 10 μM of BC12 decreased the G_0/G_1 cell population from 70% to 48% compared to untreated cells (Figure 34A and 34B, 48hrs). Treating with 20 μM of BC12 decreased the G_0/G_1 cell population from 57% to 44% at 24 hours and from 70% to 41% at 48 hours, resulting in an increase in sub-G_0/G_1 population (Figure 34A and 34B). Notably, BC12 did not measurably affect both cell counts and percentage of S+G_2/M-phase population at both time-points (Figure 34A and 34C). These data indicate that BC12 does not cause cell cycle arrest in LY18 cells and preferably induces apoptosis in cells in G_0/G_1-phase.

Finally, we tested BC12 on human primary B cell viability. Human primary B cells were obtained from healthy donors' blood and treated with increasing dose of BC12 for 24 and 48 hours. BC12 induced about 70% cell death at doses of 50 μM or higher. At a dose of 20 μM, BC12 induced about 50% cell death in human primary B cells (Figure 35), as compared to about 95% cell death in LY18 cells (Figure 29). Taken together, BC12 induces cell death in human primary B cells in a dose-dependent manner, while prolonged treatment did not significantly increase the effectiveness. Moreover, there

exists a dose window that BC12 induces significantly higher percentage of cell death in human malignant LY18 cells than primary B cells.

BC12 induces apoptosis in U937 cells

U937 is a human leukemia monocyte cell line [166]. We sought to use the U937 cell line as a model system for human malignant monocytes. To investigate the effects of *in vitro* PDE inhibitors on U937 cells, we started with testing four compounds on U937 cells at a dose of 20 μM for 24 and 48 hours (Figure 36). Similarly as in LY18 cells, BC12 treatment resulted in above 90% cell death at both time-points. BC38 induced approximately 33% cell death at 48 hours, while both BC51 and BC54 did not exhibit measurable effects on U937 cell viability compared to media control (Figure 36). A dose-dependent effect of BC12 was confirmed by titration of BC12 on U937 cell viability for 24 and 48 hours (Figure 37). BC12 potently decreases U937 cell viability at a dose of 20 μM, but not 10 μM (Figure 37).

Next, we sought to determine whether U937 cells were undergoing apoptosis after BC12 treatment by TUNEL assay (Figure 38). At both 24 and 48 hours, 10 μM of BC12 only showed a minimal effect in inducing apoptosis compared to DMSO control. Treating cells with 20 μM of BC12 induced about 80% apoptosis at 24 hours and 70% at 48 hours (Figure 38). These results confirmed that decreased U937 cell viability by BC12 treatment was due to apoptosis.

We then evaluated caspase and PARP activation in U937 cells. Similarly as in LY18 cells, caspase 8 and caspase 3 were both cleaved and activated in U937 cells treated with 20 μM of BC12 (Figure 39A and 39B). The full-length caspase 8 and 3

started to decrease at 9 hours to about 50% and 20% respectively. Cleavage of both caspase 8 and 3 was observed beginning at 6 hours, which continued to increase from 6 hours to 12 hours post treatment. Both full-length and cleaved caspase 8 were almost undetectable at 24 hours (Figure 39A, BC12). PARP cleavage was observed at 6 hours and almost completed at 12 hours (Figure 40). Staining and flow cytometric analysis indicated that about 90% of cells activated caspase 3 at 12 to 48 hours (Figure 39B). Interestingly, unlike LY18 cells, in which a great amount of caspase proteins remained in pro-enzyme forms, majority of the caspase 8 and 3 proteins were cleaved and activated during the apoptosis process in U937 cells (Figure 39 and 31).

Next, we also evaluated cell cycle progression of U937 cells treated with BC12. Treating with 10 μM of BC12 decreased the percentage of cells in G_0/G_1 phase by approximately 15% at all time points examined and $S+G_2/M$ phase by 10% at 15 and 24 hours, resulting in increased hypodiploid DNA (Figure 41A, 41B and 41C). 20 μM of BC12 resulted in a 30-40% decrease in G_0/G_1 phase, a 10-20% decrease in $S+G_2/M$ phases, and an increase in hypodiploid DNA (Figure 41A, 41B and 41C). These data indicated that BC12 did not halt cell cycle progression of U937 cells.

To obtain further evidence that BC12 does not block cell cycle progression in U937 cells, we sought to examine the level of DNA synthesis by BrdU incorporation (Figure 42). 40% of DMSO treated control cells incorporated BrdU at 24 hours and 35% at 48 hours (Figure 42, DMSO). Compared to media or DMSO control, BC12 treatment resulted in a slight increase in the percentage of cells with BrdU incorporation, approximately 57% at both 24 and 48 hours (Figure 42, BC12). This increase in percentage is very likely due to a higher amount of cell loss in other phases of cell cycle

than in S-phase, since the cells were undergoing apoptosis after BC12 treatment. Taken together, these results suggest that BC12 did not block cell cycle progression or inhibit DNA synthesis in U937 cells.

FIGURES AND LEGENDS

Figure 28. *In vitro* PDE7 inhibitors have various effects on LY18 cell viability. *A,* LY18 cells were cultured in media in the presence of DMSO, or various *in vitro* PDE inhibitors with increasing doses (0.1 μM, 1 μM, 10 μM, 50 μM and 100 μM) for 48 hours. Titration of BC54 was repeated at doses 10 μM, 50 μM and 100 μM. Treatment with other compounds was repeated at the highest dose. *B,* LY18 cells were cultured in media, or in the presence of 20 μM *in vitro* PDE inhibitor BC12, BC38 or rolipram for indicated lengths of time. Cells were collected and cell viability was determined by propidium iodide staining. Samples were analyzed by flow cytometry as described in *Material and Methods*. The data are represented as the percentage of cells that are positive for propidium iodide staining. The data are representative of 10,000 cells.

Figure 28

A

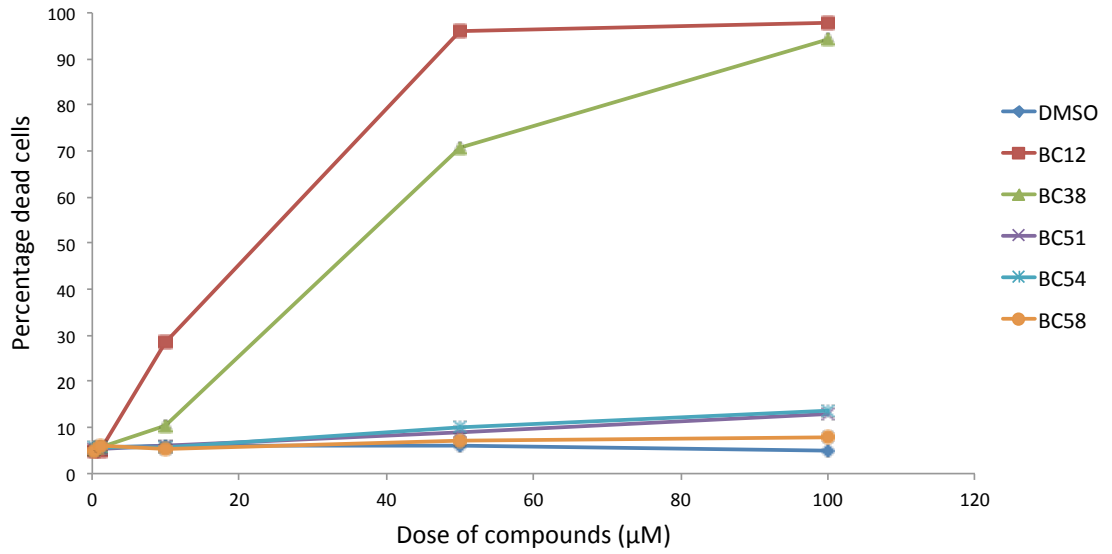
Percentage dead cells
Dose of compounds (µM)
DMSO
BC12
BC38
BC51
BC54
BC58

B

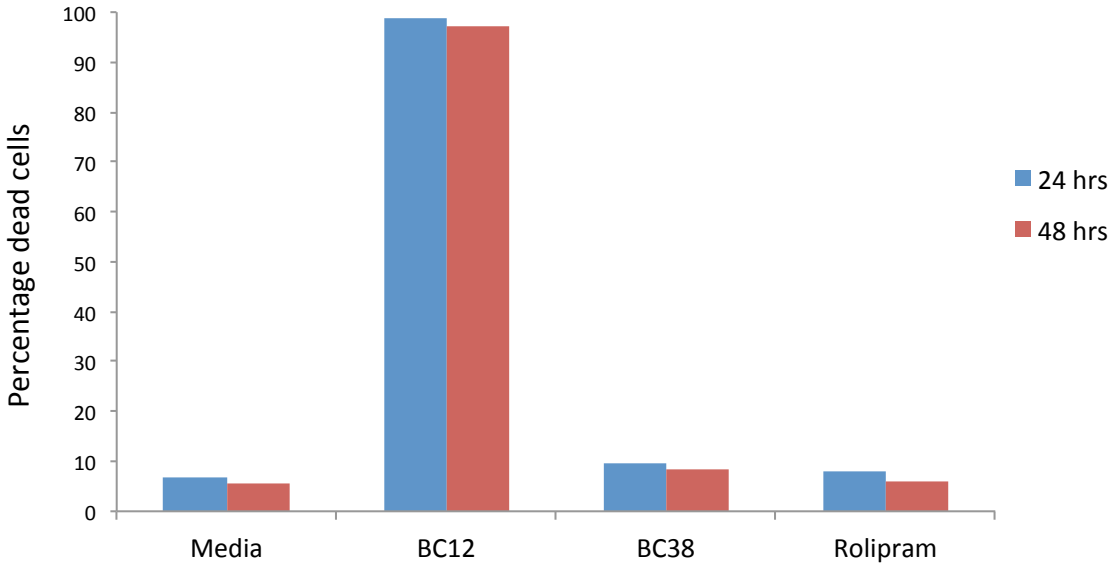
Percentage dead cells
Media
BC12
BC38
Rolipram
24 hrs
48 hrs

Figure 29. BC12 induces dose-dependent decrease of cell viability in LY18 cells. LY18 cells were cultured in media alone, or with increasing dose of BC12 (0.1 μM, 1 μM, 10 μM, 20 μM and 50 μM). At the indicated times, cells were collected and cell viability was determined by propidium iodide staining. Samples were analyzed by flow cytometry as described in *Material and Methods*. The data are represented as the percentage of cells that are positive for propidium iodide staining. The data are representative of 10,000 cells. Titration of BC12 was repeated at doses 10 μM, 20 μM and 50 μM. The same trend was observed in two independent experiments.

Figure 29

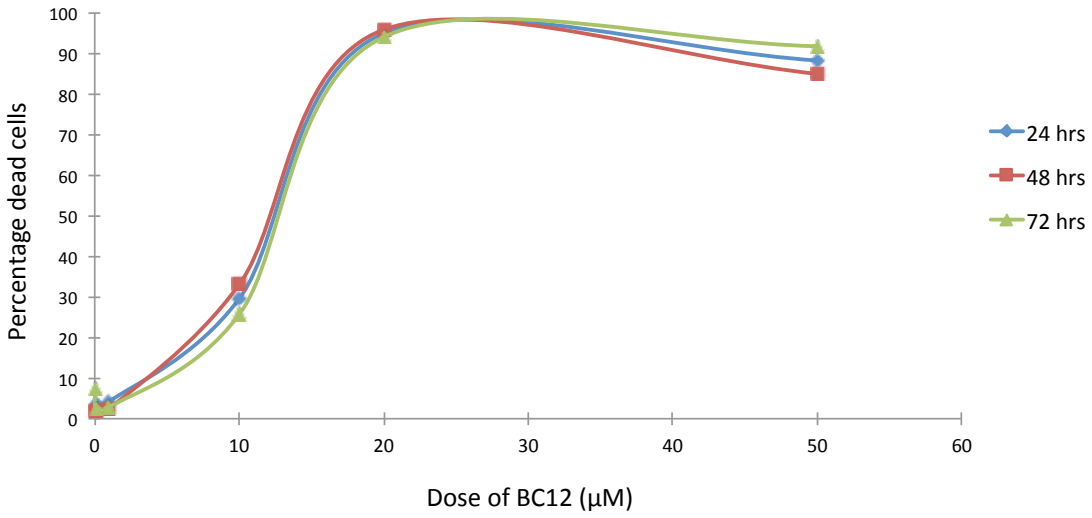
Percentage dead cells
100
90
80
70
60
50
40
30
20
10
0
0
10
20
30
40
50
60
Dose of BC12 (µM)
24 hrs
48 hrs
72 hrs

Figure 30. BC12 induces apoptosis in LY18 cells. LY18 cells were cultured in media with DMSO, 10 μM or 20 μM of BC12. At the indicated times, cells were collected and cell apoptosis was analyzed by TUNEL assay as described in *Material and Methods*. The data are represented as the percentage of cells that are positive for FITC staining. The data are representative of 10,000 cells, completed as two independent experiments.

Figure 30

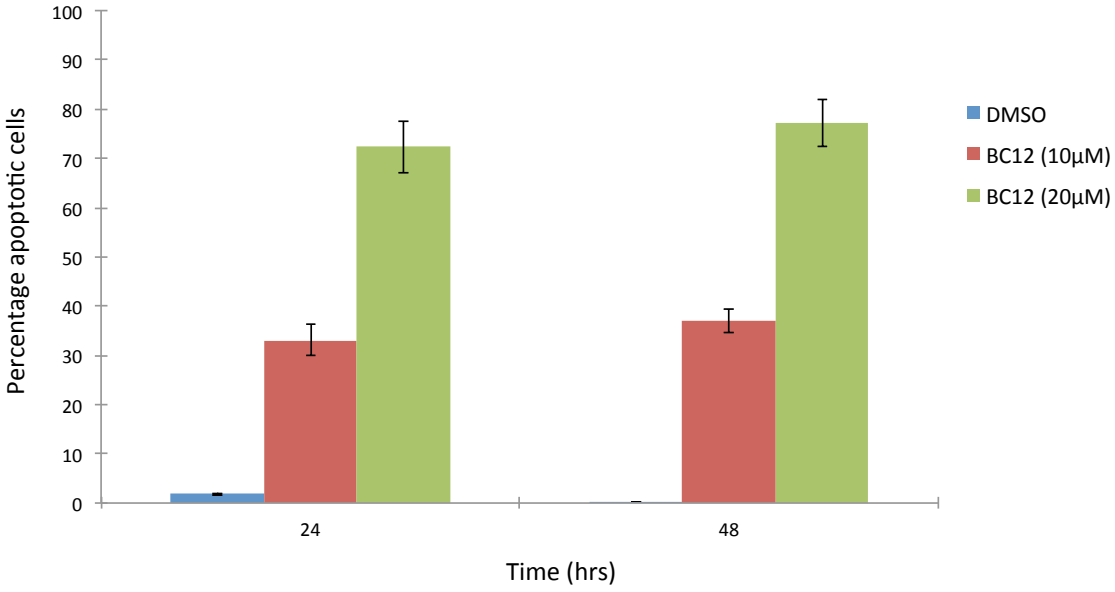
100
90
80
70
60
50
40
30
20
10
0
Percentage apoptotic cells
24
48
Time (hrs)
DMSO
BC12 (10µM)
BC12 (20µM)

Figure 31. BC12 activates caspase pathway in LY18 cells. *A,* LY18 cells were cultured in media with DMSO or 20 μM of BC12 for indicated lengths of time. Whole cell extracts were prepared and Western blotting was performed with anti-caspase 8 and anti-caspase 3 antibodies that recognize both full length and cleaved caspases as described in *Material and Methods*. The blot was stripped and reprobed for anti-HSP90 antibody to ensure equal loading of each sample. Quantification of the Western blotting bands was obtained with ImageJ software (v1.45s). Both top and bottom band densities are listed as fold increase above first detected band relative to HSP90 loading control. The data are representative of two independent experiments. *B,* LY18 cells were cultured in media with DMSO or 20 μM of BC12 for indicated lengths of time. Cells were collected and stained with FITC-conjugated anti-active caspase 3 antibody, followed by flow cytometric analysis as described in *Material and Methods*. The data are represented as the percentage of cells that are positive for active caspase 3 staining. The data are representative of 10,000 cells, completed as two independent experiments.

Figure 31

A

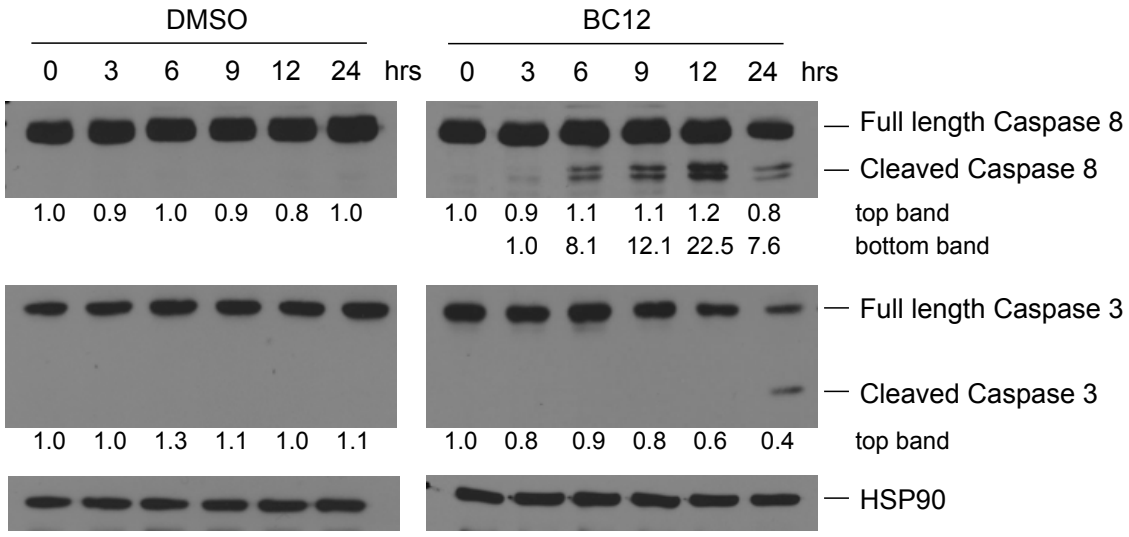
DMSO
BC12
0 3 6 9 12 24 hrs
0 3 6 9 12 24 hrs
Full length Caspase 8
Cleaved Caspase 8
1.0 0.9 1.0 0.9 0.8 1.0
1.0 0.9 1.1 1.1 1.2 0.8
top band
1.0 8.1 12.1 22.5 7.6
bottom band
Full length Caspase 3
Cleaved Caspase 3
1.0 1.0 1.3 1.1 1.0 1.1
1.0 0.8 0.9 0.8 0.6 0.4
top band
HSP90

B

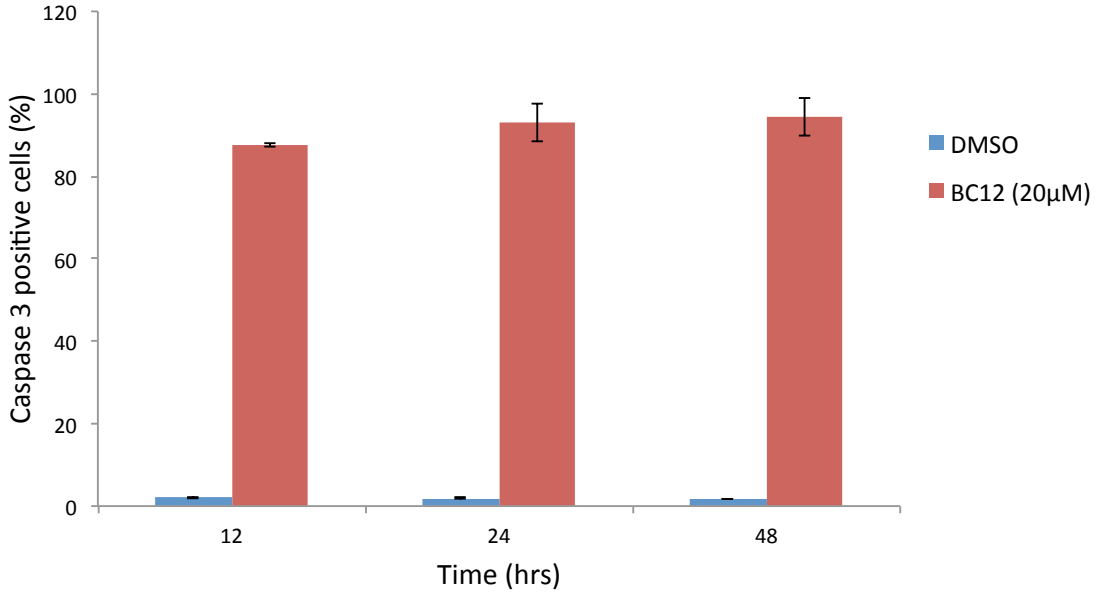
Caspase 3 positive cells (%)
120
100
80
60
40
20
0
12
24
48
Time (hrs)
DMSO
BC12 (20µM)

Figure 32. BC12 induces PARP cleavage and activation in LY18 cells. LY18 cells were cultured in media with DMSO or 20 μM of BC12 for indicated lengths of time. Whole cell extracts were prepared and Western blotting was performed with anti-PARP antibody that recognizes full length and cleaved PARP as described in *Material and Methods*. The blot was stripped and reprobed for anti-HSP90 antibody to ensure equal loading of each sample. Quantification of the Western blotting bands was obtained with ImageJ software (v1.45s). Both top and bottom band densities are listed as fold increase above first detected band relative to HSP90 loading control. The data are representative of two independent experiments.

Figure 32

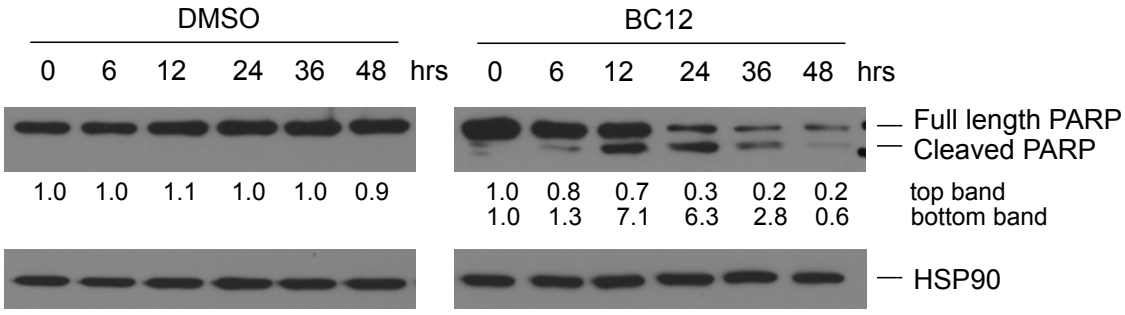
DMSO
BC12
0 6 12 24 36 48 hrs
0 6 12 24 36 48 hrs
Full length PARP
Cleaved PARP
1.0 1.0 1.1 1.0 1.0 0.9
1.0 0.8 0.7 0.3 0.2 0.2
1.0 1.3 7.1 6.3 2.8 0.6
top band
bottom band
HSP90

Figure 33. BC12 analogs have various effects on LY18 cell viability. LY18 cells were cultured in media, or treated with 20 μM of BC12 derivatives. Cells were collected at the indicated times and cell viability was determined by propidium iodide staining. Samples were analyzed by flow cytometry as described in *Material and Methods*. The data are represented as the percentage of cells that are positive for propidium iodide staining. The data are representative of 10,000 cells, completed as two independent experiments.

Figure 33

A

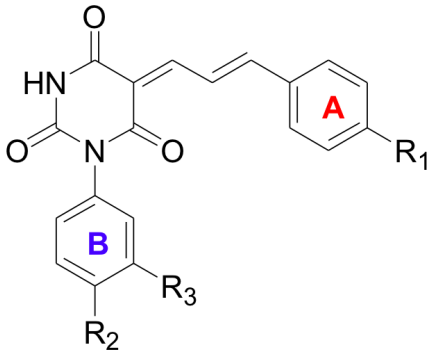

Compound	R_1	R_2	R_3
BC12	$N(CH_3)_2$	H	H
BC12-1	$N(CH_3)_2$	CH_3	H
BC12-2	$N(CH_3)_2$	Br	H
BC12-4	H	H	H
BC12-5	$N(CH_3)_2$	Cl	H
BC12-6	$N(CH_3)_2$	F	H
BC12-7	$N(CH_3)_2$	H	CH_3

B

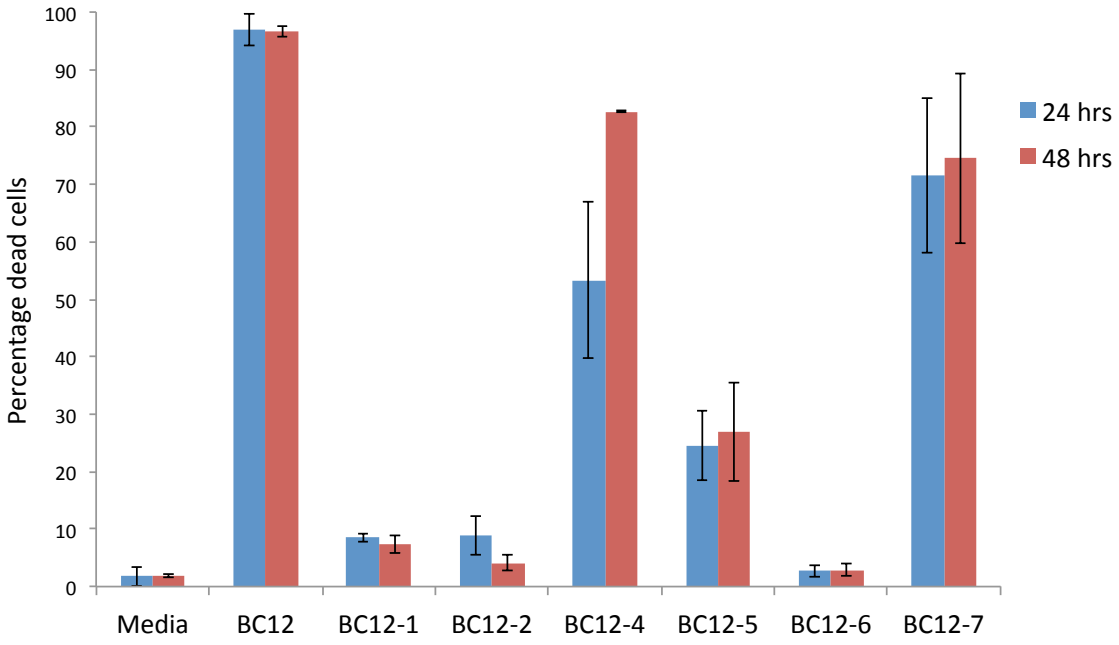

Figure 34. BC12 does not inhibit cell cycle progression in LY18 cells. LY18 cells were cultured in media alone or in the presence of 10 μM, or 20 μM BC12. At the indicated times, LY18 cells were stained with propidium iodide and cell cycle analyzed by flow cytometry as described in *Materials and Methods*. *A,* The data are presented as overlay graphs with the number of cells (counts) versus propidium iodide (PI-A). *B,* The data are represented as the percentage of LY18 cells in the G_0/G_1-phase of the cell cycle. *C,* The data are represented as the percentage of LY18 cells in the $S+G_2/M$-phase of the cell cycle. The data are representative of 10,000 cells.

Figure 34

A

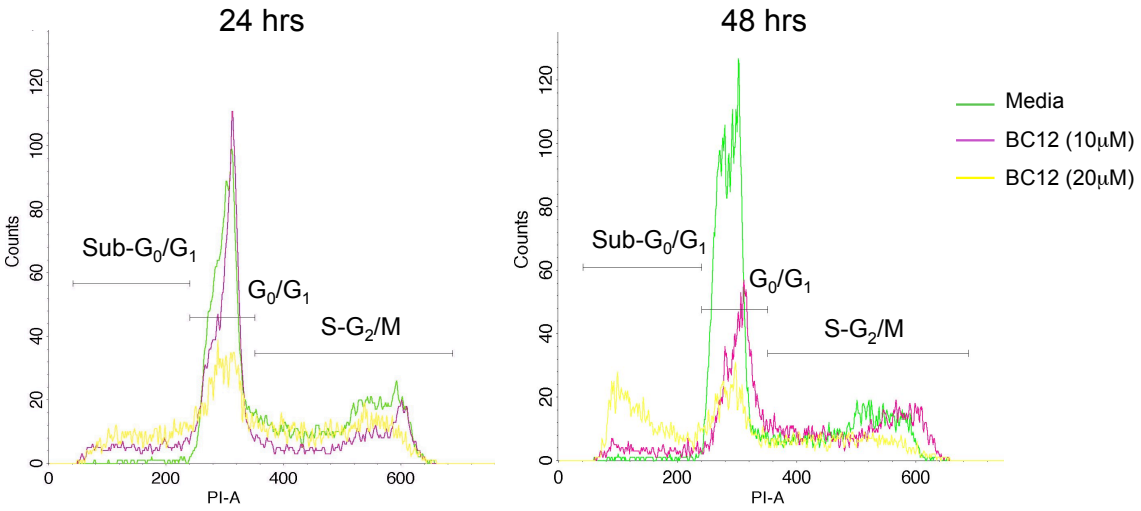

B

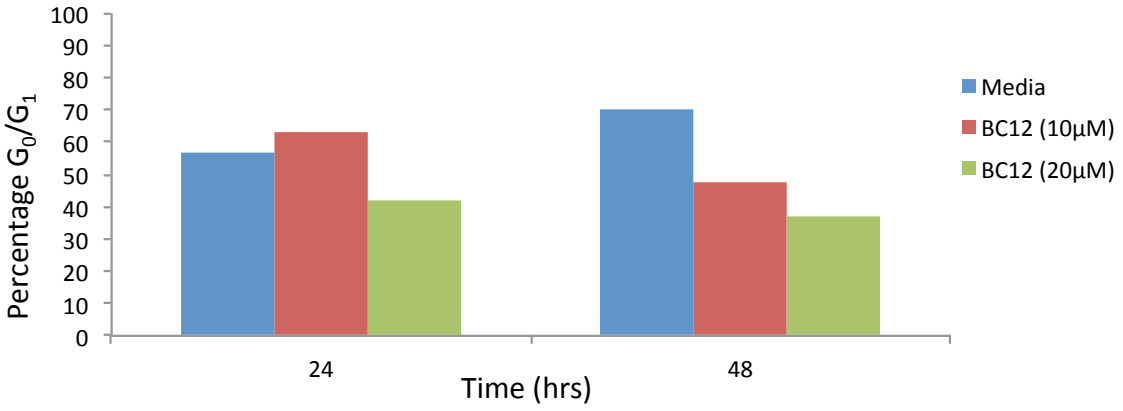

C

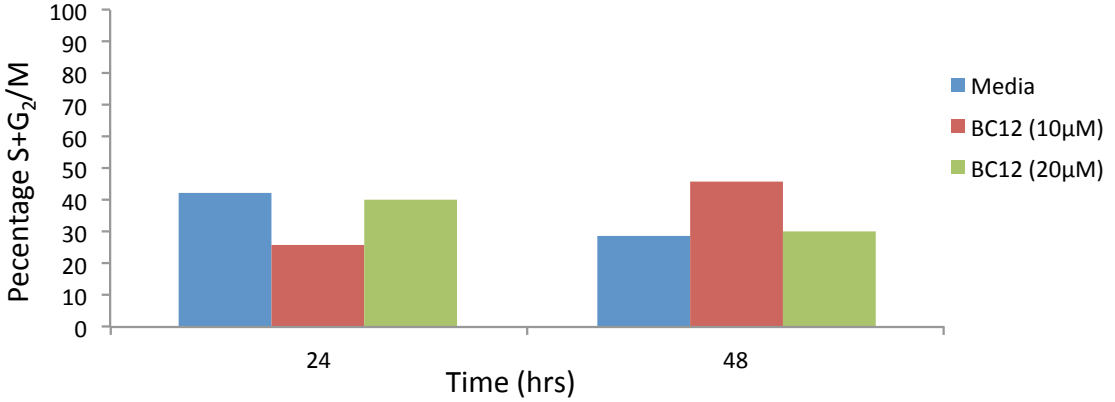

Figure 35. BC12 induces cell death in human primary B cells. Human primary B cells were isolated from donor's blood as described in *Material and Methods*. Cells were cultured in media alone, or with increasing dose of BC12 (0.05 μM, 0.5 μM, 2.5 μM, 5 μM, 10 μM, 25 μM, 50 μM and 100 μM). At the indicated times, cells were collected and cell viability was determined by propidium iodide staining. Samples were analyzed by flow cytometry as described in *Material and Methods*. The data are represented as the percentage of cells that are positive for propidium iodide staining. The data are representative of 10,000 cells. Titration of BC12 was repeated at doses 10 μM, 25 μM, 50 μM and 100 μM. The same trend was observed in two independent experiments.

Figure 35

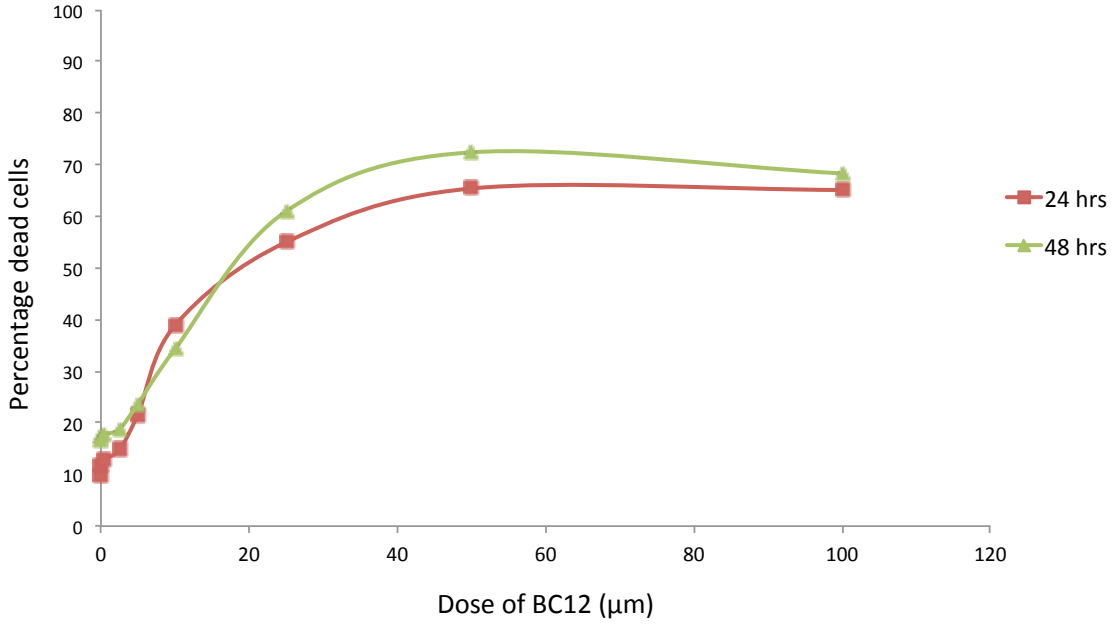
Percentage dead cells
100
90
80
70
60
50
40
30
20
10
0
0
20
40
60
80
100
120
Dose of BC12 (µm)
24 hrs
48 hrs

Figure 36. *In vitro* PDE7 inhibitors have various effects on U937 cell viability. U937 cells were cultured in media, or treated with various *in vitro* PDE7 inhibitors at a dose of 20 μM. Cells were collected at the indicated times and cell viability was determined by propidium iodide staining. Samples were analyzed by flow cytometry as described in *Material and Methods*. The data are represented as the percentage of cells that are positive for propidium iodide staining. The data are representative of 10,000 cells.

Figure 36

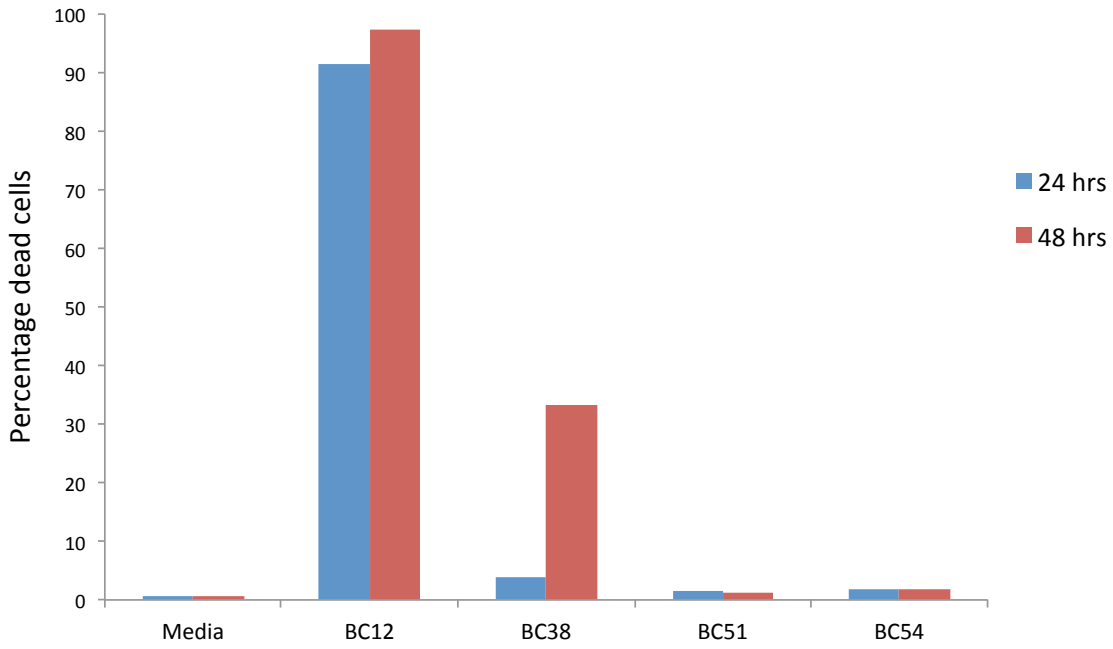
Percentage dead cells
100
90
80
70
60
50
40
30
20
10
0
Media
BC12
BC38
BC51
BC54
24 hrs
48 hrs

Figure 37. BC12 induces dose-dependent decrease of cell viability in U937 cells. U937 cells were cultured in media alone, or with increasing dose of BC12 (0.5 μM, 1 μM, 5 μM, 10 μM, 20 μM and 50 μM). At the indicated times, cells were collected and cell viability was determined by propidium iodide staining. Samples were analyzed by flow cytometry as described in *Material and Methods*. The data are represented as the percentage of cells that are positive for propidium iodide staining. The data are representative of 10,000 cells. Titration of BC12 was repeated at doses 10 μM, 20 μM and 50 μM. The same trend was observed in two independent experiments.

Figure 37

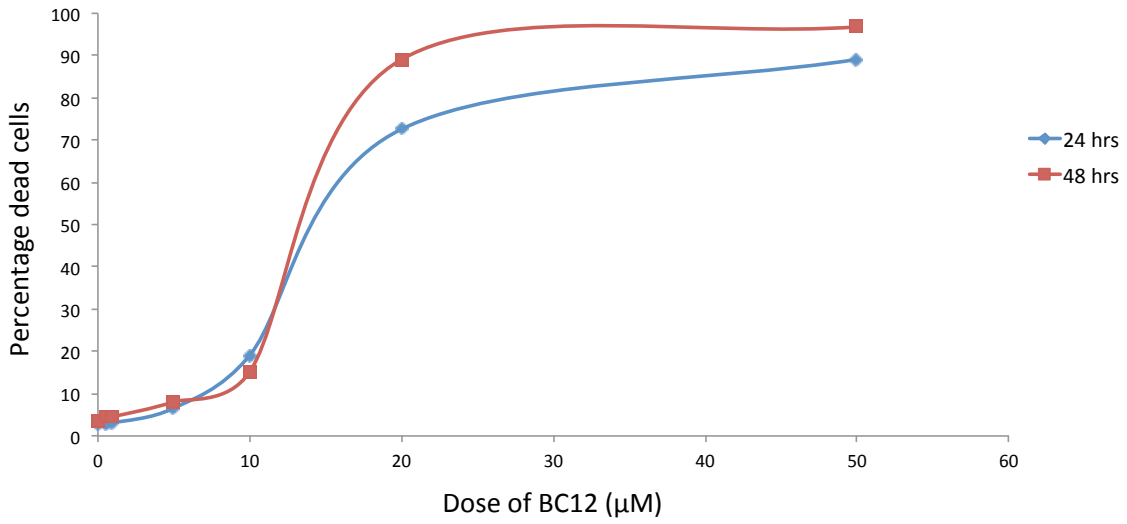
Percentage dead cells
100
90
80
70
60
50
40
30
20
10
0
0
10
20
30
40
50
60
Dose of BC12 (µM)
24 hrs
48 hrs

Figure 38. BC12 induces apoptosis in U937 cells. U937 cells were cultured in media with DMSO, 10 μM or 20 μM of BC12. At the indicated times, cells were collected and cell apoptosis was analyzed by TUNEL assay as described in *Material and Methods*. The data are represented as the percentage of cells that are positive for FITC staining. The data are representative of 10,000 cells and two independent experiments.

Figure 38

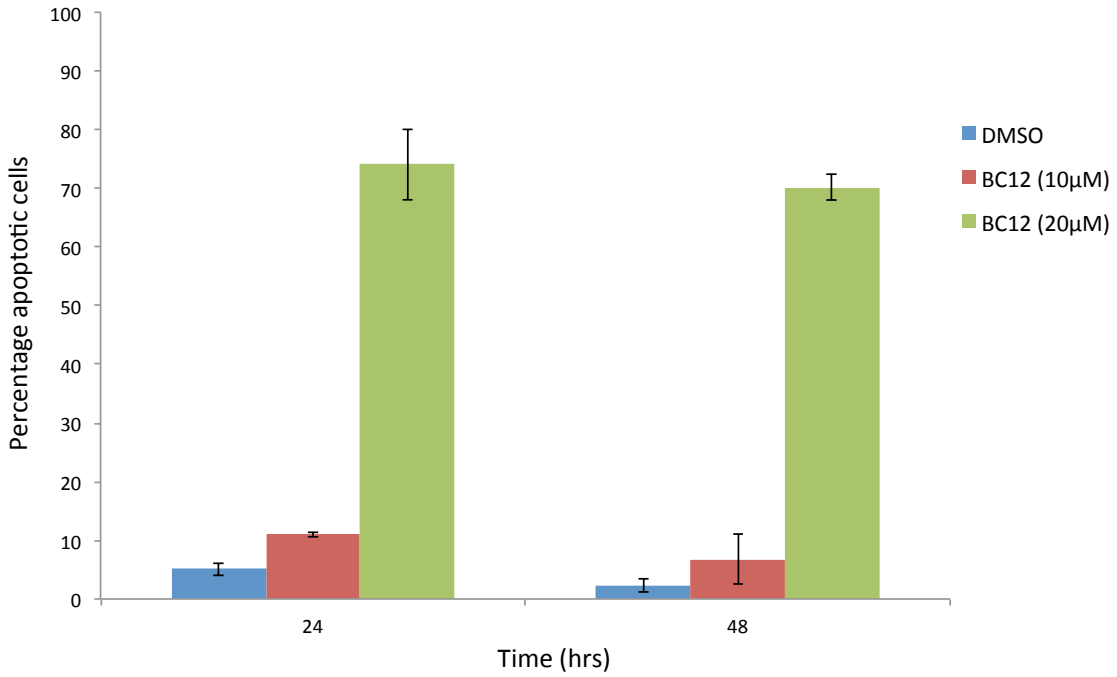
100
90
80
70
60
50
40
30
20
10
0
Percentage apoptotic cells
24
48
Time (hrs)
DMSO
BC12 (10µM)
BC12 (20µM)

Figure 39. BC12 activates caspase pathway in U937 cells. *A,* U937 cells were cultured in media with DMSO or 20 μM of BC12 for indicated length of time. Whole cell extracts were prepared and Western blotting was performed with anti-caspase 8 and anti-caspase 3 antibodies that recognize both full length and cleaved caspases as described in *Material and Methods*. The blot was stripped and reprobed for anti-HSP90 antibody to ensure equal loading of each sample. Quantification of the Western blotting bands was obtained with ImageJ software (v1.45s). Both top and bottom band densities are listed as fold increase above first detected band relative to HSP90 loading control. The data are representative of two independent experiments. *B,* U937 cells were cultured in media with DMSO or 20 μM of BC12 for indicated length of time. Cells were collected and stained with FITC-conjugated anti-active caspase 3 antibody, followed by flow cytometric analysis as described in *Material and Methods*. The data are represented as the percentage of cells that are positive for active caspase 3 staining. The data are representative of 10,000 cells, completed as two independent experiments.

Figure 39

A

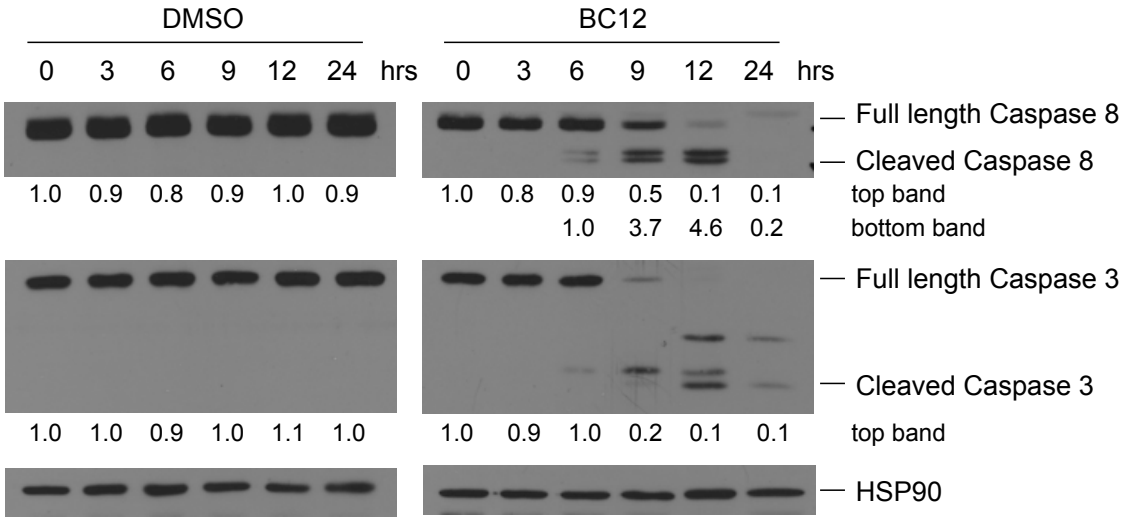
DMSO
BC12
0 3 6 9 12 24 hrs
0 3 6 9 12 24 hrs
Full length Caspase 8
Cleaved Caspase 8
1.0 0.9 0.8 0.9 1.0 0.9
1.0 0.8 0.9 0.5 0.1 0.1
top band
1.0 3.7 4.6 0.2
bottom band
Full length Caspase 3
Cleaved Caspase 3
1.0 1.0 0.9 1.0 1.1 1.0
1.0 0.9 1.0 0.2 0.1 0.1
top band
HSP90

B

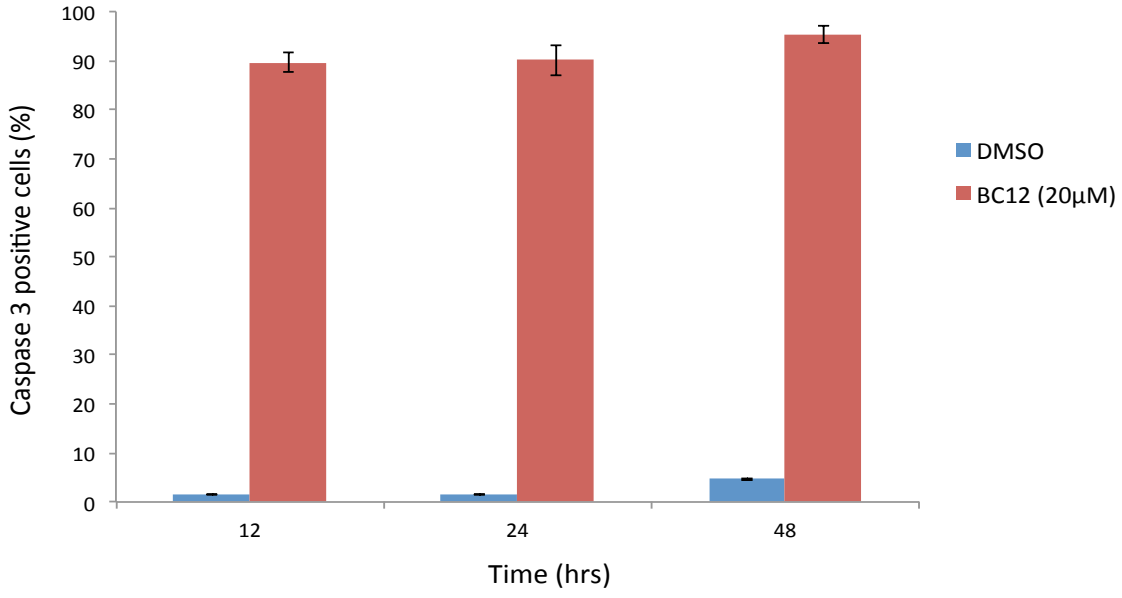
Caspase 3 positive cells (%)
100
90
80
70
60
50
40
30
20
10
0
12
24
48
Time (hrs)
DMSO
BC12 (20μM)

Figure 40. BC12 induces PARP cleavage and activation in U937 cells. U937 cells were cultured in media with DMSO or 20 μM of BC12 for indicated length of time. Whole cell extracts were prepared and Western blotting was performed with anti-PARP antibody that recognizes full length and cleaved PARP as described in *Material and Methods*. The blot was stripped and reprobed for anti-HSP90 antibody to ensure equal loading of each sample. Quantification of the Western blotting bands was obtained with ImageJ software (v1.45s). Both top and bottom band densities are listed as fold increase above first detected band relative to HSP90 loading control. The data are representative of two independent experiments.

Figure 40

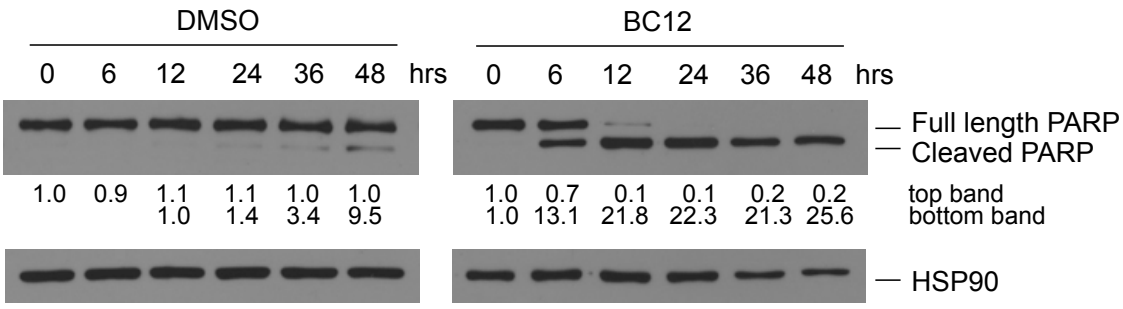
DMSO
BC12
0 6 12 24 36 48 hrs
0 6 12 24 36 48 hrs
Full length PARP
Cleaved PARP
1.0 0.9 1.1 1.1 1.0 1.0
1.0 1.0 1.4 3.4 9.5
1.0 0.7 0.1 0.1 0.2 0.2
1.0 13.1 21.8 22.3 21.3 25.6
top band
bottom band
HSP90

Figure 41. BC12 does not inhibit cell cycle progression in U937 cells. U937 cells were cultured in media alone or in the presence of 10 μM, or 20 μM BC12. At the indicated times, U937 cells were stained with propidium iodide and cell cycle analyzed by flow cytometry as described in *Materials and Methods*. *A,* The data are represented as the percentage of U937 cells in the G_0/G_1-phase of the cell cycle. *B,* The data are represented as the percentage of cells in the $S+G_2/M$-phase. *C,* The data are represented as the percentage of cells in the sub-G_0/G_1-phase. The data are representative of 10,000 cells.

Figure 41

A

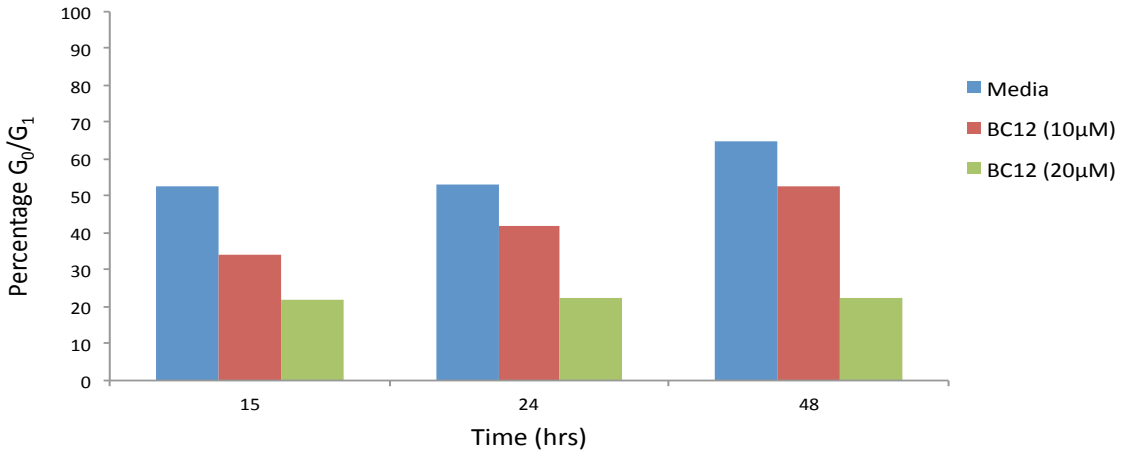

B

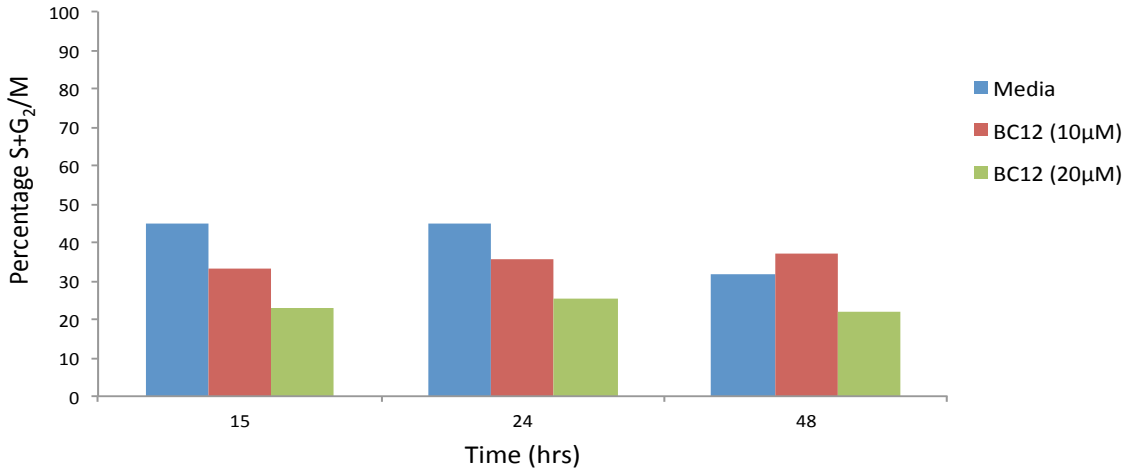

C

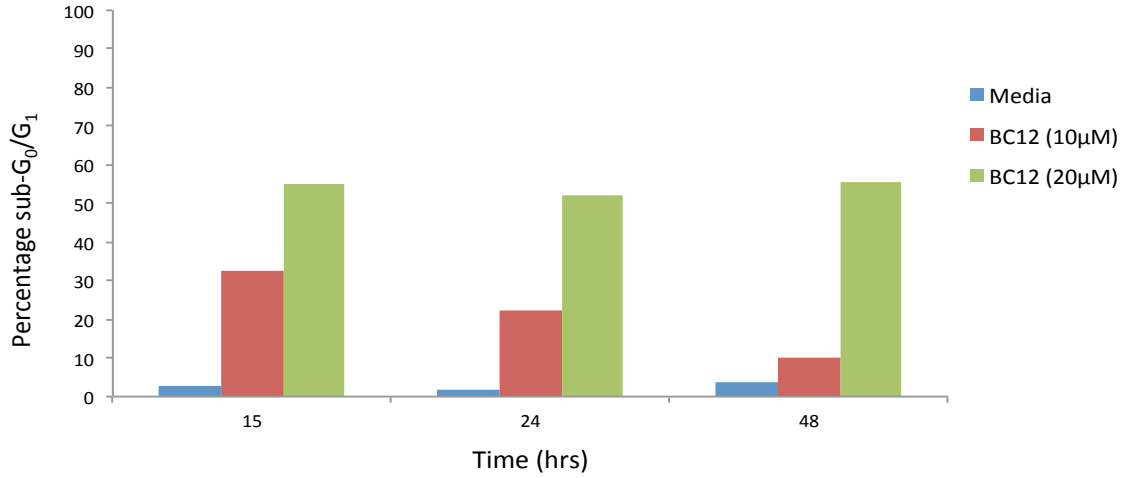

Figure 42. BC12 does not inhibit DNA synthesis in U937 cells. U937 cells were cultured in media alone, with DMSO or 20 μM of BC12. At the indicated times, cells were collected and DNA synthesis was monitored by BrdU incorporation and analyzed by flow cytometry as described in *Materials and Methods.* The data are representative of 10,000 cells and are presented as cell number (counts) versus BrdU (FITC-A). The bars reflect the percentage of BrdU positive U937 cells. The data are representative of two independent experiments.

Figure 42

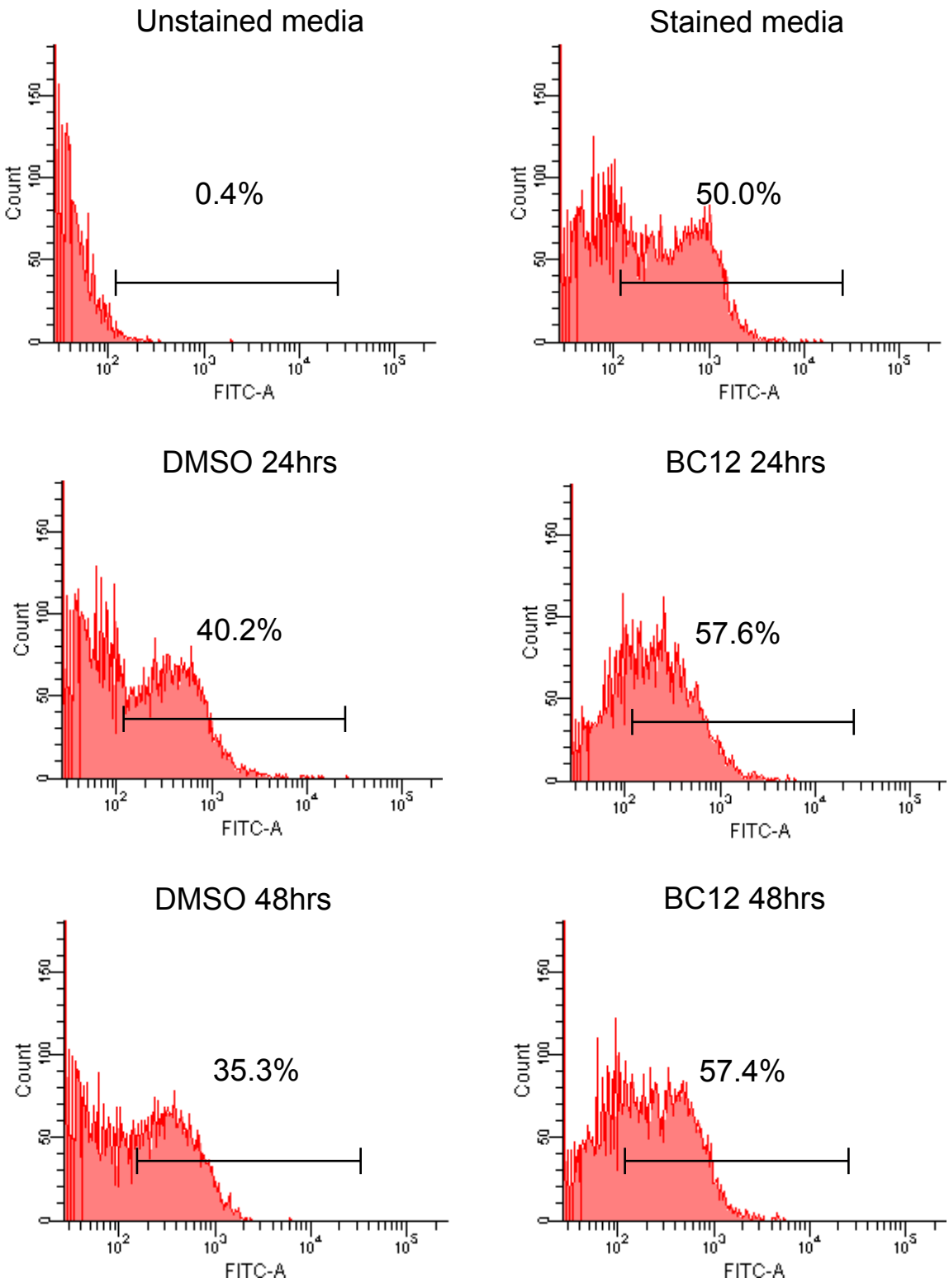
Unstained media
0.4%
Stained media
50.0%
DMSO 24hrs
40.2%
BC12 24hrs
57.6%
DMSO 48hrs
35.3%
BC12 48hrs
57.4%
Count
FITC-A

DISCUSSION

I. Chapter One

PDE4 inhibitors have been proved effective therapeutic agents for alleviating chronic inflammation such as asthma and COPD. However, these inhibitors are compromised by dose-limiting side effects that are difficult to overcome [181]. PDE7A is proposed to be a new therapeutic target in addition to PDE4 [11], for its ubiquitous expression in proinflammatory and immune cells [22]. Emerging evidence has suggested that PDE7A plays an important role in regulating T cell activation [4, 5]. Despite the immunomodulatory potential of PDE7, selective inhibitors of PDE7 are lacking. BRL50481 is the only commercially available PDE7 inhibitor [27]. Herein, we characterized a novel *in vitro* PDE7 inhibitor, BC12, for its immunosuppressive activity in mammalian T cells.

IL-2 is a key cytokine of T cell activation. The *de novo* synthesis of IL-2 is an immediate event following TCR and costimulatory molecule ligation [57]. Using human Jurkat cells as a model for human T lymphocytes, we first demonstrate that BC12 inhibits IL-2 secretion in activated Jurkat cells in a dose-dependent manner without significantly reducing cell viability. Since IL-2 production is an outcome of gene expression, protein translation, transport and secretion, we were able to assesse the endogenous IL-2 protein level with the aid of a Golgi inhibitor and confirmed that BC12 inhibits endogenous IL-2 protein production. Relative *IL-2* mRNA levels were then evaluated by semi-quantitative real-time PCR. Our data demonstrate that *IL-2* mRNA expression was blocked by BC12. We did not directly examine IL-2 protein translation; therefore cannot rule out the

possibility that IL-2 protein translation is also inhibited by BC12. It is important to note that the inhibitory effects of BC12 on both protein production and mRNA expression were initiated at the earliest time point we examined and persisted for at least 24 hours as the longest time point we observed.

As a key growth cytokine for T cells, *IL-2* expression is controlled at multiple levels, including transcriptional and post-transcriptional regulation. *IL-2* mRNA contains several AU-rich elements in 3'-UTR as well as additional elements in 5'-UTR and within the coding region, providing regulatory sites for mRNA stability in response to TCR and CD28 costimulation [123–127]. Our studies used CsA to inhibit *IL-2* transcription by blocking calcineurin-dependent nuclear import of NFAT [146]. In the presence of CsA, we were able to assess *IL-2* mRNA degradation rate by real-time PCR. Our results indicate that BC12 does not accelerate *IL-2* mRNA degradation. Thus, inhibited *IL-2* gene expression by BC12 is due to transcriptional repression.

Transcriptional regulation of *IL-2* gene is well characterized. Positive regulatory elements in the 300 bp minimal promoter region of *IL-2* gene need to be occupied by corresponding transcription factors for optimal transcription [74]. Microarray analysis of the whole genome expression profile of Jurkat cells was performed to study the interaction effect of BC12 and stimuli. Among transcription factor families NFAT, NFκB, Fos, Jun and Oct-1, NFκB regulated genes are most affected by BC12. In NFκB family proteins, RelA (p65), NFκB1 (p50), and c-Rel are three demonstrated targets of TCR and CD28 signaling [88]. Western blotting of nuclear extracts suggests that all three proteins show impaired nuclear translocation in the presence of BC12. Inhibition of NFκB pathway was further validated by EMSA, indicating BC12 inhibits NFκB proteins

binding to their specific DNA probe. In resting T cells, NFκB heterodimers reside in cytoplasm in complex with IκB protein. Upon TCR/CD28 stimulation, nuclear translocation of NFκB depends on phosphorylation-induced degradation of IκB [86]. The multi-subunit IKK complex is the central component of the NFκB signaling pathway, which phosphorylates IκB and targets its ubiquitination [88]. Our data suggest that BC12 suppresses NFκB pathway by inhibiting IκB phosphorylation and degradation. However, phosphorylation status of IKKα/β complex seems unaffected by BC12 based on Western blotting. The phospho-IKKα/β antibody in our study detects phosphorylation of Ser176/180 in IKKα and Ser177/181 in IKKβ, which is required for activation of IKK complex [183–185]. To directly assess the kinase activity of the IKK complex, IKKα/β kinases can be immunoprecipitated from cells treated with stimuli and BC12. *In vitro* kinase assay can be conducted using recombinant IκB protein as a substrate. In addition to IKKα/β phosphorylation, recent findings have demonstrated other regulatory mechanisms required for IKK activation [20, 21]. Specifically, in complex with the catalytic subunits IKKα/β, IKKγ is an essential structural and regulatory subunit of the IKK complex [20, 22] and IKK activation depends on IKKγ polyubiquitination [20, 21]. A recent publication reports that a compound cordycepin suppresses NFκB activation by blocking IKKγ ubiquitination [188]. Therefore, we can also evaluate other modifications of IKK complex in addition to IKKα/β phosphorylation.

In addition to NFκB, our EMSA data also suggest that the NFAT pathway is inhibited by BC12 in activated Jurkat cells. Two different NFAT binding DNA probes were used to validate the findings. Super-shift assay using anti-NFATc2 and anti-

NFATc1 antibodies reveals that both NFAT family proteins are present in the nucleus to bind to the DNA probe. However, Western blotting of nuclear proteins indicated that nuclear translocation of NFATc2 protein was not significantly affected. Since the preparation of nuclear extracts may result in inter-contamination of nuclear and cytoplasmic proteins, other approaches can be employed to validate the data. Immunofluorescence microscopy using antibodies specific to NFATc2, NFATc1, and other transcription factors of interest can be used to image the localization of the proteins in response to stimuli and BC12.

As our studies demonstrate thus far, BC12 inhibits *IL-2* gene transcription in activated Jurkat cells through NFκB and NFAT-mediated pathways. To validate our findings based on EMSA, we attempted chromatin immunoprecipitation (ChIP) using antibodies specific to NFATc2 or RelA(p65) and amplified precipitated DNA using primers specific to *IL-2* promoter region. However, the ChIP experiments were not successful due to low affinity of the antibodies. This approach could be repeated if antibodies with high affinity are available. Furthermore, luciferase assay with NFAT or NFκB-driven reporter gene transfected to Jurkat cells can be used to confirm the inhibitory effect of BC12 on these pathways.

Importantly, although we initially hypothesized PDE7 as the *in vivo* target of BC12 in Jurkat cells, we found that BC12 inhibited *IL-2* transcription not through PDE by comparison analysis. BC12-4, BC12-6, BC54 and BC12 were used to treat Jurkat cells simultaneously with stimuli. Besides BC12, its structural analog BC12-4 displayed potent inhibitory effects on IL-2 production in activated Jurkat cells. The extent of reduction in IL-2 production by BC12-6 and BC54 was approximately 25%, similar to that of

commercially available PDE4 inhibitor rolipram (unpublished data by Hoffman Lab). Among these compounds, BC54 is the most potent PDE4 and PDE7 dual inhibitor; BC12-6 and BC12 exhibit similar PDE7A inhibitory activity in *in vitro* PDE assay; BC12-4 has no measurable PDE7A inhibitory activity (unpublished data by Hoffman Lab). Thus, we can speculate that the inhibitory effect on IL-2 production is not correlated with their *in vitro* PDE inhibitory capacity. However, the possibility that BC54 and BC12-6 have a lower accessibility to cells although treated at the same dosage, cannot be completely ruled out. This issue was partially addressed by previous studies from Hoffman Lab, which showed that BC54 potently inhibited TNFα secretion from U937 cells and induced apoptosis in B-CLL cells (unpublished data). These findings demonstrated an anti-inflammatory effect of BC54 and its ability to cross the cell membrane. To further confirm that PDE7 is not the *in vivo* target of BC12 that leads to IL-2 inhibition, intracellular cAMP levels can be assessed after cells were treated by BC12. Alternatively, cAMP antagonist that specifically inhibits downstream effector enzymes such as PKA can be used along with BC12 to treat Jurkat cells. If BC12 works through elevating intracellular cAMP level by inhibiting PDE, its effect should be reversed by a cAMP antagonist.

Structurally, BC12 is a barbiturate-based compound. Accumulating evidence suggests that clinical use of barbiturates for neuroprotection is associated with a loss of protective immunity as a side effect [24, 25]. It has been reported that barbiturates, such as thiopental and thiamylal, directly inhibit calmodulin/calcineurin complex, leading to inhibition of NFAT pathway. NFAT-driven reporter genes, as well as IL-2 and IFNγ production in activated human T lymphocytes, were suppressed [29]. Another report also

indicates that thiopental inhibits NFκB mediated transcription in Jurkat cells and human primary T lymphocytes, with possible involvement of reduced degradation of IκBα [191]. Thiopental has some level of structural similarity with BC12; however, the dose of thiopental reported to achieve an inhibitory effect on IL-2 production is more than 100-fold higher than BC12 [29].

Inhibitors of T cell activation function through targeting different pathways. Cyclosporin A (CsA) and tarolimus target calcium calmodulin-dependent phosphatase calcineurin, thus inhibit NFAT regulated *IL-2* expression [146]. Rapamycin blocks IL-2 post-receptor signaling by targeting mTOR [144]. PDE4/7 dual inhibitors, such as T-2585, inhibit human T cell proliferation and cytokine production [182]. Our compound BC12 inhibits T cell activation by targeting NFAT and NFκB pathways. It is important to note that BC12 does not completely block either pathway; instead, partially reduces the activity of both pathways, resulting in suppression of *IL-2* expression. Recently, therapies that target multiple pathways have been increasingly designed to achieve a collective effect to treat complex diseases such as cancer [192]. It has been suggested that partial inhibition of multiple targets can be more efficient than the complete inhibition of a single target [193]. Therefore, BC12 can be a very promising multi-target drug that inhibits T cell activation.

An interesting finding from our study is that BC12 augments phosphorylation status of signaling proteins in the AP-1 signaling pathway in stimulated Jurkat cells, while BC12 alone does not induce activation of signaling pathway. In agreement with the Western blotting data, EMSA result suggests that BC12 considerably increases the binding of AP-1 proteins to their specific DNA probe. We also conducted ChIP

experiment using antibody specific to c-Jun (data not shown), which showed increased occupation of c-Jun to *IL-2* promoter region when treated with BC12 along with stimuli. Microarray data also indicate that the expression levels of several AP-1 regulated genes are increased by BC12 in the presence of stimuli. Taken together, BC12 augments AP-1 signaling pathway, resulting in increased binding of AP-1 to its corresponding regulatory elements in DNA, which may be responsible for increased expression of *c-Fos*, *c-Jun* and *IL-8* as revealed by microarray data. However, the relation between increased AP-1 activation and inhibited *IL-2* expression has not been resolved. Feedback loops commonly exist to regulate signaling pathways. It has been reported that *IL-2* transcription is transient and self-limited by an auto-regulatory feedback loop, in which IL-2 inhibits its own expression [58]. We can speculate that a novel feedback loop may exist such that repressed downstream *IL-2* expression resulted in hyper-activation of upstream signaling pathways. Further experiments need to be conducted to validate this hypothesis.

We further investigated the effects of BC12 and its derivative compounds in activated mouse and human primary T cells. Our findings in Jurkat cells were well recapitulated in both primary T cell cultures. Specifically, BC12 and BC12-4 both inhibit IL-2 production in activated mouse and human primary T cells, whereas BC12-6 does not exhibit a significant effect. It was confirmed in human primary T cells that inhibition of IL-2 production is attributable to transcriptional repression by real-time PCR. It is important to note that BC12 alone, or in combination of stimuli does not induce significant cell death at the dose that inhibits IL-2 production. Therefore, the

immunosuppressive activity of BC12 is not limited to transformed cell line, but also effective in primary T cells.

$CD4^+$ helper T cells are divided into distinct subsets based on cytokine production and immune function. Th1 cells produce IL-12 and IFNγ, promoting cell-mediated immune response. Th2 cells produce IL-4, IL-5 and IL-13, promoting humoral immunity. Th17 cells produce IL-17, IL-22 and IL-6, which mediate neutrophil inflammation and are increasingly implicated in steroid-insensitive asthma [194]. We sought to investigate the effect of BC12 on T helper cell specific cytokine secretion in activated human primary $CD4^+$ T cells. Our data indicate that BC12 selectively inhibits Th2 cytokine and some of the Th17 cytokine secretions. Production of the key Th1 cytokine IFNγ is not significantly affected by BC12. These findings, although preliminary, are very promising. Abnormal polarization of Th2 response is a key event in allergic diseases. Predominant Th2 profile cytokine expression and a reduced production of Th1 cytokine IFNγ is noted [141]. Th2 cytokines drive the differentiation and function of B cells and mast cells. IL-4 promotes antibody class-switching in B cells, leading to the secretion of IgE. IgE binds to receptors on mast cells, resulting in release of mediators such as histamines that lead to tissue inflammation. IL-5 stimulates B cell growth and antibody secretion and mediates eosinophil activation [195]. Immunomodulatory compounds such as suplatast tosilate, which inhibits IL-4 and IL-5 production but not IFNγ [196], have been proven effective in clinical application [32, 33]. The potential of BC12 on selectively inhibiting Th2 cytokines is a very interesting and promising direction for developing novel therapeutic agents to treat allergic diseases. Further experiments need to be carried out to confirm the effects of BC12 on key cytokine production and gene expression such as IL-4, IL-5 and

IFNγ. Instead of total $CD4^+$ T cells, Th1 and Th2 cells can be induced for more specific analysis. Furthermore, in addition to cytokine inhibition, BC12 can be tested for its potential to inhibit Th2 cell differentiation and to increase Th1/Th2 ratio.

In summary, our studies report that BC12, a novel *in vitro* PDE7 inhibitor, inhibits *IL-2* expression in activated Jurkat cells, mouse and human primary T cells, by targeting NFAT and NFκB-mediated pathways as summarized in Figure 7. Moreover, our findings also suggest that BC12 has a potential to selectively inhibit Th2 cytokines. The immunosuppressive and potential immunomodulatory effects mark BC12 a promising therapeutic agent that worth further investigation.

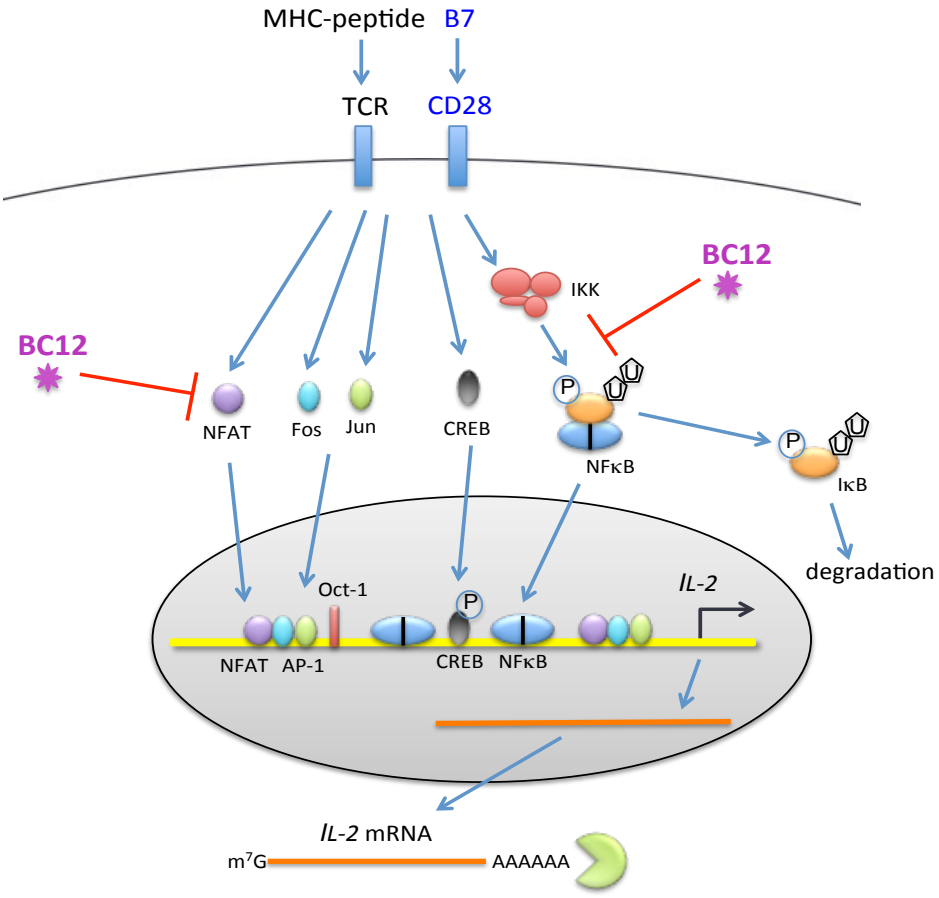

Figure 7. Summary of mechanism of inhibition of BC12.

II. Chapter Two

Elevating intracellular cAMP levels can result in growth arrest and apoptosis in cancer cells, marking PDEs as potential targets for cancer treatment [199]. The development of family-specific PDE inhibitors allows insight into the therapeutic effects of targeting specific PDEs. PDE inhibitors have been shown to induce apoptosis in hematological malignant cells, either alone or in synergy with glucocorticoids [6–10]. It was reported that PDE4B overexpression correlates with higher risk of relapse of DLBCL and limits cAMP-associated apoptosis in DLBCL [10]. PDE7B overexpression was observed in B-CLL [7]. Both inhibitors of PDE7 and a dual inhibitor of PDE4/7 selectively induce apoptosis in CLL cells compared to normal B cells, suggesting PDE7B as a potential therapeutic target for CLL [7]. However, inhibitors that selectively and potently inhibit PDE7B are in need to confirm its role in CLL malignancy. As the only commercially available PDE7 specific inhibitor, BRL50481 is a potent PDE7A inhibitor with IC_{50} of 150 nM, but poor PDE7B inhibitor with IC_{50} of 12 μM [28]. Our novel *in vitro* PDE7 inhibitor BC12 inhibits PDE7A catalytic domain with IC_{50} of 1 μM and full-length rat PDE7B with IC_{50} of 200 nM, exhibiting significantly stronger PDE7B inhibitory activity than BRL50481.

Using human LY18 cell line and U937 cell line as models for human DLBCL cells and malignant monocytes, we characterized the ability of several PDE4 and/or PDE7 inhibitors to induce cell death in human malignant B cells and monocytes. Our data demonstrate that BC12 is the most potent compound among several *in vitro* PDE inhibitors to induce cell death in both cell lines. BC12 induces cell death in a dose-dependent manner. With a dose of 20 μM, BC12 results in approximately 90% cell death.

To compare the effect of BC12 on normal B cells and malignant LY18 cells, we also titrated BC12 on human primary B cell viability. At 20 μM, BC12 induces significantly less cell death in primary B cells than in LY18 cells, suggesting that BC12 has selectivity in killing DLBCL cells over normal B cells. Of note, cell lines usually derive from high-grade malignancies that carry greater abnormalities than primary tumor samples for its ability to survive in cell culture environment. Therefore, BC12 has the potential to be more effective in killing primary DLBCL cells than LY18 cell line.

We also confirm that BC12 induces apoptosis in both LY18 and U937 cells, evidenced by DNA fragmentation and caspase pathway activation, which results in the decreased viability. There are two main pathways of apoptosis in vertebrates, the extrinsic and intrinsic pathways [200]. Extrinsic signals ligate death receptors such as Fas receptor to activate initiator caspases such as caspase 8. Initiator caspases cleave and activate effector caspases, such as caspase 3 and caspase 7. In the intrinsic pathway, a BH3-only protein such as Bid triggers mitochondria permeabilization and cytochrome c release to cytosol. Cytochrome c triggers the oligomerization of Apaf-1 and formation of the apoptosome, where caspase 9 is activated. Caspase 9 cleaves and activates effector caspases such as caspase 3 and caspase 7 [200]. Our data revealed that caspase 8 and caspase 3 are activated in both cell lines treated with BC12, suggesting an involvement of extrinsic pathway in BC12 induced apoptosis. The contribution of intrinsic pathway cannot be ruled out and needs to be further investigated. Inhibition of cell cycle progression can ultimately lead to apoptosis. Cell cycle analysis and BrdU staining revealed that BC12 does not cause cell cycle arrest; instead, directly induces apoptosis while cells are still proliferating.

To decipher the correlation of *in vitro* PDE7 inhibitory activity and apoptotic effects in LY18 cells, derivative compounds of BC12 were tested on LY18 cell viability for structural-activity analysis. BC12-4, which has no PDE7 inhibitory activity, reduces LY18 cell viability to the similar level as BC12. In contrast, BC12-6, which is the most potent PDE7 inhibitor among the derivatives except BC12, does not decrease LY18 viability. In addition, BC54, the most potent PDE4/7 dual inhibitor, does not exhibit any effect on LY18 viability up to a dose of 100 μM. These data all together suggest that the *in vivo* target of BC12 that induces apoptotic effects in LY18 cells is not PDE7. It is important to note that the apoptotic effects of BC12 derivative compounds in LY18 cells coincide with the IL-2 inhibitory effects in Jurkat cells as investigated in Chapter One. Specifically, BC12, BC12-7, BC12-4 and BC12-5 all displayed potent effects in both cell lines, whereas BC12-1, BC12-2 and BC12-6 did not. Based on these findings, we can speculate that the *in vivo* targets that lead to either IL-2 inhibition in Jurkat cells or apoptosis in LY18 cells may be the same.

In Chapter One, we demonstrate that NFκB pathway is inhibited by BC12 in human Jurkat cells. NFκB factors regulate a vast series of genes in immune cells that control inflammation, cell growth, differentiation or apoptosis [201]. Aberrant activation of NFκB pathway has been frequently observed in hematologic malignancies and NFκB-blocking approaches have been investigated as anti-caner strategies [201]. A compound specifically targeting NFκB activity by inhibiting IκB phosphorylation induces apoptosis of CLL cells in a dose-dependent manner [202]. The pro-apoptotic effect of NFκB inhibitor rely on the block of NFκB-mediated expression of apoptosis-modulating genes,

such as *BCL-2* family genes [201]. Moreover, NFκB and tumor suppressor p53 can inhibit each other's transactivation possibly through competing for binding to the p300/CBP coactivator [203]. It is important to note that LY18 cells carry rearranged *p53*, *BCL-2* and *MYC* genes [160]. MYC promotes cell growth activity, whereas p53 and BCL-2 mutation permit the cells to escape apoptotic death and are responsible for the resistance of the cell line to anti-cancer treatment [160]. Taken together, we can hypothesize that inhibiting p53 and BCL-2 activity by targeting NFκB pathway can induce a differential apoptotic effect between LY18 cells and human normal B cells, which is a reasonable mechanism of action by BC12. Further experiments need to be conducted to confirm this hypothesis.

In summary, our data demonstrate that BC12 induces apoptosis in human LY18 and U937 cell lines in a dose-dependent manner. Titration of BC12 on LY18 cells and human primary B cells revealed that BC12 induces cell death more effectively in DLBCL LY18 cell line than normal B cells, which merits this compound further investigation as an anti-cancer agent.

REFERENCES

[1] C. Lugnier, "Cyclic nucleotide phosphodiesterase (PDE) superfamily: a new target for the development of specific therapeutic agents.," *Pharmacology & therapeutics*, vol. 109, no. 3, pp. 366–98, Mar. 2006.

[2] S. Pierre, T. Eschenhagen, G. Geisslinger, and K. Scholich, "Capturing adenylyl cyclases as potential drug targets.," *Nature reviews. Drug discovery*, vol. 8, no. 4, pp. 321–35, Apr. 2009.

[3] D. M. Essayan, "Cyclic nucleotide phosphodiesterases.," *The Journal of allergy and clinical immunology*, vol. 108, no. 5, pp. 671–80, Nov. 2001.

[4] H. R. Bourne, L. M. Lichtenstein, K. L. Melmon, C. S. Henney, Y. Weinstein, and G. M. Shearer, "Modulation of inflammation and immunity by cyclic AMP.," *Science (New York, N.Y.)*, vol. 184, no. 4132, pp. 19–28, Apr. 1974.

[5] A. Castro, M. J. Jerez, C. Gil, and A. Martinez, "Cyclic nucleotide phosphodiesterases and their role in immunomodulatory responses: advances in the development of specific phosphodiesterase inhibitors.," *Medicinal research reviews*, vol. 25, no. 2, pp. 229–44, Mar. 2005.

[6] J. A. Meyers, D. W. Su, and A. Lerner, "Chronic lymphocytic leukemia and B and T cells differ in their response to cyclic nucleotide phosphodiesterase inhibitors.," *Journal of immunology (Baltimore, Md. : 1950)*, vol. 182, no. 9, pp. 5400–11, May 2009.

[7] L. Zhang, F. Murray, A. Zahno, J. R. Kanter, D. Chou, R. Suda, M. Fenlon, L. Rassenti, H. Cottam, T. J. Kipps, and P. A. Insel, "Cyclic nucleotide phosphodiesterase profiling reveals increased expression of phosphodiesterase 7B in chronic lymphocytic leukemia.," *Proceedings of the National Academy of Sciences of the United States of America*, vol. 105, no. 49, pp. 19532–7, Dec. 2008.

[8] L. Zhang and P. A. Insel, "The pro-apoptotic protein Bim is a convergence point for cAMP/protein kinase A- and glucocorticoid-promoted apoptosis of lymphoid cells.," *The Journal of biological chemistry*, vol. 279, no. 20, pp. 20858–65, May 2004.

[9] S. Tiwari, H. Dong, E. J. Kim, L. Weintraub, P. M. Epstein, and A. Lerner, "Type 4 cAMP phosphodiesterase (PDE4) inhibitors augment glucocorticoid-mediated apoptosis in B cell chronic lymphocytic leukemia (B-CLL) in the absence of exogenous adenylyl cyclase stimulation.," *Biochemical pharmacology*, vol. 69, no. 3, pp. 473–83, Feb. 2005.

[10] P. G. Smith, F. Wang, K. N. Wilkinson, K. J. Savage, U. Klein, D. S. Neuberg, G. Bollag, M. A. Shipp, and R. C. T. Aguiar, "The phosphodiesterase PDE4B limits cAMP-associated PI3K/AKT-dependent apoptosis in diffuse large B-cell lymphoma.," *Blood*, vol. 105, no. 1, pp. 308–16, Jan. 2005.

[11] M. A. Giembycz and S. J. Smith, “Phosphodiesterase 7A: a new therapeutic target for alleviating chronic inflammation?,” *Current pharmaceutical design*, vol. 12, no. 25, pp. 3207–20, Jan. 2006.

[12] K.-E. Andersson, S. Uckert, C. Stief, and P. Hedlund, “Phosphodiesterases (PDEs) and PDE inhibitors for treatment of LUTS.,” *Neurourology and urodynamics*, vol. 26, no. 6 Suppl, pp. 928–33, Oct. 2007.

[13] M. A. Giembycz, C. J. Corrigan, J. Seybold, R. Newton, and P. J. Barnes, “Identification of cyclic AMP phosphodiesterases 3, 4 and 7 in human CD4+ and CD8+ T-lymphocytes: role in regulating proliferation and the biosynthesis of interleukin-2.,” *British journal of pharmacology*, vol. 118, no. 8, pp. 1945–58, Aug. 1996.

[14] R. W. BUTCHER and E. W. SUTHERLAND, “Adenosine 3’,5'-phosphate in biological materials. I. Purification and properties of cyclic 3',5'-nucleotide phosphodiesterase and use of this enzyme to characterize adenosine 3',5'-phosphate in human urine.,” *The Journal of biological chemistry*, vol. 237, pp. 1244–50, Apr. 1962.

[15] K. Fan Chung, “Phosphodiesterase inhibitors in airways disease.,” *European journal of pharmacology*, vol. 533, no. 1–3, pp. 110–7, Mar. 2006.

[16] C. Kroegel and M. Foerster, “Phosphodiesterase-4 inhibitors as a novel approach for the treatment of respiratory disease: cilomilast.,” *Expert opinion on investigational drugs*, vol. 16, no. 1, pp. 109–24, Jan. 2007.

[17] S. G. Dastidar, D. Rajagopal, and A. Ray, “Therapeutic benefit of PDE4 inhibitors in inflammatory diseases.,” *Current opinion in investigational drugs (London, England : 2000)*, vol. 8, no. 5, pp. 364–72, May 2007.

[18] T. Michaeli, T. J. Bloom, T. Martins, K. Loughney, K. Ferguson, M. Riggs, L. Rodgers, J. A. Beavo, and M. Wigler, “Isolation and characterization of a previously undetected human cAMP phosphodiesterase by complementation of cAMP phosphodiesterase-deficient Saccharomyces cerevisiae.,” *The Journal of biological chemistry*, vol. 268, no. 17, pp. 12925–32, Jun. 1993.

[19] T. Sasaki, J. Kotera, K. Yuasa, and K. Omori, “Identification of human PDE7B, a cAMP-specific phosphodiesterase.,” *Biochemical and biophysical research communications*, vol. 271, no. 3, pp. 575–83, May 2000.

[20] T. Sasaki, J. Kotera, and K. Omori, “Novel alternative splice variants of rat phosphodiesterase 7B showing unique tissue-specific expression and phosphorylation.,” *The Biochemical journal*, vol. 361, no. Pt 2, pp. 211–20, Jan. 2002.

[21] J. M. Hetman, S. H. Soderling, N. A. Glavas, and J. A. Beavo, “Cloning and characterization of PDE7B, a cAMP-specific phosphodiesterase.,” *Proceedings of the National Academy of Sciences of the United States of America*, vol. 97, no. 1, pp. 472–6, Jan. 2000.

[22] S. J. Smith, S. Brookes-Fazakerley, L. E. Donnelly, P. J. Barnes, M. S. Barnette, and M. A. Giembycz, "Ubiquitous expression of phosphodiesterase 7A in human proinflammatory and immune cells.," *American journal of physiology. Lung cellular and molecular physiology*, vol. 284, no. 2, pp. L279–89, Feb. 2003.

[23] N. A. Glavas, C. Ostenson, J. B. Schaefer, V. Vasta, and J. A. Beavo, "T cell activation up-regulates cyclic nucleotide phosphodiesterases 8A1 and 7A3.," *Proceedings of the National Academy of Sciences of the United States of America*, vol. 98, no. 11, pp. 6319–24, May 2001.

[24] R. Lee, S. Wolda, E. Moon, J. Esselstyn, C. Hertel, and A. Lerner, "PDE7A is expressed in human B-lymphocytes and is up-regulated by elevation of intracellular cAMP.," *Cellular signalling*, vol. 14, no. 3, pp. 277–84, Mar. 2002.

[25] L. Li, "CD3- and CD28-Dependent Induction of PDE7 Required for T Cell Activation," *Science*, vol. 283, no. 5403, pp. 848–851, Feb. 1999.

[26] G. Yang, K. W. McIntyre, R. M. Townsend, H. H. Shen, W. J. Pitts, J. H. Dodd, S. G. Nadler, M. McKinnon, and A. J. Watson, "Phosphodiesterase 7A-deficient mice have functional T cells.," *Journal of immunology (Baltimore, Md. : 1950)*, vol. 171, no. 12, pp. 6414–20, Dec. 2003.

[27] L. Macrophages, C. D. T-lymphocytes, S. J. Smith, L. B. Cieslinski, R. Newton, L. E. Donnelly, P. S. Fenwick, A. G. Nicholson, P. J. Barnes, M. S. Barnette, and M. A. Giembycz, "Discovery of BRL 50481 [3- (N , N-dimethylsulfonamido) -4- methyl-nitrobenzene], a Selective Inhibitor of Phosphodiesterase 7 : In Vitro Studies in Human Monocytes ," vol. 66, no. 6, pp. 1679–1689, 2004.

[28] M. A. Alaamery, A. R. Wyman, F. D. Ivey, C. Allain, D. Demirbas, L. Wang, O. Ceyhan, C. S. Hoffman, B. College, C. Ave, and H. H. Rm, "New classes of PDE7 inhibitors identified by a fission yeast-based HTS," *J Biomol Screen*, vol. 15, no. 4, pp. 359–367, 2011.

[29] M. Humar, S. E. Pischke, T. Loop, A. Hoetzel, R. Schmidt, C. Klaas, H. L. Pahl, K. K. Geiger, and B. H. J. Pannen, "Barbiturates directly inhibit the calmodulin/calcineurin complex: a novel mechanism of inhibition of nuclear factor of activated T cells.," *Molecular pharmacology*, vol. 65, no. 2, pp. 350–61, Feb. 2004.

[30] M. Humar, N. Andriopoulos, S. E. Pischke, T. Loop, R. Schmidt, A. Hoetzel, M. Roesslein, H. L. Pahl, K. K. Geiger, and B. H. J. Pannen, "Inhibition of activator protein 1 by barbiturates is mediated by differential effects on mitogen-activated protein kinases and the small G proteins ras and rac-1.," *The Journal of pharmacology and experimental therapeutics*, vol. 311, no. 3, pp. 1232–40, Dec. 2004.

[31] C. A. J. Janeway, P. Travers, M. Walport, and M. J. Shlomchik, *Immunobiology the immune system in health and disease 6th edition*. Garland Science, 2005.

[32] E. Sebzda, S. Mariathasan, T. Ohteki, R. Jones, M. F. Bachmann, and P. S. Ohashi, "Selection of the T cell repertoire," *Annual review of immunology*, vol. 17, no. 3, pp. 829–874, 1999.

[33] E. V Rothenberg, "T-lineage specification and commitment : a gene regulation perspective," vol. 14, no. 02, pp. 431–440, 2002.

[34] C. a London, a K. Abbas, and a Kelso, "Helper T cell subsets: heterogeneity, functions and development.," *Veterinary immunology and immunopathology*, vol. 63, no. 1–2, pp. 37–44, May 1998.

[35] D. R. Littman and A. Y. Rudensky, "Th17 and regulatory T cells in mediating and restraining inflammation.," *Cell*, vol. 140, no. 6, pp. 845–58, Mar. 2010.

[36] Y. K. Lee, R. Mukasa, R. D. Hatton, and C. T. Weaver, "Developmental plasticity of Th17 and Treg cells.," *Current opinion in immunology*, vol. 21, no. 3, pp. 274–80, Jun. 2009.

[37] S. Chapoval, P. Dasgupta, N. J. Dorsey, and A. D. Keegan, "Regulation of the T helper cell type 2 (Th2)/T regulatory cell (Treg) balance by IL-4 and STAT6.," *Journal of leukocyte biology*, vol. 87, no. 6, pp. 1011–8, Jun. 2010.

[38] E. Bettelli, Y. Carrier, W. Gao, T. Korn, T. B. Strom, M. Oukka, H. L. Weiner, and V. K. Kuchroo, "Reciprocal developmental pathways for the generation of pathogenic effector TH17 and regulatory T cells.," *Nature*, vol. 441, no. 7090, pp. 235–8, May 2006.

[39] C. T. Weaver and R. D. Hatton, "Interplay between the TH17 and TReg cell lineages: a (co-)evolutionary perspective.," *Nature reviews. Immunology*, vol. 9, no. 12, pp. 883–9, Dec. 2009.

[40] D. Mucida, Y. Park, G. Kim, O. Turovskaya, I. Scott, M. Kronenberg, and H. Cheroutre, "Reciprocal TH17 and regulatory T cell differentiation mediated by retinoic acid.," *Science (New York, N.Y.)*, vol. 317, no. 5835, pp. 256–60, Jul. 2007.

[41] J. L. Coombes, K. R. R. Siddiqui, C. V Arancibia-Cárcamo, J. Hall, C.-M. Sun, Y. Belkaid, and F. Powrie, "A functionally specialized population of mucosal CD103+ DCs induces Foxp3+ regulatory T cells via a TGF-beta and retinoic acid-dependent mechanism.," *The Journal of experimental medicine*, vol. 204, no. 8, pp. 1757–64, Aug. 2007.

[42] C.-M. Sun, J. A. Hall, R. B. Blank, N. Bouladoux, M. Oukka, J. R. Mora, and Y. Belkaid, "Small intestine lamina propria dendritic cells promote de novo generation of Foxp3 T reg cells via retinoic acid.," *The Journal of experimental medicine*, vol. 204, no. 8, pp. 1775–85, Aug. 2007.

[43] M. J. Benson, K. Pino-Lagos, M. Rosemblatt, and R. J. Noelle, "All-trans retinoic acid mediates enhanced T reg cell growth, differentiation, and gut homing in the face of high

levels of co-stimulation.," *The Journal of experimental medicine*, vol. 204, no. 8, pp. 1765–74, Aug. 2007.

[44] I. I. Ivanov, B. S. McKenzie, L. Zhou, C. E. Tadokoro, A. Lepelley, J. J. Lafaille, D. J. Cua, and D. R. Littman, "The orphan nuclear receptor RORgammat directs the differentiation program of proinflammatory IL-17+ T helper cells.," *Cell*, vol. 126, no. 6, pp. 1121–33, Sep. 2006.

[45] S. G. Ward, "CD28: a signalling perspective.," *The Biochemical journal*, vol. 318, pp. 361–77, Sep. 1996.

[46] D. Cantrell, "T cell antigen receptor signal transduction pathways.," *Annual review of immunology*, vol. 14, pp. 259–74, Jan. 1996.

[47] R. J. Salmond, A. Filby, I. Qureshi, S. Caserta, and R. Zamoyska, "T-cell receptor proximal signaling via the Src-family kinases, Lck and Fyn, influences T-cell activation, differentiation, and tolerance.," *Immunological reviews*, vol. 228, no. 1, pp. 9–22, Mar. 2009.

[48] S. L. Gaffen and K. D. Liu, "Overview of interleukin-2 function, production and clinical applications.," *Cytokine*, vol. 28, no. 3, pp. 109–23, Nov. 2004.

[49] J. D. Powell, J. a Ragheb, S. Kitagawa-Sakakida, and R. H. Schwartz, "Molecular regulation of interleukin-2 expression by CD28 co-stimulation and anergy.," *Immunological reviews*, vol. 165, pp. 287–300, Oct. 1998.

[50] O. Acuto, S. Mise-Omata, G. Mangino, and F. Michel, "Molecular modifiers of T cell antigen receptor triggering threshold: the mechanism of CD28 costimulatory receptor.," *Immunological reviews*, vol. 192, pp. 21–31, Apr. 2003.

[51] C. E. Rudd, A. Taylor, and H. Schneider, "CD28 and CTLA-4 coreceptor expression and signal transduction.," *Immunological reviews*, vol. 229, no. 1, pp. 12–26, May 2009.

[52] N. Isakov and A. Altman, "Protein kinase C(theta) in T cell activation.," *Annual review of immunology*, vol. 20, pp. 761–94, Jan. 2002.

[53] "ScienceDirect.com - The Lancet - Acute lymphoblastic leukaemia." [Online]. Available: http://www.sciencedirect.com.proxy.bc.edu/science/article/pii/S0140673608604572#. [Accessed: 19-Jan-2013].

[54] U. Schneider, H. U. Schwenk, and G. Bornkamm, "Characterization of EBV-genome negative 'null' and 'T' cell lines derived from children with acute lymphoblastic leukemia and leukemic transformed non-Hodgkin lymphoma.," *International journal of cancer. Journal international du cancer*, vol. 19, no. 5, pp. 621–6, May 1977.

[55] G. Pawelec, A. Borowitz, P. H. Krammer, and P. Wernet, "Constitutive interleukin 2 production by the JURKAT human leukemic T cell line.," *European journal of immunology*, vol. 12, no. 5, pp. 387–92, May 1982.

[56] D. A. Morgan, F. W. Ruscetti, and R. Gallo, “Selective in vitro growth of T lymphocytes from normal human bone marrows.,” *Science*, vol. 193, no. 4257, pp. 1007–8, Sep. 1976.

[57] W. Liao, J.-X. Lin, and W. J. Leonard, “IL-2 family cytokines: new insights into the complex roles of IL-2 as a broad regulator of T helper cell differentiation.,” *Current opinion in immunology*, vol. 23, no. 5, pp. 598–604, Oct. 2011.

[58] T. R. Malek, “The biology of interleukin-2.,” *Annual review of immunology*, vol. 26, pp. 453–79, Jan. 2008.

[59] L. Van Parijs and A. K. Abbas, “Homeostasis and self-tolerance in the immune system: turning lymphocytes off.,” *Science*, vol. 280, no. 5361, pp. 243–8, Apr. 1998.

[60] T. R. Malek and A. L. Bayer, “Tolerance, not immunity, crucially depends on IL-2.,” *Nature reviews. Immunology*, vol. 4, no. 9, pp. 665–74, Sep. 2004.

[61] O. Boyman and J. Sprent, “The role of interleukin-2 during homeostasis and activation of the immune system.,” *Nature reviews. Immunology*, vol. 12, no. 3, pp. 180–90, Jan. 2012.

[62] W. Strober and R. O. Ehrhardt, “Chronic intestinal inflammation: an unexpected outcome in cytokine or T cell receptor mutant mice.,” *Cell*, vol. 75, no. 2, pp. 203–5, Oct. 1993.

[63] B. Sadlack, J. Löhler, H. Schorle, G. Klebb, H. Haber, E. Sickel, R. J. Noelle, and I. Horak, “Generalized autoimmune disease in interleukin-2-deficient mice is triggered by an uncontrolled activation and proliferation of CD4+ T cells.,” *European journal of immunology*, vol. 25, no. 11, pp. 3053–9, Nov. 1995.

[64] M. Wolf, A. Schimpl, and T. Hünig, “Control of T cell hyperactivation in IL-2-deficient mice by CD4(+)CD25(-) and CD4(+)CD25(+) T cells: evidence for two distinct regulatory mechanisms.,” *European journal of immunology*, vol. 31, no. 6, pp. 1637–45, Jun. 2001.

[65] T. R. Malek, A. Yu, V. Vincek, P. Scibelli, and L. Kong, “CD4 regulatory T cells prevent lethal autoimmunity in IL-2Rbeta-deficient mice. Implications for the nonredundant function of IL-2.,” *Immunity*, vol. 17, no. 2, pp. 167–78, Aug. 2002.

[66] M. A. Burchill, C. A. Goetz, M. Prlic, J. J. O’Neil, I. R. Harmon, S. J. Bensinger, L. A. Turka, P. Brennan, S. C. Jameson, and M. A. Farrar, “Distinct effects of STAT5 activation on CD4+ and CD8+ T cell homeostasis: development of CD4+CD25+ regulatory T cells versus CD8+ memory T cells.,” *Journal of immunology (Baltimore, Md. : 1950)*, vol. 171, no. 11, pp. 5853–64, Dec. 2003.

[67] J. W. Snow, N. Abraham, M. C. Ma, B. G. Herndier, A. W. Pastuszak, and M. A. Goldsmith, “Loss of tolerance and autoimmunity affecting multiple organs in STAT5A/5B-deficient mice.,” *Journal of immunology (Baltimore, Md. : 1950)*, vol. 171, no. 10, pp. 5042–50, Nov. 2003.

[68] A. Antov, L. Yang, M. Vig, D. Baltimore, and L. Van Parijs, “Essential role for STAT5 signaling in CD25+CD4+ regulatory T cell homeostasis and the maintenance of self-tolerance.,” *Journal of immunology (Baltimore, Md. : 1950)*, vol. 171, no. 7, pp. 3435–41, Oct. 2003.

[69] W. Liao, J.-X. Lin, L. Wang, P. Li, and W. J. Leonard, “Modulation of cytokine receptors by IL-2 broadly regulates differentiation into helper T cell lineages.,” *Nature immunology*, vol. 12, no. 6, pp. 551–9, Jun. 2011.

[70] J. Cote-Sierra, G. Foucras, L. Guo, L. Chiodetti, H. A. Young, J. Hu-Li, J. Zhu, and W. E. Paul, “Interleukin 2 plays a central role in Th2 differentiation.,” *Proceedings of the National Academy of Sciences of the United States of America*, vol. 101, no. 11, pp. 3880–5, Mar. 2004.

[71] W. Liao, D. E. Schones, J. Oh, Y. Cui, K. Cui, T.-Y. Roh, K. Zhao, and W. J. Leonard, “Priming for T helper type 2 differentiation by interleukin 2-mediated induction of interleukin 4 receptor alpha-chain expression.,” *Nature immunology*, vol. 9, no. 11, pp. 1288–96, Nov. 2008.

[72] X.-P. Yang, K. Ghoreschi, S. M. Steward-Tharp, J. Rodriguez-Canales, J. Zhu, J. R. Grainger, K. Hirahara, H.-W. Sun, L. Wei, G. Vahedi, Y. Kanno, J. J. O’Shea, and A. Laurence, “Opposing regulation of the locus encoding IL-17 through direct, reciprocal actions of STAT3 and STAT5.,” *Nature immunology*, vol. 12, no. 3, pp. 247–54, Mar. 2011.

[73] A. Laurence, C. M. Tato, T. S. Davidson, Y. Kanno, Z. Chen, Z. Yao, R. B. Blank, F. Meylan, R. Siegel, L. Hennighausen, E. M. Shevach, and J. J. O’shea, “Interleukin-2 signaling via STAT5 constrains T helper 17 cell generation.,” *Immunity*, vol. 26, no. 3, pp. 371–81, Mar. 2007.

[74] H. P. Kim, J. Imbert, and W. J. Leonard, “Both integrated and differential regulation of components of the IL-2/IL-2 receptor system.,” *Cytokine & growth factor reviews*, vol. 17, no. 5, pp. 349–66, Oct. 2006.

[75] J. C. Crispín and G. C. Tsokos, “Transcriptional regulation of IL-2 in health and autoimmunity.,” *Autoimmunity reviews*, vol. 8, no. 3, pp. 190–5, Jan. 2009.

[76] J. Jain, C. Loh, and A. Rao, “Transcriptional regulation of the IL-2 gene.,” *Current opinion in immunology*, vol. 7, no. 3, pp. 333–42, Jun. 1995.

[77] C. Loh, K. T. Shaw, J. Carew, J. P. Viola, C. Luo, B. A. Perrino, and A. Rao, “Calcineurin binds the transcription factor NFAT1 and reversibly regulates its activity.,” *The Journal of biological chemistry*, vol. 271, no. 18, pp. 10884–91, May 1996.

[78] F. Macian, “NFAT proteins: key regulators of T-cell development and function.,” *Nature reviews. Immunology*, vol. 5, no. 6, pp. 472–84, Jun. 2005.

[79] H. Yoshida, H. Nishina, H. Takimoto, L. E. Marengère, A. C. Wakeham, D. Bouchard, Y. Y. Kong, T. Ohteki, A. Shahinian, M. Bachmann, P. S. Ohashi, J. M. Penninger, G. R. Crabtree, and T. W. Mak, "The transcription factor NF-ATc1 regulates lymphocyte proliferation and Th2 cytokine production.," *Immunity*, vol. 8, no. 1, pp. 115–24, Jan. 1998.

[80] M. R. Hodge, A. M. Ranger, F. Charles de la Brousse, T. Hoey, M. J. Grusby, and L. H. Glimcher, "Hyperproliferation and dysregulation of IL-4 expression in NF-ATp-deficient mice.," *Immunity*, vol. 4, no. 4, pp. 397–405, Apr. 1996.

[81] S. L. Peng, A. J. Gerth, A. M. Ranger, and L. H. Glimcher, "NFATc1 and NFATc2 together control both T and B cell activation and differentiation.," *Immunity*, vol. 14, no. 1, pp. 13–20, Jan. 2001.

[82] E. Shaulian and M. Karin, "AP-1 as a regulator of cell life and death.," *Nature cell biology*, vol. 4, no. 5, pp. E131–6, May 2002.

[83] Q. Meng and Y. Xia, "c-Jun, at the crossroad of the signaling network.," *Protein & cell*, vol. 2, no. 11, pp. 889–98, Nov. 2011.

[84] K. J. Kovács, "c-Fos as a transcription factor: a stressful (re)view from a functional map.," *Neurochemistry international*, vol. 33, no. 4, pp. 287–97, Oct. 1998.

[85] D. Petrak, S. A. Memon, M. J. Birrer, J. D. Ashwell, and C. M. Zacharchuk, "Dominant negative mutant of c-Jun inhibits NF-AT transcriptional activity and prevents IL-2 gene transcription.," *Journal of immunology*, vol. 153, no. 5, pp. 2046–51, Sep. 1994.

[86] M. Karin and Y. Ben-Neriah, "Phosphorylation meets ubiquitination: the control of NF-[kappa]B activity.," *Annual review of immunology*, vol. 18, pp. 621–63, Jan. 2000.

[87] D. Thanos and T. Maniatis, "NF-kappa B: a lesson in family values.," *Cell*, vol. 80, no. 4, pp. 529–32, Feb. 1995.

[88] L. P. Kane, J. Lin, and A. Weiss, "It's all Rel-ative: NF-kappaB and CD28 costimulation of T-cell activation.," *Trends in immunology*, vol. 23, no. 8, pp. 413–20, Aug. 2002.

[89] O. Gaide, B. Favier, D. F. Legler, D. Bonnet, B. Brissoni, S. Valitutti, C. Bron, J. Tschopp, and M. Thome, "CARMA1 is a critical lipid raft-associated regulator of TCR-induced NF-kappa B activation.," *Nature immunology*, vol. 3, no. 9, pp. 836–43, Sep. 2002.

[90] D. Wang, Y. You, S. M. Case, L. M. McAllister-Lucas, L. Wang, P. S. DiStefano, G. Nuñez, J. Bertin, and X. Lin, "A requirement for CARMA1 in TCR-induced NF-kappa B activation.," *Nature immunology*, vol. 3, no. 9, pp. 830–5, Sep. 2002.

[91] O. Gaide, F. Martinon, O. Micheau, D. Bonnet, M. Thome, and J. Tschopp, "Carma1, a CARD-containing binding partner of Bcl10, induces Bcl10 phosphorylation and NF-kappaB activation.," *FEBS letters*, vol. 496, no. 2–3, pp. 121–7, May 2001.

[92] J. Cheng, A. Montecalvo, and L. P. Kane, "Regulation of NF-κB induction by TCR/CD28.," *Immunologic research*, vol. 50, no. 2–3, pp. 113–7, Aug. 2011.

[93] H. Sebban, S. Yamaoka, and G. Courtois, "Posttranslational modifications of NEMO and its partners in NF-kappaB signaling.," *Trends in cell biology*, vol. 16, no. 11, pp. 569–77, Nov. 2006.

[94] H. Häcker and M. Karin, "Regulation and function of IKK and IKK-related kinases.," *Science's STKE : signal transduction knowledge environment*, vol. 2006, no. 357, p. re13, Oct. 2006.

[95] A. Oeckinghaus, M. S. Hayden, and S. Ghosh, "Crosstalk in NF-κB signaling pathways.," *Nature immunology*, vol. 12, no. 8, pp. 695–708, Aug. 2011.

[96] S. Ghosh and M. Karin, "Missing pieces in the NF-kappaB puzzle.," *Cell*, vol. 109 Suppl, pp. S81–96, Apr. 2002.

[97] V. S. Shapiro, K. E. Truitt, J. B. Imboden, and a Weiss, "CD28 mediates transcriptional upregulation of the interleukin-2 (IL-2) promoter through a composite element containing the CD28RE and NF-IL-2B AP-1 sites.," *Molecular and cellular biology*, vol. 17, no. 7, pp. 4051–8, Jul. 1997.

[98] M. P. Kamps, L. Corcoran, J. H. LeBowitz, and D. Baltimore, "The promoter of the human interleukin-2 gene contains two octamer-binding sites and is partially activated by the expression of Oct-2.," *Molecular and cellular biology*, vol. 10, no. 10, pp. 5464–72, Oct. 1990.

[99] I. Pfeuffer, S. Klein-Hessling, A. Heinfling, S. Chuvpilo, C. Escher, T. Brabletz, B. Hentsch, H. Schwarzenbach, P. Matthias, and E. Serfling, "Octamer factors exert a dual effect on the IL-2 and IL-4 promoters.," *Journal of immunology*, vol. 153, no. 12, pp. 5572–85, Dec. 1994.

[100] B. Mayr and M. Montminy, "Transcriptional regulation by the phosphorylation-dependent factor CREB.," *Nature reviews. Molecular cell biology*, vol. 2, no. 8, pp. 599–609, Aug. 2001.

[101] A. Y. Wen, K. M. Sakamoto, and L. S. Miller, "The role of the transcription factor CREB in immune function.," *Journal of immunology (Baltimore, Md. : 1950)*, vol. 185, no. 11, pp. 6413–9, Dec. 2010.

[102] E. E. Solomou, Y. T. Juang, and G. C. Tsokos, "Protein kinase C-theta participates in the activation of cyclic AMP-responsive element-binding protein and its subsequent binding to the -180 site of the IL-2 promoter in normal human T lymphocytes.," *Journal of immunology (Baltimore, Md. : 1950)*, vol. 166, no. 9, pp. 5665–74, May 2001.

[103] K. Barton, N. Muthusamy, M. Chanyangam, C. Fischer, C. Clendenin, and J. M. Leiden, "Defective thymocyte proliferation and IL-2 production in transgenic mice expressing a dominant-negative form of CREB.," *Nature*, vol. 379, no. 6560, pp. 81–5, Jan. 1996.

[104] D. De Cesare, G. M. Fimia, and P. Sassone-Corsi, “Signaling routes to CREM and CREB: plasticity in transcriptional activation.,” *Trends in biochemical sciences*, vol. 24, no. 7, pp. 281–5, Jul. 1999.

[105] C. M. Hedrich, T. Rauen, and G. C. Tsokos, “cAMP-responsive element modulator (CREM)α protein signaling mediates epigenetic remodeling of the human interleukin-2 gene: implications in systemic lupus erythematosus.,” *The Journal of biological chemistry*, vol. 286, no. 50, pp. 43429–36, Dec. 2011.

[106] K. Tenbrock, Y.-T. Juang, M. F. Gourley, M. P. Nambiar, and G. C. Tsokos, “Antisense cyclic adenosine 5’-monophosphate response element modulator up-regulates IL-2 in T cells from patients with systemic lupus erythematosus.,” *Journal of immunology*, vol. 169, no. 8, pp. 4147–52, Oct. 2002.

[107] K. Tenbrock, Y.-T. Juang, M. Tolnay, and G. C. Tsokos, “The cyclic adenosine 5’-monophosphate response element modulator suppresses IL-2 production in stimulated T cells by a chromatin-dependent mechanism.,” *Journal of immunology (Baltimore, Md. : 1950)*, vol. 170, no. 6, pp. 2971–6, Mar. 2003.

[108] C. Skerka, E. L. Decker, and P. F. Zipfel, “A regulatory element in the human interleukin 2 gene promoter is a binding site for the zinc finger proteins Sp1 and EGR-1.,” *The Journal of biological chemistry*, vol. 270, no. 38, pp. 22500–6, Sep. 1995.

[109] E. L. Decker, C. Skerka, and P. F. Zipfel, “The early growth response protein (EGR-1) regulates interleukin-2 transcription by synergistic interaction with the nuclear factor of activated T cells.,” *The Journal of biological chemistry*, vol. 273, no. 41, pp. 26923–30, Oct. 1998.

[110] S. Collins, L. A. Wolfraim, C. G. Drake, M. R. Horton, and J. D. Powell, “Cutting Edge: TCR-induced NAB2 enhances T cell function by coactivating IL-2 transcription.,” *Journal of immunology (Baltimore, Md. : 1950)*, vol. 177, no. 12, pp. 8301–5, Dec. 2006.

[111] A. Avots, A. Hoffmeyer, E. Flory, A. Cimanis, U. R. Rapp, and E. Serfling, “GABP factors bind to a distal interleukin 2 (IL-2) enhancer and contribute to c-Raf-mediated increase in IL-2 induction.,” *Molecular and cellular biology*, vol. 17, no. 8, pp. 4381–9, Aug. 1997.

[112] T. M. Williams, D. Moolten, J. Burlein, J. Romano, R. Bhaerman, A. Godillot, M. Mellon, F. J. Rauscher, and J. A. Kant, “Identification of a zinc finger protein that inhibits IL-2 gene expression.,” *Science*, vol. 254, no. 5039, pp. 1791–4, Dec. 1991.

[113] J. Wang, S. Lee, C. E.-Y. Teh, K. Bunting, L. Ma, and M. F. Shannon, “The transcription repressor, ZEB1, cooperates with CtBP2 and HDAC1 to suppress IL-2 gene activation in T cells.,” *International immunology*, vol. 21, no. 3, pp. 227–35, Mar. 2009.

[114] D. H. Yasui, T. Genetta, T. Kadesch, T. M. Williams, S. L. Swain, L. V Tsui, and B. T. Huber, “Transcriptional repression of the IL-2 gene in Th cells by ZEB.,” *Journal of immunology (Baltimore, Md. : 1950)*, vol. 160, no. 9, pp. 4433–40, May 1998.

[115] R. M. Thomas, N. Chunder, C. Chen, S. E. Umetsu, S. Winandy, and A. D. Wells, “Ikaros enforces the costimulatory requirement for IL2 gene expression and is required for anergy induction in CD4+ T lymphocytes.,” *Journal of immunology (Baltimore, Md. : 1950)*, vol. 179, no. 11, pp. 7305–15, Dec. 2007.

[116] S. Bandyopadhyay, M. Duré, M. Paroder, N. Soto-Nieves, I. Puga, and F. Macián, “Interleukin 2 gene transcription is regulated by Ikaros-induced changes in histone acetylation in anergic T cells.,” *Blood*, vol. 109, no. 7, pp. 2878–86, Apr. 2007.

[117] A. Sundstedt, M. Sigvardsson, T. Leanderson, G. Hedlund, T. Kalland, and M. Dohlsten, “In vivo anergized CD4+ T cells express perturbed AP-1 and NF-kappa B transcription factors.,” *Proceedings of the National Academy of Sciences of the United States of America*, vol. 93, no. 3, pp. 979–84, Feb. 1996.

[118] S. Grundström, P. Anderson, P. Scheipers, and A. Sundstedt, “Bcl-3 and NFkappaB p50-p50 homodimers act as transcriptional repressors in tolerant CD4+ T cells.,” *The Journal of biological chemistry*, vol. 279, no. 9, pp. 8460–8, Feb. 2004.

[119] A. Murayama, K. Sakura, M. Nakama, K. Yasuzawa-Tanaka, E. Fujita, Y. Tateishi, Y. Wang, T. Ushijima, T. Baba, K. Shibuya, A. Shibuya, Y. Kawabe, and J. Yanagisawa, “A specific CpG site demethylation in the human interleukin 2 gene promoter is an epigenetic memory.,” *The EMBO journal*, vol. 25, no. 5, pp. 1081–92, Mar. 2006.

[120] D. Bruniquel and R. H. Schwartz, “Selective, stable demethylation of the interleukin-2 gene enhances transcription by an active process.,” *Nature immunology*, vol. 4, no. 3, pp. 235–40, Mar. 2003.

[121] J. L. Attema, R. Reeves, V. Murray, I. Levichkin, M. D. Temple, D. J. Tremethick, and M. F. Shannon, “The human IL-2 gene promoter can assemble a positioned nucleosome that becomes remodeled upon T cell activation.,” *Journal of immunology (Baltimore, Md. : 1950)*, vol. 169, no. 5, pp. 2466–76, Sep. 2002.

[122] R. M. Thomas, L. Gao, and A. D. Wells, “Signals from CD28 induce stable epigenetic modification of the IL-2 promoter.,” *Journal of immunology (Baltimore, Md. : 1950)*, vol. 174, no. 8, pp. 4639–46, Apr. 2005.

[123] C. Y. Chen and A. B. Shyu, “AU-rich elements: characterization and importance in mRNA degradation.,” *Trends in biochemical sciences*, vol. 20, no. 11, pp. 465–70, Nov. 1995.

[124] T. Lindstein, C. H. June, J. A. Ledbetter, G. Stella, and C. B. Thompson, “Regulation of lymphokine messenger RNA stability by a surface-mediated T cell activation pathway.,” *Science (New York, N.Y.)*, vol. 244, no. 4902, pp. 339–43, Apr. 1989.

[125] J. Shim, H. Lim, J. R Yates, and M. Karin, “Nuclear export of NF90 is required for interleukin-2 mRNA stabilization.,” *Molecular cell*, vol. 10, no. 6, pp. 1331–44, Dec. 2002.

[126] C. Y. Chen, F. Del Gatto-Konczak, Z. Wu, and M. Karin, "Stabilization of interleukin-2 mRNA by the c-Jun NH2-terminal kinase pathway.," *Science (New York, N.Y.)*, vol. 280, no. 5371, pp. 1945–9, Jun. 1998.

[127] J. A. Ragheb, M. Deen, and R. H. Schwartz, "CD28-Mediated regulation of mRNA stability requires sequences within the coding region of the IL-2 mRNA.," *Journal of immunology (Baltimore, Md. : 1950)*, vol. 163, no. 1, pp. 120–9, Jul. 1999.

[128] Y. Pei, P. Zhu, Y. Dang, J. Wu, X. Yang, B. Wan, J. O. Liu, Q. Yi, and L. Yu, "Nuclear export of NF90 to stabilize IL-2 mRNA is mediated by AKT-dependent phosphorylation at Ser647 in response to CD28 costimulation.," *Journal of immunology (Baltimore, Md. : 1950)*, vol. 180, no. 1, pp. 222–9, Jan. 2008.

[129] C. Y. Chen, R. Gherzi, J. S. Andersen, G. Gaietta, K. Jürchott, H. D. Royer, M. Mann, and M. Karin, "Nucleolin and YB-1 are required for JNK-mediated interleukin-2 mRNA stabilization during T-cell activation.," *Genes & development*, vol. 14, no. 10, pp. 1236–48, May 2000.

[130] V. R. Moulton and G. C. Tsokos, "Abnormalities of T cell signaling in systemic lupus erythematosus.," *Arthritis research & therapy*, vol. 13, no. 2, p. 207, Jan. 2011.

[131] V. C. Kyttaris and G. C. Tsokos, "Targeting lymphocyte signaling pathways as a therapeutic approach to systemic lupus erythematosus.," *Current opinion in rheumatology*, vol. 23, no. 5, pp. 449–53, Sep. 2011.

[132] S. N. Liossis, X. Z. Ding, G. J. Dennis, and G. C. Tsokos, "Altered pattern of TCR/CD3-mediated protein-tyrosyl phosphorylation in T cells from patients with systemic lupus erythematosus. Deficient expression of the T cell receptor zeta chain.," *The Journal of clinical investigation*, vol. 101, no. 7, pp. 1448–57, Apr. 1998.

[133] D. Vassilopoulos, B. Kovacs, and G. C. Tsokos, "TCR/CD3 complex-mediated signal transduction pathway in T cells and T cell lines from patients with systemic lupus erythematosus.," *Journal of immunology (Baltimore, Md. : 1950)*, vol. 155, no. 4, pp. 2269–81, Aug. 1995.

[134] H. K. Wong, G. M. Kammer, G. Dennis, and G. C. Tsokos, "Abnormal NF-kappa B activity in T lymphocytes from patients with systemic lupus erythematosus is associated with decreased p65-RelA protein expression.," *Journal of immunology (Baltimore, Md. : 1950)*, vol. 163, no. 3, pp. 1682–9, Aug. 1999.

[135] V. C. Kyttaris, Y.-T. Juang, K. Tenbrock, A. Weinstein, and G. C. Tsokos, "Cyclic adenosine 5'-monophosphate response element modulator is responsible for the decreased expression of c-fos and activator protein-1 binding in T cells from patients with systemic lupus erythematosus.," *Journal of immunology (Baltimore, Md. : 1950)*, vol. 173, no. 5, pp. 3557–63, Sep. 2004.

[136] C. G. Katsiari, V. C. Kyttaris, Y.-T. Juang, and G. C. Tsokos, "Protein phosphatase 2A is a negative regulator of IL-2 production in patients with systemic lupus erythematosus.," *The Journal of clinical investigation*, vol. 115, no. 11, pp. 3193–204, Nov. 2005.

[137] B. Kovacs, D. Vassilopoulos, S. A. Vogelgesang, and G. C. Tsokos, “Defective CD3-mediated cell death in activated T cells from patients with systemic lupus erythematosus: role of decreased intracellular TNF-alpha.,” *Clinical immunology and immunopathology*, vol. 81, no. 3, pp. 293–302, Dec. 1996.

[138] D. A. Horwitz, J. D. Gray, and S. G. Zheng, “The potential of human regulatory T cells generated ex vivo as a treatment for lupus and other chronic inflammatory diseases.,” *Arthritis research*, vol. 4, no. 4, pp. 241–6, Jan. 2002.

[139] S. A. Long and J. H. Buckner, “CD4+FOXP3+ T regulatory cells in human autoimmunity: more than a numbers game.,” *Journal of immunology (Baltimore, Md. : 1950)*, vol. 187, no. 5, pp. 2061–6, Sep. 2011.

[140] C. M. Wilke, K. Bishop, D. Fox, and W. Zou, “Deciphering the role of Th17 cells in human disease.,” *Trends in immunology*, vol. 32, no. 12, pp. 603–11, Dec. 2011.

[141] R. G. Stirling and K. F. Chung, “New immunological approaches and cytokine targets in asthma and allergy.,” *The European respiratory journal : official journal of the European Society for Clinical Respiratory Physiology*, vol. 16, no. 6, pp. 1158–74, Dec. 2000.

[142] J. F. Alcorn, C. R. Crowe, and J. K. Kolls, “TH17 cells in asthma and COPD.,” *Annual review of physiology*, vol. 72, pp. 495–516, Jan. 2010.

[143] A. N. Thorburn and P. M. Hansbro, “Harnessing regulatory T cells to suppress asthma: from potential to therapy.,” *American journal of respiratory cell and molecular biology*, vol. 43, no. 5, pp. 511–9, Nov. 2010.

[144] M. D. Duncan and D. S. Wilkes, “Transplant-related immunosuppression: a review of immunosuppression and pulmonary infections.,” *Proceedings of the American Thoracic Society*, vol. 2, no. 5, pp. 449–55, Jan. 2005.

[145] “ScienceDirect.com - Steroids - Novel insights into mechanisms of glucocorticoid action and the development of new glucocorticoid receptor ligands.” [Online]. Available: http://www.sciencedirect.com.proxy.bc.edu/science/article/pii/S0039128X07002383#. [Accessed: 12-Dec-2012].

[146] J. Liu, J. D. Farmer, W. S. Lane, J. Friedman, I. Weissman, and S. L. Schreiber, “Calcineurin is a common target of cyclophilin-cyclosporin A and FKBP-FK506 complexes.,” *Cell*, vol. 66, no. 4, pp. 807–15, Aug. 1991.

[147] J. Chung, C. J. Kuo, G. R. Crabtree, and J. Blenis, “Rapamycin-FKBP specifically blocks growth-dependent activation of and signaling by the 70 kd S6 protein kinases.,” *Cell*, vol. 69, no. 7, pp. 1227–36, Jun. 1992.

[148] C. S. Cho, “Rapamycin antagonizes cyclosporin A- and tacrolimus (FK506)-mediated augmentation of linker for activation of T cell expression in T cells,” *International Immunology*, vol. 15, no. 11, pp. 1369–1378, Nov. 2003.

[149] G. R. Ingle, T. M. Sievers, and C. D. Holt, “Sirolimus: continuing the evolution of transplant immunosuppression.,” *The Annals of pharmacotherapy*, vol. 34, no. 9, pp. 1044–55, Sep. 2000.

[150] C. Sommerer and M. Zeier, “AEB071--a promising immunosuppressive agent.,” *Clinical transplantation*, vol. 23 Suppl 2, pp. 15–8, Dec. 2009.

[151] G.-M. Deng, L. Liu, F. R. Bahjat, P. R. Pine, and G. C. Tsokos, “Suppression of skin and kidney disease by inhibition of spleen tyrosine kinase in lupus-prone mice.,” *Arthritis and rheumatism*, vol. 62, no. 7, pp. 2086–92, Jul. 2010.

[152] M. Fuxa and J. A. Skok, “ScienceDirect.com - Current Opinion in Immunology - Transcriptional regulation in early B cell development.” [Online]. Available: http://www.sciencedirect.com.proxy.bc.edu/science/article/pii/S0952791507000106#. [Accessed: 20-Jan-2013].

[153] R. J. Benschop and J. C. Cambier, “B cell development: signal transduction by antigen receptors and their surrogates.,” *Current opinion in immunology*, vol. 11, no. 2, pp. 143–51, Apr. 1999.

[154] K. S. Campbell, “Signal transduction from the B cell antigen-receptor.,” *Current opinion in immunology*, vol. 11, no. 3, pp. 256–64, Jun. 1999.

[155] A. A. Alizadeh, M. B. Eisen, R. E. Davis, C. Ma, I. S. Lossos, A. Rosenwald, J. C. Boldrick, H. Sabet, T. Tran, X. Yu, J. I. Powell, L. Yang, G. E. Marti, T. Moore, J. Hudson, L. Lu, D. B. Lewis, R. Tibshirani, G. Sherlock, W. C. Chan, T. C. Greiner, D. D. Weisenburger, J. O. Armitage, R. Warnke, R. Levy, W. Wilson, M. R. Grever, J. C. Byrd, D. Botstein, P. O. Brown, and L. M. Staudt, “Distinct types of diffuse large B-cell lymphoma identified by gene expression profiling.,” *Nature*, vol. 403, no. 6769, pp. 503–11, Feb. 2000.

[156] L. M. Staudt, “Molecular Diagnosis of the Hematologic Cancers — NEJM.” [Online]. Available: http://www.nejm.org/doi/full/10.1056/NEJMra020067. [Accessed: 21-Jan-2013].

[157] P. Tsang, E. Cesarman, A. Chadburn, Y. F. Liu, and D. M. Knowles, “Molecular characterization of primary mediastinal B cell lymphoma.,” *The American journal of pathology*, vol. 148, no. 6, pp. 2017–25, Jun. 1996.

[158] M. Sánchez-Beato, A. Sánchez-Aguilera, and M. A. Piris, “Cell cycle deregulation in B-cell lymphomas.,” *Blood*, vol. 101, no. 4, pp. 1220–35, Feb. 2003.

[159] H. Chang, H. A. Messner, X. H. Wang, C. Yee, L. Addy, J. Meharchand, and M. D. Minden, “A human lymphoma cell line with multiple immunoglobulin rearrangements.,” *The Journal of clinical investigation*, vol. 89, no. 3, pp. 1014–20, Mar. 1992.

[160] H. Chang, J. A. Blondal, S. Benchimol, M. D. Minden, and H. A. Messner, "p53 mutations, c-myc and bcl-2 rearrangements in human non-Hodgkin's lymphoma cell lines.," *Leukemia & lymphoma*, vol. 19, no. 1–2, pp. 165–71, Sep. 1995.

[161] A. D. Friedman, "Transcriptional control of granulocyte and monocyte development.," *Oncogene*, vol. 26, no. 47, pp. 6816–28, Oct. 2007.

[162] D. Strauss-Ayali, S. M. Conrad, and D. M. Mosser, "Monocyte subpopulations and their differentiation patterns during infection.," *Journal of leukocyte biology*, vol. 82, no. 2, pp. 244–52, Aug. 2007.

[163] C. Shi and E. G. Pamer, "Monocyte recruitment during infection and inflammation.," *Nature reviews. Immunology*, vol. 11, no. 11, pp. 762–74, Nov. 2011.

[164] N. V Serbina, T. Jia, T. M. Hohl, and E. G. Pamer, "Monocyte-mediated defense against microbial pathogens.," *Annual review of immunology*, vol. 26, pp. 421–52, Jan. 2008.

[165] F. Geissmann, M. G. Manz, S. Jung, M. H. Sieweke, M. Merad, and K. Ley, "Development of monocytes, macrophages, and dendritic cells.," *Science (New York, N.Y.)*, vol. 327, no. 5966, pp. 656–61, Feb. 2010.

[166] C. Sundström and K. Nilsson, "Establishment and characterization of a human histiocytic lymphoma cell line (U-937).," *International journal of cancer. Journal international du cancer*, vol. 17, no. 5, pp. 565–77, May 1976.

[167] H. S. Koren, S. J. Anderson, and J. W. Larrick, "In vitro activation of a human macrophage-like cell line.," *Nature*, vol. 279, no. 5711, pp. 328–31, May 1979.

[168] J. W. Larrick, D. G. Fischer, S. J. Anderson, and H. S. Koren, "Characterization of a human macrophage-like cell line stimulated in vitro: a model of macrophage functions.," *Journal of immunology (Baltimore, Md. : 1950)*, vol. 125, no. 1, pp. 6–12, Jul. 1980.

[169] C. Härtel, G. Bein, H. Kirchner, and H. Klüter, "A human whole-blood assay for analysis of T-cell function by quantification of cytokine mRNA.," *Scandinavian journal of immunology*, vol. 49, no. 6, pp. 649–54, Jun. 1999.

[170] A. M. Hidalgo-Estévez, E. González, C. Punzón, and M. Fresno, "Human immunodeficiency virus type 1 Tat increases cooperation between AP-1 and NFAT transcription factors in T cells.," *The Journal of general virology*, vol. 87, no. Pt 6, pp. 1603–12, Jun. 2006.

[171] J. M. Trevillyan, X. G. Chiou, Y. W. Chen, S. J. Ballaron, M. P. Sheets, M. L. Smith, P. E. Wiedeman, U. Warrior, J. Wilkins, E. J. Gubbins, G. D. Gagne, J. Fagerland, G. W. Carter, J. R. Luly, K. W. Mollison, and S. W. Djuric, "Potent inhibition of NFAT activation and T cell cytokine production by novel low molecular weight pyrazole compounds.," *The Journal of biological chemistry*, vol. 276, no. 51, pp. 48118–26, Dec. 2001.

[172] J. E. Kay, “Mechanisms of T lymphocyte activation.,” *Immunology letters*, vol. 29, no. 1–2, pp. 51–4, Jul. 1991.

[173] M. Sanchez-Lockhart and J. Miller, “Engagement of CD28 outside of the immunological synapse results in up-regulation of IL-2 mRNA stability but not IL-2 transcription.,” *Journal of immunology (Baltimore, Md. : 1950)*, vol. 176, no. 8, pp. 4778–84, Apr. 2006.

[174] X. Shan, M. J. Czar, S. C. Bunnell, P. Liu, Y. Liu, P. L. Schwartzberg, and R. L. Wange, “Deficiency of PTEN in Jurkat T cells causes constitutive localization of Itk to the plasma membrane and hyperresponsiveness to CD3 stimulation.,” *Molecular and cellular biology*, vol. 20, no. 18, pp. 6945–57, Sep. 2000.

[175] S. Merluzzi, O. D’Orlando, A. Leonardi, G. Vitale, and C. Pucillo, “TRAF2 and p38 are involved in B cells CD40-mediated APE/Ref-1 nuclear translocation: a novel pathway in B cell activation.,” *Molecular immunology*, vol. 45, no. 1, pp. 76–86, Jan. 2008.

[176] M.-H. Cheong, S.-R. Lee, H.-S. Yoo, J.-W. Jeong, G.-Y. Kim, W.-J. Kim, I.-C. Jung, and Y. H. Choi, “Anti-inflammatory effects of Polygala tenuifolia root through inhibition of NF-κB activation in lipopolysaccharide-induced BV2 microglial cells.,” *Journal of ethnopharmacology*, vol. 137, no. 3, pp. 1402–8, Oct. 2011.

[177] A. M. Hidalgo-Estévez, E. González, C. Punzón, and M. Fresno, “Human immunodeficiency virus type 1 Tat increases cooperation between AP-1 and NFAT transcription factors in T cells.,” *The Journal of general virology*, vol. 87, no. Pt 6, pp. 1603–12, Jun. 2006.

[178] J. Park, N. R. Yaseen, P. G. Hogan, A. Rao, and S. Sharma, “Phosphorylation of the transcription factor NFATp inhibits its DNA binding activity in cyclosporin A-treated human B and T cells.,” *The Journal of biological chemistry*, vol. 270, no. 35, pp. 20653–9, Sep. 1995.

[179] A. Truneh, F. Albert, P. Golstein, and A. M. Schmitt-Verhulst, “Early steps of lymphocyte activation bypassed by synergy between calcium ionophores and phorbol ester.,” *Nature*, vol. 313, no. 6000, pp. 318–20.

[180] D. W. Nicholson, A. Ali, N. A. Thornberry, J. P. Vaillancourt, C. K. Ding, M. Gallant, Y. Gareau, P. R. Griffin, M. Labelle, and Y. A. Lazebnik, “Identification and inhibition of the ICE/CED-3 protease necessary for mammalian apoptosis.,” *Nature*, vol. 376, no. 6535, pp. 37–43, Jul. 1995.

[181] M. A. Giembycz, “Phosphodiesterase 4 inhibitors and the treatment of asthma: where are we now and where do we go from here?,” *Drugs*, vol. 59, no. 2, pp. 193–212, Feb. 2000.

[182] A. Nakata, K. Ogawa, T. Sasaki, N. Koyama, K. Wada, J. Kotera, H. Kikkawa, K. Omori, and O. Kaminuma, “Potential role of phosphodiesterase 7 in human T cell function: comparative effects of two phosphodiesterase inhibitors.,” *Clinical and experimental immunology*, vol. 128, no. 3, pp. 460–6, Jun. 2002.

[183] M. Delhase, M. Hayakawa, Y. Chen, and M. Karin, “Positive and negative regulation of IkappaB kinase activity through IKKbeta subunit phosphorylation.,” *Science (New York, N.Y.)*, vol. 284, no. 5412, pp. 309–13, Apr. 1999.

[184] J. A. DiDonato, M. Hayakawa, D. M. Rothwarf, E. Zandi, and M. Karin, “A cytokine-responsive IkappaB kinase that activates the transcription factor NF-kappaB.,” *Nature*, vol. 388, no. 6642, pp. 548–54, Aug. 1997.

[185] F. Mercurio, H. Zhu, B. W. Murray, A. Shevchenko, B. L. Bennett, J. Li, D. B. Young, M. Barbosa, M. Mann, A. Manning, and A. Rao, “IKK-1 and IKK-2: cytokine-activated IkappaB kinases essential for NF-kappaB activation.,” *Science (New York, N.Y.)*, vol. 278, no. 5339, pp. 860–6, Oct. 1997.

[186] A. Israël, “NF-kappaB activation: Nondegradative ubiquitination implicates NEMO.,” *Trends in immunology*, vol. 27, no. 9, pp. 395–7, Sep. 2006.

[187] D. M. Rothwarf, E. Zandi, G. Natoli, and M. Karin, “IKK-gamma is an essential regulatory subunit of the IkappaB kinase complex.,” *Nature*, vol. 395, no. 6699, pp. 297–300, Sep. 1998.

[188] Z. Ren, J. Cui, Z. Huo, J. Xue, H. Cui, B. Luo, L. Jiang, and R. Yang, “Cordycepin suppresses TNF-α-induced NF-κB activation by reducing p65 transcriptional activity, inhibiting IκBα phosphorylation, and blocking IKKγ ubiquitination.,” *International immunopharmacology*, vol. 14, no. 4, pp. 698–703, Dec. 2012.

[189] C. Corrêa-Sales, C. E. Tosta, and L. V Rizzo, “The effects of anesthesia with thiopental on T lymphocyte responses to antigen and mitogens in vivo and in vitro.,” *International journal of immunopharmacology*, vol. 19, no. 2, pp. 117–28, Feb. 1997.

[190] K. Nishina, H. Akamatsu, K. Mikawa, M. Shiga, N. Maekawa, H. Obara, and Y. Niwa, “The inhibitory effects of thiopental, midazolam, and ketamine on human neutrophil functions.,” *Anesthesia and analgesia*, vol. 86, no. 1, pp. 159–65, Jan. 1998.

[191] T. Loop, Z. Liu, M. Humar, A. Hoetzel, A. Benzing, H. L. Pahl, K. K. Geiger, and B. H. J Pannen, “Thiopental inhibits the activation of nuclear factor kappaB.,” *Anesthesiology*, vol. 96, no. 5, pp. 1202–13, May 2002.

[192] L. Gossage and T. Eisen, “Targeting multiple kinase pathways: a change in paradigm.,” *Clinical cancer research : an official journal of the American Association for Cancer Research*, vol. 16, no. 7, pp. 1973–8, Apr. 2010.

[193] P. Csermely, V. Agoston, and S. Pongor, “The efficiency of multi-target drugs: the network approach might help drug design.,” *Trends in pharmacological sciences*, vol. 26, no. 4, pp. 178–82, Apr. 2005.

[194] L. McKinley, J. F. Alcorn, A. Peterson, R. B. Dupont, S. Kapadia, A. Logar, A. Henry, C. G. Irvin, J. D. Piganelli, A. Ray, and J. K. Kolls, “TH17 cells mediate steroid-resistant

airway inflammation and airway hyperresponsiveness in mice.," *Journal of immunology (Baltimore, Md. : 1950)*, vol. 181, no. 6, pp. 4089–97, Sep. 2008.

[195] W. C. Rowan, J. L. Smith, K. Affleck, and A. Amour, "Targeting phosphoinositide 3-kinase δ for allergic asthma.," *Biochemical Society transactions*, vol. 40, no. 1, pp. 240–5, Feb. 2012.

[196] N. Oda, K. Minoguchi, T. Yokoe, T. Hashimoto, K. Wada, M. Miyamoto, A. Tanaka, Y. Kohno, and M. Adachi, "Effect of suplatast tosilate (IPD-1151T) on cytokine production by allergen-specific human Th1 and Th2 cell lines.," *Life sciences*, vol. 65, no. 8, pp. 763–70, Jan. 1999.

[197] M. Yoshida, H. Aizawa, H. Inoue, K. Matsumoto, H. Koto, M. Komori, S. Fukuyama, M. Okamoto, and N. Hara, "Effect of suplatast tosilate on airway hyperresponsiveness and inflammation in asthma patients.," *The Journal of asthma : official journal of the Association for the Care of Asthma*, vol. 39, no. 6, pp. 545–52, Sep. 2002.

[198] S. Yoshihara, H. Fukuda, and O. Arisaka, "Usefulness of suplatast tosilate, a Th2 cytokine inhibitor based on the Th1/Th2 ratio for allergic disease in children: a retrospective study.," *Arzneimittel-Forschung*, vol. 61, no. 7, pp. 421–4, Jan. 2011.

[199] R. Savai, S. S. Pullamsetti, G.-A. Banat, N. Weissmann, H. A. Ghofrani, F. Grimminger, and R. T. Schermuly, "Targeting cancer with phosphodiesterase inhibitors.," *Expert opinion on investigational drugs*, vol. 19, no. 1, pp. 117–31, Jan. 2010.

[200] C. Muñoz-Pinedo, "Signaling pathways that regulate life and cell death: evolution of apoptosis in the context of self-defense.," *Advances in experimental medicine and biology*, vol. 738, pp. 124–43, Jan. 2012.

[201] M. C. Turco, M. F. Romano, A. Petrella, R. Bisogni, P. Tassone, and S. Venuta, "NF-kappaB/Rel-mediated regulation of apoptosis in hematologic malignancies and normal hematopoietic progenitors.," *Leukemia : official journal of the Leukemia Society of America, Leukemia Research Fund, U.K*, vol. 18, no. 1, pp. 11–7, Jan. 2004.

[202] M. Kanduri, G. Tobin, A. Aleskog, K. Nilsson, and R. Rosenquist, "The novel NF-κB inhibitor IMD-0354 induces apoptosis in chronic lymphocytic leukemia.," *Blood cancer journal*, vol. 1, no. 3, p. e12, Mar. 2011.

[203] G. A. Webster and N. D. Perkins, "Transcriptional cross talk between NF-kappaB and p53.," *Molecular and cellular biology*, vol. 19, no. 5, pp. 3485–95, May 1999.